

POST-TENSIONED REINFORCED CONCRETE  
AS APPLIED TO  
THE CONSTRUCTION OF SHIPS

James Daniel Ertner



POST-TENSIONED REINFORCED CONCRETE  
AS APPLIED TO  
THE CONSTRUCTION OF SHIPS

by

JAMES DANIEL ERTNER  
B.S., Wheaton College (Illinois)  
1968

SUBMITTED IN PARTIAL FULFILLMENT  
OF THE REQUIREMENTS FOR THE  
DEGREE OF OCEAN ENGINEER  
AND THE  
DEGREE OF MASTER OF SCIENCE IN  
NAVAL ARCHITECTURE AND MARINE ENGINEERING  
at the  
MASSACHUSETTS INSTITUTE OF TECHNOLOGY





POST-TENSIONED REINFORCED CONCRETE  
AS APPLIED TO  
THE CONSTRUCTION OF SHIPS

by

James Daniel Ertner

Submitted to the Department of Ocean Engineering on  
May 9, 1975, in partial fulfillment of the requirements for  
the degree of Ocean Engineer and the degree of Master of  
Science in Naval Architecture and Marine Engineering.

ABSTRACT

Post-tensioned reinforced concrete is a material which integrates the advantages of concrete, steel, reinforced concrete, and prestressed concrete. Unlike ferro-cement (which has been limited to small boats), post-tensioned reinforced concrete has the potential for being applied to the construction of larger ships, such as liquified natural gas tankers. An investigation of its engineering properties, permissible stresses under loading, design considerations (cracking, corrosion, concrete cover thickness, etc.), and its flexural behavior, all lead to the application of post-tensioned reinforced concrete to a tanker midship section. The key parameters in the design of such a midship section (excluding the principal ship dimensions) are: concrete cover thickness, diameter of ordinary reinforcing rods, total area of ordinary reinforcing steel, diameter of post-tensioning tendons, total area of post-tensioning steel, strength of the respective steels and the concrete, and modular ratio. The three parameters with the greatest impact on section properties (i.e., moment of inertia and section modulus) are modular ratio, overall steel area, and concrete area. The effect on moment of inertia (determined with the aid of a computer program) of varying these parameters is presented graphically. One particularly significant conclusion is that, for a constant moment of inertia, the weight of a midship section can be reduced by increasing the modular ratio while decreasing the steel area and/or the concrete area; furthermore, the steel stress increases considerably, whereas the concrete tensile stress (the critical stress in post-tensioned reinforced concrete structures) is virtually unaffected.

Thesis Supervisor: J. Harvey Evans  
Title: Professor of Naval Architecture



ACKNOWLEDGEMENT

For originally suggesting the thesis topic, for always being enthusiastically willing to discuss its progress, for freely offering professional advice, and for making the year's work a pleasurable experience, I want to heartily and gratefully thank Professor J. Harvey Evans. Appreciation is also due Mr. Keatinge Keays, Administration Officer of the Ocean Engineering Department, for granting me use of his computer program.

The excellent typing is the handiwork of my dear wife, Jenny, for which I express a loving thanks. And even though my beautiful daughter, Gail, is too young to understand what this is all about, she nevertheless deserves congratulations for being such a well-behaved baby, and thereby indirectly helping me with my thesis.

Last, but certainly not least, a sincere note of gratitude is extended to the United States Navy, without whose sponsorship my three-year course of study at M.I.T. would not have been possible.



TABLE OF CONTENTS

	<u>Page</u>
Title Page	1
Abstract	2
Acknowledgement	3
Table of Contents	4
List of Tables	8
List of Figures	10
Nomenclature	12
CHAPTER I: INTRODUCTION	15
A.    Historical Perspective	15
1.    Ferro-cement	15
2.    Reinforced Concrete	16
B.    Fundamentals and Problem Definition	18
CHAPTER II: POST-TENSIONED REINFORCED CONCRETE	22
A.    Preliminary Arguments	22
B.    Engineering Properties	25
1.    Steel	25
2.    Concrete	28
C.    Permissible Stresses	35
1.    Steel	35
2.    Concrete	36
D.    Material Selection -- Theoretical Aspects	40
1.    Steel	41
2.    Concrete	43



Page

E.	Material Selection -- Economic Aspects	55
1.	Steel	55
2.	Concrete	61
F.	Selection of Concrete Mix for a Ship	64
CHAPTER III: DESIGN CONSIDERATIONS		69
A.	Cracking of Concrete	69
1.	Fracture Mechanics	70
2.	Application of Fracture Mechanics to Concrete	73
3.	Application of Fracture Mechanics to Reinforced Concrete	75
4.	Cracking as a Design Factor	77
B.	Corrosion and Concrete	94
C.	Cover of Concrete	101
D.	Spacing of Rods	105
E.	Cost Considerations	109
CHAPTER IV: FLEXURAL ANALYSIS OF CONCRETE BEAMS		112
A.	Bending of Reinforced Concrete Members	112
1.	Reinforced Concrete Beam Bending Analysis	113
2.	Applications	118
3.	Use of Codes in Reinforced Concrete Bending	120
B.	Bending of Prestressed Concrete Members	128
1.	Flexural Analysis of Prestressed Concrete	128
2.	Use of Codes in Prestressed Concrete Bending	134





Page

C.	Bending of Post-Tensioned Reinforced Concrete Members	135
1.	Synthesis of Reinforced and Prestressed Concrete	138
2.	Calculation of Section Properties	140
3.	Applications	144
CHAPTER V: APPLICATION TO THE DESIGN OF A TANKER MIDSHIP SECTION		147
A.	Calculation of Section Modulus	148
1.	Post-Tensioned Reinforced Concrete Beam	149
2.	Computerized Extension to a Tanker Midship Section	151
B.	Effect on Tanker Midship Section Modulus of Varying Key Parameters	153
1.	Selection of Parameter Range of Values	154
2.	Application of Computer Program	156
C.	Results and Conclusions	161
1.	Treatment of Cover Thickness	161
2.	Effect of Varying Depth and Breadth	163
3.	Effect of Five Key Parameters	164
4.	Effect of the Three Primary Parameters	170
5.	Minimum Weight Considerations	184
D.	Stress Diagram	186
E.	Recommendations	193
APPENDICES		197
A.	Conversion Table	197



Page

B.	Effect on Beam Depth of Varying Modular Ratio	198
C.	Effect on Beam Depth of Varying Steel Stress	200
D.	Effect on Beam Weight of Varying Depth	202
E.	Analytical Expression for Minimum Weight of Beam	204
F.	Effect on Stress and Section Modulus of Varying Beam Depth	207
G.	Effect on Stress and Section Modulus of Varying Steel Area and Distribution	211
H.	Determination of Post-Tensioning Steel Area	214
I.	Determination of Nonprestressed and Prestressed Steel Area	219
J.	Modified Computer Program to Calculate the Section Modulus of a Post-Tensioned Reinforced Concrete Ship	222
K.	Effect on Moment of Inertia of Varying Primary Parameters	227
L.	Minimum Weight Considerations	230
REFERENCES		232



LIST OF TABLES

<u>Table</u>	<u>Page</u>
1. Types and Strengths of Portland Cement	47
2. Aggregates Commonly Used in Concrete	50
(a) Weight of Aggregates	
(b) Strength of Aggregates	
3. Aggregate-Cement Ratio (By Weight) Required to Give Four Degrees of Workability with Different Gradings for Rounded 3/4 inch Aggregate	53
4. Size and Weight of Ordinary Reinforcing Bars	56
5. Cost of Steel Used for Post-Tensioning Tendons	60
6. Average Cost of Aggregates	63
7. Constants for Use in Determination of Required Area of Nonprestressed Reinforcement (Equation 19)	82
8. Allowable Tensile Stresses for Class 2 Post-Tensioned Members	86
9. Allowable Tensile Stresses for Class 3 Post-Tensioned Members	88
10. Factors to be Multiplied by Allowable Tensile Stresses in Table 9	88
11. Stress in Post-Tensioning Tendons for Determination of Ultimate Moment (Equation 57)	136
12. Calculation of Neutral Axis Location and Moment of Inertia for Example in Figure 12	152
13. Possible Combinations of the Five Key Parameters	166
14. Computer Results of the Thirty-two Combinations of Five Key Parameters (for $n = 7$ )	168



<u>Table</u>	<u>Page</u>
15. Effect on Total Stress of Varying Modular Ratio	191
F1. Effect on Stress and Section Modulus of Varying Beam Depth	210
G1. Effect on Stress and Section Modulus of Varying Steel Area and Distribution	213





# LIST OF FIGURES

<u>Figure</u>		<u>Page</u>
1.	Typical Stress-Strain Curves for Concrete Reinforcement	26
2.	Typical Stress-Strain Curves for Prestressing Steels	27
3.	Typical Stress-Strain Curve for Concrete	29
4.	Tangent and Secant Concrete Moduli of Elasticity	30
5.	Permissible Tensile Stress in Concrete	39
6.	Relation Between Concrete Compressive Strength and Water-Cement Ratio	45
7.	Rectangular Reinforced Concrete Beam	115
8.	Rectangular Reinforced Concrete Beam (ACI Code)	123
9.	Rectangular Beam with Both Tension and Compression Reinforcement	125
10.	Determination of Stresses (a) Plain Concrete Beam (b) Prestressed Concrete Beam	131
11.	Post-Tensioned Reinforced Concrete Beam	142
12.	Post-Tensioned Reinforced Concrete Beam with Both Tension and Compression Reinforcement	150
13.	Post-Tensioned Reinforced Concrete Rectangular Midship Section	157
14.	Moment of Inertia vs. Modular Ratio (for constant concrete area)	173
15.	Moment of Inertia vs. Modular Ratio (for constant steel area)	175
16.	Moment of Inertia vs. Concrete Area (for constant modular ratio)	176



FigurePage

17.	Moment of Inertia vs. Concrete Area (for constant steel area)	177
18.	Moment of Inertia vs. Steel Area (for constant concrete area)	178
19.	Moment of Inertia vs. Steel Area (for constant modular ratio)	179
20.	Effect on Moment of Inertia of Increasing Modular Ratio and Decreasing Concrete Area	181
21.	Effect on Moment of Inertia of Increasing Modular Ratio and Decreasing Steel Area	182
22.	Effect on Moment of Inertia of Increasing Concrete Area and Decreasing Steel Area	183
23.	Stress Diagram for a Post-Tensioned Reinforced Concrete Tanker Midship Section	192



NOMENCLATURE

$A$	cross-sectional area
$A_c$	area of concrete
$A_{eq}$	equivalent concrete area = $A_g - A_s + nA_s$
$A_g$	gross sectional area of concrete
$A_{ps}$	area of prestressed reinforcement
$A_s$	area of nonprestressed tension reinforcement
$A'_s$	area of nonprestressed compression reinforcement
$a_{cr}$	distance from surface to nearest reinforcing bar
$b$	breadth
$C$	total compressive force in concrete
$c$	distance from neutral axis to extreme fiber; depth of notch; half the initial crack length
$c_{min}$	minimum concrete cover thickness to reinforcement
$D$	reinforcement rod diameter
$d$	depth of beam from top to center of tension reinforcement
$d'$	depth from top of beam to center of compression reinforcement
$d_o$	overall depth of beam
$E_c$	Young's modulus of elasticity for concrete
$E_s$	Young's modulus of elasticity for steel
$e$	strain; eccentricity
$f$	bending stresses
$f_c$	concrete stress at service loads
$f'_c$	specified compressive strength of concrete



$f_{pb}$	tensile stress in prestressing tendon at failure
$f_{ps}$	stress in prestressing steel at design loads
$f_{pu}$	ultimate strength of prestressing steel
$f_r$	modulus of rupture of concrete
$f_s$	stress in tension reinforcement at service loads
$f'_s$	stress in compression steel at service loads
$f_y$	yield strength of nonprestressed tension reinforcement
$f'_y$	yield strength of nonprestressed compression reinforcement
$G$	strain energy release rate
$h$	overall depth of reinforced concrete beam; net depth of beam with notch = $d_o - c$
$h_{agg}$	maximum diameter of aggregate
$I$	moment of inertia
$j$	ratio of moment arm of C-T couple to depth
$K$	stress intensity factor
$k$	ratio of location of neutral axis to depth
$M$	bending moment
$n$	modular ratio = $E_s/E_c$
$P$	applied load
$p$	percentage of nonprestressed tension steel = $A_s/bd$
$p'$	percentage of nonprestressed compression steel = $A'_s/bd$
$p_p$	percentage of prestressed reinforcement = $A_{ps}/bd$
pcf	pounds per cubic foot
psi	pounds per squared inch





q	prestressing steel reinforcement ratio = $p_p f_{pu} / f'_c$
q'	alternative prestressing steel reinforcement ratio = $p_p f_{ps} / f'_c$
R	ratio of distances from the neutral axis to the tension face and to the reinforcement centroid
r	radius from crack tip to any point
S	section modulus = $I/c$ ; specific surface energy
T	total tensile force; surface energy
U	elastic strain energy
u	Poisson's ratio
W	unit weight of concrete
$w_{max}$	maximum crack width
x	distance from surface to neutral axis
z	moment arm = $jd$
$\rho$	density; radius of curvature of crack tip
$\sigma$	applied stress
$\sigma_c$	critical stress for failure
$\sigma_n$	nominal stress at the notch root
$\phi$	capacity reduction factor



## CHAPTER I

### INTRODUCTION

The application of concrete to ship construction affords two immediate advantages in times of rising material prices and rapidly diminishing natural resources, namely, low relative cost and general availability. The raw materials for making cement and aggregates are essentially limitless, since practically all of the earth's crust can be used, assuming that the energy requirements for such production can be met. Further, concrete is the one construction material the engineer can personally formulate, within limits, to meet specific individual job requirements of durability and strength. The prospect of applying concrete to ship design and construction thus offers a potential benefit which merits serious consideration.

#### A. Historical Perspective

1. Ferro-cement. The first floating structures made of portland cement mortar, the forerunner of today's ferro-cement type of construction, were the ten-foot long reinforced mortar rowboats built in the late 1840's by J.L. Lambot in France (1). The mortar hulls were reinforced with wire fabric and iron grid. Until 1967, at which time it was transferred to a French museum, one of



these boats was still afloat in a pond on Lambot's estate.

Present-day ferro-cement construction was developed by the Italian architect P.L. Nervi (2). In 1946, Nervi built his largest ferro-cement vessel; with a displacement of 165 tons, the hull was nearly 1-1/2 inches thick and reinforcement consisted of three layers of 1/4 inch round steel bars at 4 inch centers and eight layers of wire fabric. After eight years of sea service, the vessel required no maintenance -- unfortunately, it was wrecked on a rocky coast during a storm in 1959.

Ferro-cement is currently receiving widespread attention from the United States Navy (3, 4, 5, 6, 7), individuals (8, 9), and professional societies (10). In fact, the Society of Naval Architects and Marine Engineers has formed a committee whose technical objective is the development and standardization of ferro-cement for marine purposes. However, the applicability of the aforementioned references has been limited to small boats, primarily due to the limited tensile strength of such structures. It is, thus, unlikely that ferro-cement construction will ever be practical for large ships (say, longer than 200 feet).

2. Reinforced Concrete. One solution to this problem is reinforced concrete. As opposed to ferro-cement which is formed in relatively thin layers on the



order of 1 to 1-1/2 inches, ordinary reinforced concrete is typically cast in sections approaching 6 inches and more. Whereas ferro-cement contains thin rods and/or wire mesh, reinforced concrete is reinforced with thicker steel bars. Tensile cracking is considered negligible and structures are designed so that all design tensile loads are carried by the bars, the concrete being used to carry compression loads.

The first large reinforced concrete ocean-going ship produced in the United States was the "Faith"; constructed in 1917, this vessel displaced 3,427 tons and had a hull thickness varying from 4 to 4-1/2 inches. The U.S. Shipping Board Emergency Fleet Corporation program constructed twelve concrete ships for World War I use (six of them were tankers); ranging in length from 260 to 434 feet, the hulls of these ships incorporated steel reinforcing bars ranging from 3/8 to 1-3/8 inches in diameter; hull thicknesses varied from 4 to 6 inches. The average compressive strength of the concrete was 4,000 pounds per squared inch (psi) at age 28 days. Crushed lightweight (expanded clay) aggregate was utilized in the 120 pounds per cubic foot (pcf) concrete (11). It is apropos to note that drill cores extracted about 1953 from the hull of the wrecked "Selma", one of these twelve ships, revealed no corrosion of reinforcing steel after 35 years of exposure to seawater.





During World War II, the U.S. Maritime Commission constructed a total of 104 concrete hulls: 24 of these were for self-propelled dry cargo ships each 350 feet long; the remainder were for seagoing oil barges, with a cargo capacity of 5,000 to 7,000 tons. The concrete in all of these vessels incorporated lightweight aggregate (maximum size = 1/2 inch) and modified portland cement (ASTM Type II). Minimum compressive strength required at age 28 days was 5,000 psi; hull thicknesses ranged from 4 to 6-1/2 inches (12).

#### B. Fundamentals and Problem Definition

Before progressing any further, it is fitting that a few key terms be identified. Ferro-cement, suffice it to say, is characterized by a thin wire mesh of the chicken wire variety covered by mortar that, in general, can be applied with a trowel. Its application has been limited to small boats. Reinforced concrete, on the other hand, is concrete containing steel bar reinforcement, and, like ferro-cement, is designed on the assumption that the two materials act together in resisting forces (13).

Concrete, on its own, is a material which is relatively weak in tension; steel reinforcing rods are therefore embedded in that part of a beam subject to tensile strain, e.g., the lower layer in a simply supported beam. (A ship, idealized as a beam on a  $1.1(L)^{0.5}$  wave, experiences



alternating loads in a seaway, and thus requires reinforcing rods at both deck and keel). Standard textbooks on reinforced concrete (14, 15) present the fundamental characteristics, and traditional strength of materials texts include sections on the bending analysis of reinforced concrete beams (16, 17). The concrete ships constructed during World Wars I and II were of this material.

Prestressed concrete is reinforced concrete in which there have been introduced internal stresses of such magnitude and distribution that the stresses resulting from loads are counteracted to a desired degree (13). Two principal methods of prestressing are post-tensioning and pre-tensioning, in which tendons embodied in the concrete are tensioned after the concrete has hardened and before the concrete is placed, respectively.

Post-tensioned prestressed concrete incorporates the use of tensioned tendons in preformed voids or ducts throughout the length of the member. The tendons are stressed by hydraulic jacks and anchored after the concrete has developed a specified strength (generally after about 14 to 28 days). As a final operation, the ducts or voids are pressure grouted to protect the tendons against corrosion and also to provide bond between the tendon and the concrete.

One of the main advantages of prestressing is that it



tends to minimize tensile cracking in the concrete. This is accomplished by means of the "prestress", namely, the compression induced in the concrete by the external pressure (tension) applied to the tendons. Thus, under conditions of superimposed loading, the normal tendency for tensile stress to develop only goes towards nullifying the artificial compressive prestress.

Resulting advantages are that the concrete is in compression, high prestress tends to increase durability of the concrete, impact resistance is good, and fatigue resistance is high. Prestressed concrete textbooks (18, 19, 20, 21) cover the various engineering properties, specifically as applied to land-based structures. The adaptation of prestressed concrete to ships is a recent phenomenon and is sparsely represented in the literature (22, 23, 24).

A significant point must be made at this juncture. References on reinforced concrete (a binary system consisting of concrete + reinforcing rods) and prestressed concrete (a binary system consisting of concrete + reinforcing rods that have been post- or pre-tensioned) are amply available. However, a survey of the literature does not reveal any references dealing strictly with reinforced as well as prestressed concrete. I will thus define, for purposes of this thesis, a tertiary system consisting of the "union" of the above two binary "sets",



and will call it "prestressed (or, post-tensioned) reinforced concrete". Therefore:

Post-Tensioned Reinforced Concrete =

Concrete  
+  
Reinforcing Rods  
+  
Post-Tensioned Tendons

The purpose of this thesis is thus to investigate the feasibility of applying post-tensioned reinforced concrete to the construction of ships.





## CHAPTER II

POST-TENSIONED REINFORCED CONCRETE

Despite the fact that the ocean-going concrete ships and barges of Chapter I were structurally sound, further development was apparently undesirable because conventionally reinforced thick concrete hulls are heavier than comparatively thin steel hulls. Furthermore, even if no immediate structural degradation or leakage resulted, tensile cracking in a ship operating in a seaway (experiencing large hogging and sagging bending moments) would act to pump salt water into the structure and onto the bars, causing corrosion. This in turn requires a larger cover of cement to prevent tensile cracks from reaching the reinforcing bars, contributing further to size and weight of the structure.

The weight of the hull thus seems to be the most damaging drawback in using concrete for large ships. The alternating loads in a seaway present difficulties in utilizing concrete properties. However, numerous advantages indicate that consideration of this material as applied to the construction of ships should not be neglected.

A. Preliminary Arguments

Some of these advantages of prestressed concrete



include: economy of construction vis-à-vis steel structures; high prestress tends to increase durability of the concrete; low maintenance (e.g., no drydocking due to concrete durability); sparkproof, fire resistant, and extremely advantageous for transporting flammable or explosive cargo. Prestressed concrete has high fatigue strength, due chiefly to the small stress variations in the prestressing steel; prestressing improves ability for energy absorption under impact loads. Prestressed concrete has a favorable mode of failure under accident or over-stress conditions, such as grounding, collision, and explosion -- it develops localized cracks or disruption, but does not rip or tear as metals do; if a ship hull is damaged, repairs are rapid and relatively inexpensive (chip away cracked areas, apply bonding compound to the contact surface, and pour a concrete patch). Prestressed concrete is virtually corrosion resistant, and is less likely than many other structural materials to exhibit brittle fracture at low temperatures. A favorable result of corrosion resistance is that rusting would be precluded in the cargo compartments: further ramifications would be minimization of cargo contamination and no expensive gas freeing procedures incidental to hot work or chipping of rusted steel hulls. Another advantage of prestressed concrete is that thermal conductivity is only one-sixth that of steel hulls, thereby



holding condensation in cargo holds to a minimum.

The weight disadvantage of concrete ships previously alluded to might be overcome by resorting to post-tensioned reinforced concrete hulls. Prestressed concrete usually employs high-strength materials and therefore requires less of them for the same load, which results in lighter members. The small steel area (due to the use of high-strength steel) warrants thinner members which are also more flexible than conventionally reinforced concrete members. Furthermore, prestressing is intended to minimize the formation of tension cracks under working loads. With this reduction of (or hopefully, lack of) cracking, the entire cross-section remains effective for stress; a smaller required section normally results.

Any weight disadvantage would be further allayed if post-tensioned reinforced concrete were used in the construction of ships designed to carry a typically light cargo, e.g., a liquified natural gas (LNG) tanker. Not only would the light cargo counteract the heavier (compared to steel) concrete hull, but the concrete hull would also preclude (or at least greatly minimize) the taking on of ballast upon off-loading the cargo. The preceding discussion of the corrosion resistant advantage of prestressed concrete, as well as cracking minimization, are both also particularly applicable to tankers. Thus,



there seems to be ample evidence to justify further investigation into the applicability of post-tensioned reinforced concrete to large ship construction.

## B. Engineering Properties

Before the load-carrying behavior of post-tensioned reinforced concrete attains meaning, the basic physical properties of concrete and steel (both prestressing and nonprestressed) must be understood.

Prestressed concrete combines the best properties of concrete and steel. Concrete is capable of resisting relatively high compressive stresses, although its tensile strength is only 10 to 15 percent of its compressive strength. On the other hand, steel is strong in tension. Prestressing combines these two materials in the most efficient manner: by stretching the steel before it is bonded to the concrete, compressive forces are placed in the concrete; and if the steel and the resultant compressive portion are located in the ship hull area where tensile forces occur under loading, these materials will be utilized most efficiently.

1. Steel. Turning briefly first to steel, as it is the more familiar material (at least to naval architects), the stress-strain relationship deserves attention. Figures 1 and 2 portray typical stress-strain curves for several steels. There are three basic differences







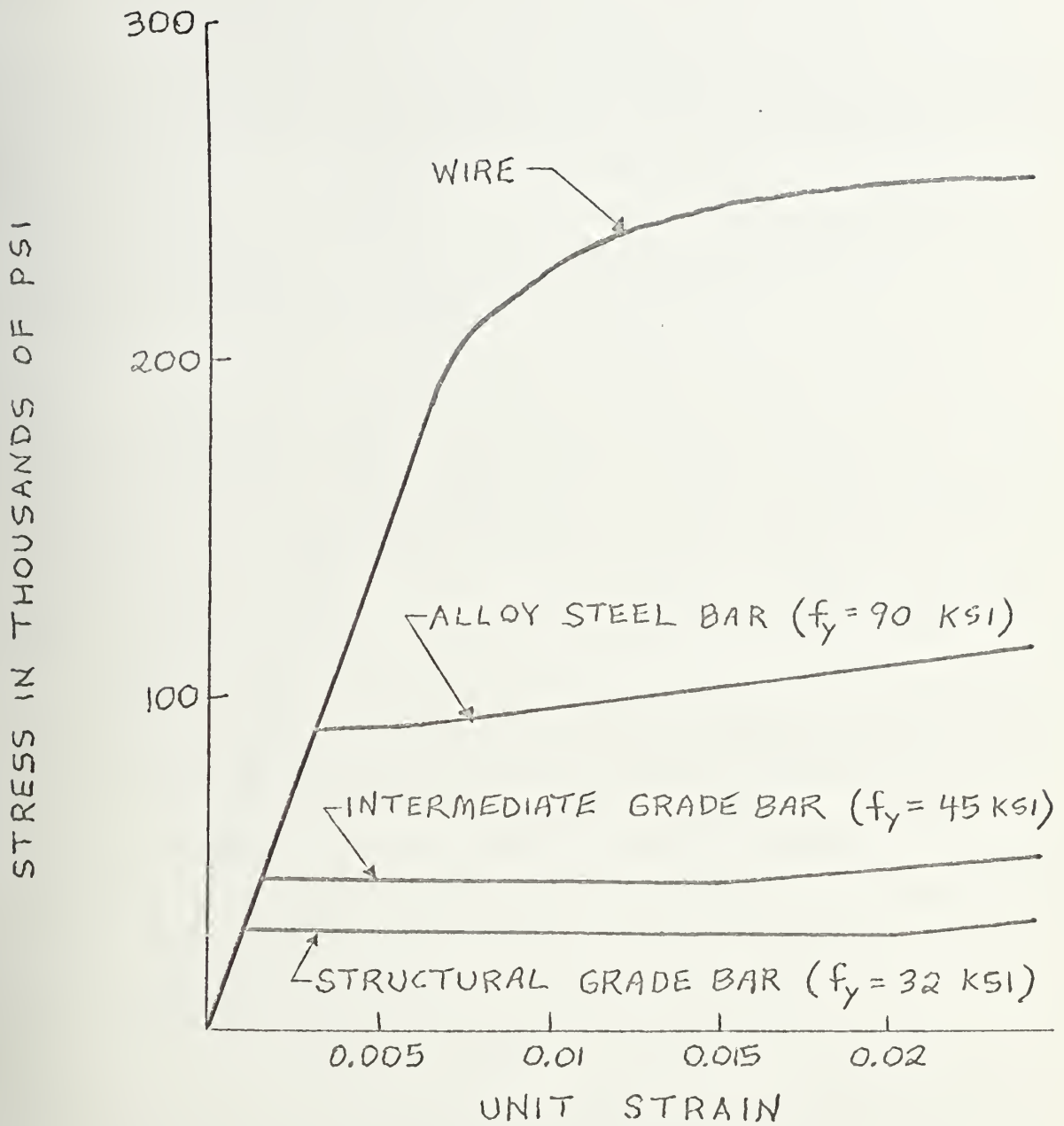


FIGURE 1

TYPICAL STRESS-STRAIN CURVES  
FOR CONCRETE REINFORCEMENT



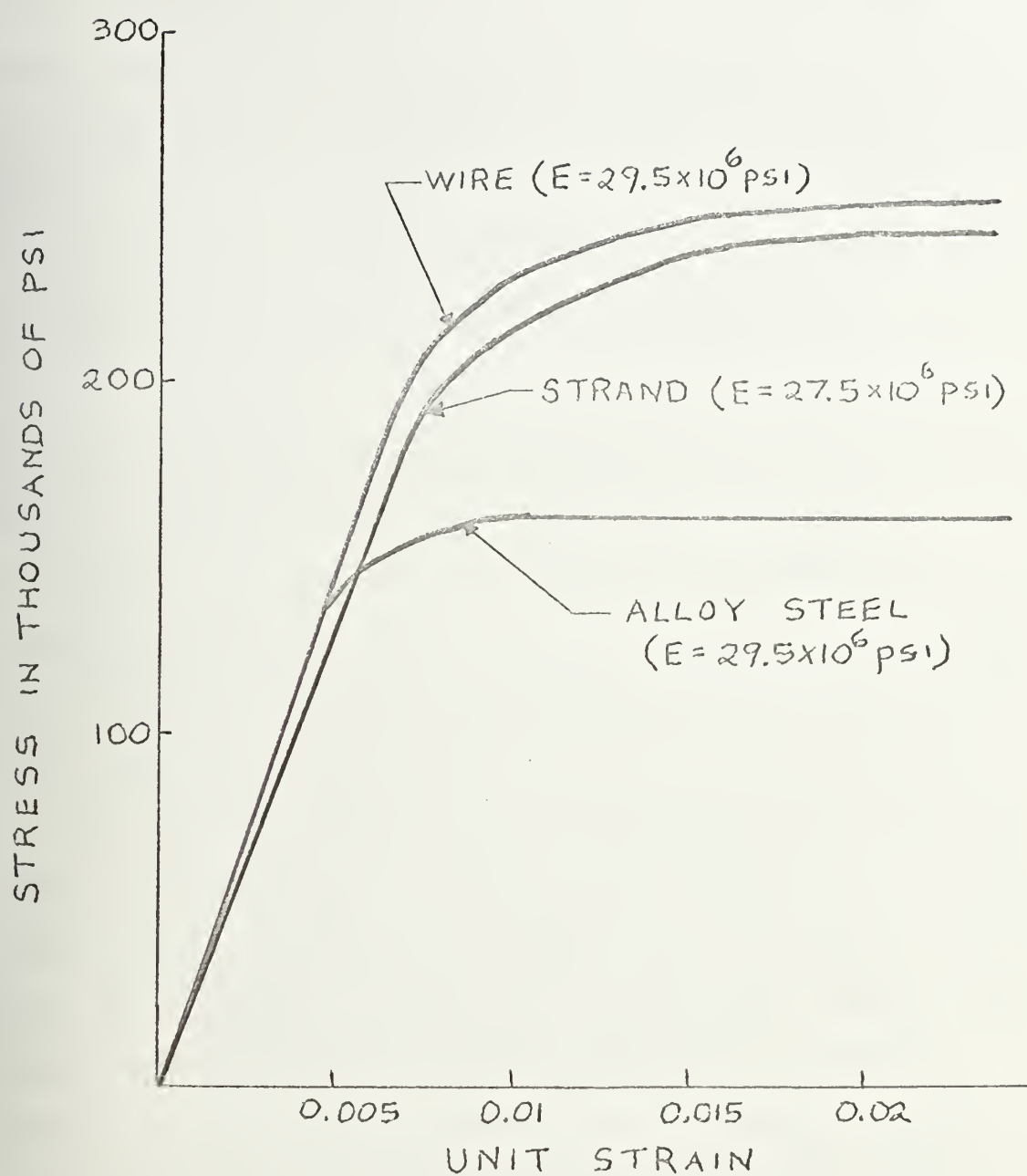


FIGURE 2  
TYPICAL STRESS-STRAIN CURVES  
FOR PRESTRESSING STEELS



between the stress-strain relationship of prestressing steels and those of ordinary concrete reinforcement usually used (25): (a) high tensile strength of prestressing steel; (b) absence of a well-defined yield point on the high-strength steel curve; and (c) reduced modulus of elasticity of stranded wire (most widely used for pre-tensioned concrete).

2. Concrete. Since concrete is a heterogeneous mixture of divers and sundry components, it is inevitable that its physical properties will vary over wide ranges. For example, the modulus of elasticity of steel is approximately  $29 \times 10^6$  psi regardless of its type. On the other hand, the modulus of elasticity of concrete may vary from 1.5 to  $7.0 \times 10^6$  psi.

The typical stress-strain diagram of concrete, as shown in Figure 3, is a smooth curve which has no proportional limit; strictly speaking, Young's modulus does not apply to concrete. Figure 4 indicates two moduli, the tangent modulus and the secant modulus. Of greater significance for design purposes is the secant modulus at design stress. It is defined as the slope of the line joining zero stress and the design stress on the stress-strain diagram. For higher strength concretes, as the concrete modulus of elasticity ( $E_c$ ) increases, the stress-strain curve approaches a straight line relationship



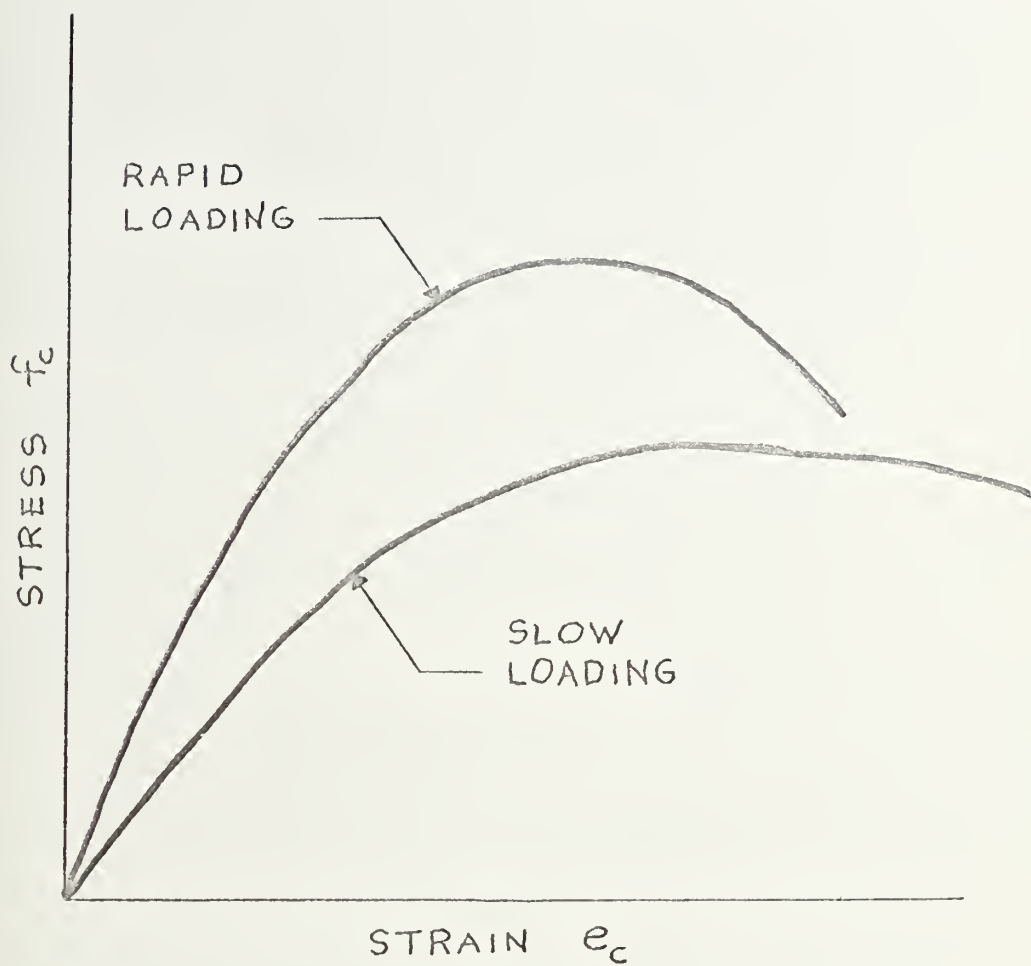


FIGURE 3  
TYPICAL STRESS-STRAIN CURVE FOR CONCRETE





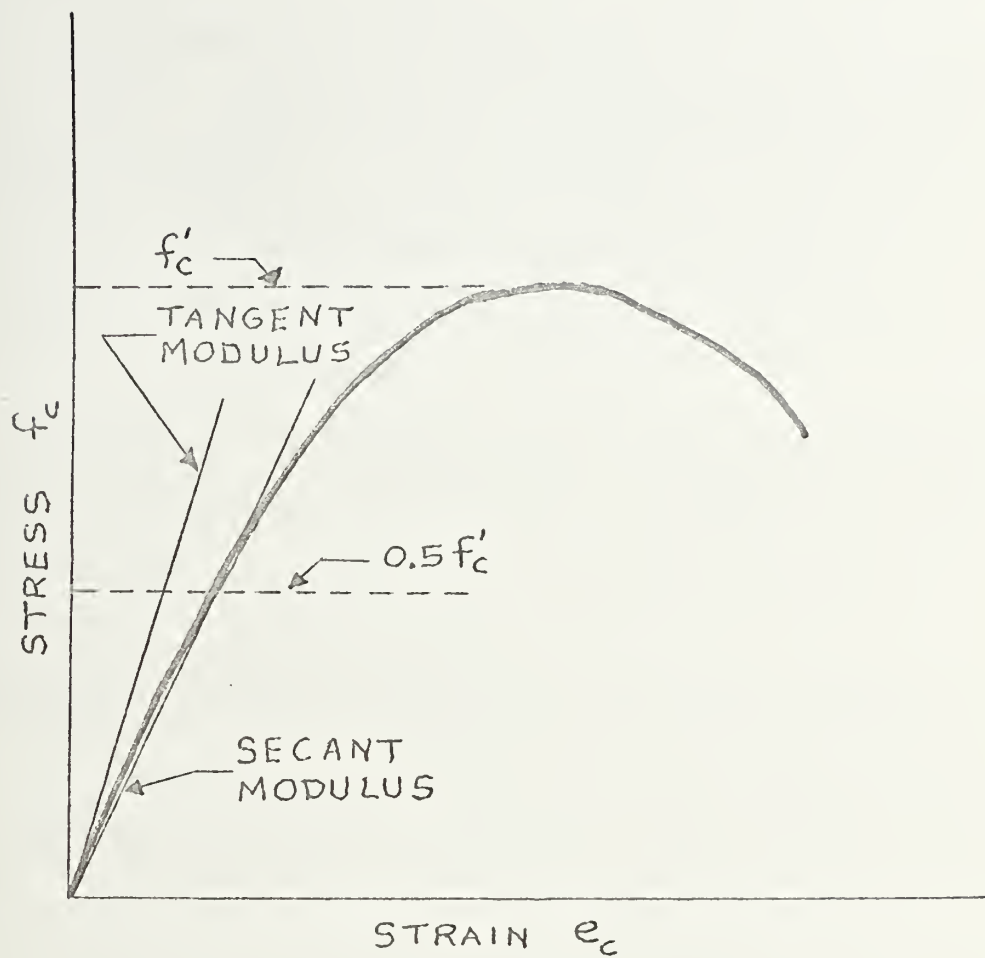


FIGURE 4

TANGENT AND SECANT CONCRETE MODULII OF ELASTICITY



for a larger range of stresses so that the two moduli become nearly identical. Such is the case for concrete encountered in prestressed concretes.

A term that is characteristic of reinforced concrete is the modular ratio ( $n$ ). It is defined as the ratio of steel modulus of elasticity ( $E_s$ ) to concrete modulus of elasticity ( $E_c$ ). Thus,

$$n = E_s / E_c \quad (1)$$

It can be shown that the stress in the steel reinforcement ( $f_s$ ) is greater than the stress in the concrete ( $f_c$ ) by a factor equal to the modular ratio. The proof is as follows:

(a) Assume that the steel reinforcing rods and concrete have the same strain; this is true since both components are physically constrained to move as a single unit and thus undergo the same deflections at their interfaces.

In other words,

$$e_c = e_s \quad (2)$$

(b) Assume that both materials are not stressed above their proportional limits and that Hooke's Law applies to both (although concrete does not strictly follow Hooke's Law). Then,

$$\begin{aligned} \text{and} \quad f_c &= e_c E_c \\ f_s &= e_s E_s \end{aligned} \quad (3)$$

Re-writing equations (3) results in:



$$\begin{aligned} \text{and} \quad e_c &= f_c/E_c \\ e_s &= f_s/E_s \end{aligned}$$

and substituting in equation (2) yields:

$$f_c/E_c = f_s/E_s$$

Thus,

$$f_s = f_c E_s / E_c = n f_c \quad (4)$$

A secant modulus determined at one-half the specified compressive strength of concrete ( $0.5f'_c$ ) is normally used for design purposes. Several formulae have been proposed to estimate the modulus, among which the following are well known:

$$\text{ACI 318-71 Code: } E_c = 33(f'_c)^{0.5} W^{1.5} \quad (5)$$

$$\text{Jensen's Equation: } E_c = (6 \times 10^6 f'_c) / (f'_c + 2000) \quad (6)$$

$$\text{Parson's Equation: } E_c = 12,000(f'_c)^{0.7} \quad (7)$$

$$\text{Lyse's Equation: } E_c = 1.8 \times 10^6 + 460f'_c \quad (8)$$

where  $W$  = unit weight of concrete (pcf).

Equations (6), (7) and (8) are reasonably accurate for average concretes of average materials, although predicted moduli tend to be too high when  $f'_c$  exceeds 5000 psi. Equation (5) has been adopted by the American Concrete Institute to provide a single equation suitable both for normal and lightweight concretes throughout the presently utilized range of compressive strengths (13). For simplicity of calculation, equation (5) can be re-written as

$$E_c = 33(W^3 f'_c)^{0.5} \quad (5a)$$



and is valid for values of  $W$  between 90 and 155 pcf.

Two other properties with particular significance to concrete are (a) creep and (b) shrinkage.

(a) The initial strain in concrete on first loading at low unit stresses is nearly elastic, but this strain increases with time even under constant load. This increased deformation with time is called creep. Factors tending to increase creep include loading at an early age, using concrete with a high water-cement ratio, and exposing the concrete to drying conditions.

(b) Among the more important factors that influence drying shrinkage are the water-cement ratio of the paste, the amount of paste in the concrete, the mix proportions, the curing conditions, the length of the drying period, the humidity of the surrounding air, the maximum size and composition of the aggregate, and the size and shape of the concrete mass (30). The most important single factor affecting shrinkage is the amount of water placed in the mix per unit volume of concrete. The shrinkage of concrete is mainly due to the evaporation of the mixing water. Since moisture is never uniformly withdrawn throughout the concrete, the differential moisture changes cause differential shrinkage tendencies and internal stresses. In plain concrete completely unrestrained against contraction, a uniform shrinkage would cause no stress; with reinforced concrete, however, even uniform





shrinkage causes stresses, namely, compression in the steel and tension in the concrete.

Creep and shrinkage present a disadvantage and an advantage to post-tensioned reinforced concrete. They reduce the prestressing force. On the other side of the ledger, however, creep prevents concrete from being a brittle material which would shatter when subjected to a high concentration of stress at any point; creep allows the high stress at one point to flow to nearby areas, thus relieving the concentrations. The advantage of this stress relieving outweighs the disadvantage of prestress loss, provided the creep does not produce undesirable camber, deflection, or stresses in fully or partially restrained members (25).

Because of elastic shortening, creep and shrinkage of concrete, and stress-relaxation (creep) of steel, the initial prestressing force gradually diminishes. This decrease is termed loss of prestress. Losses in post-tensioned members fall into three groups: losses occurring during the process of tensioning (due to friction within the duct), the loss occurring at the stage of anchoring (due to slip of the tendons), and losses arising subsequently (due to creep, shrinkage, etc.). The magnitude of prestress loss does not significantly affect the ultimate capacity of a member. For post-tensioning, steel stress losses may be assumed to be



25,000 psi or 15 percent of the prestressing steel ultimate strength, whichever is less.

### C. Permissible Stresses

Having accomplished the prerequisite step of presenting the various engineering properties involved, the maximum allowable stresses in the three components of post-tensioned reinforced concrete must next be determined.

1. Steel. Once again disposing of the more familiar (and less problematical) material first, let us consider steel. Stresses in the steel reinforcement should be less than or equal to the specified yield strength of nonprestressed reinforcement ( $f_y$ ), or about 32,000 psi if mild steel is used. Theoretically, stresses in the post-tensioning tendons should not exceed the ultimate strength of prestressing steel ( $f_{pu}$ ), where  $f_{pu}$  (not to be confused with  $f_y$ ) of HY-80 is around 100,000 psi. In practice, however, steel stresses are limited to provide a margin of safety on the steel, and also to avoid excessive stress-relaxation due to creep of the steel. In this way, the risk of permanent deformation from overload is also reduced. The British Standards Institution (26) specifies that the initial tensile stress should not exceed 70 percent of the ultimate strength, nor 85 percent of the 0.2 percent



proof stress, whichever is less. The American counterpart (13) to this reference limits prestressing steel stresses to  $0.80f_{pu}$  due to jacking, and  $0.70f_{pu}$  immediately after anchoring of the post-tensioning tendons. Gerwick (23) adopts the less conservative figure of  $0.85f_{pu}$ .

2. Concrete. The determination of permissible stresses in concrete is not as straightforward. Concrete strength is dependent upon many factors and fluctuates accordingly; allowable stress as a percentage of ultimate strength will thus vary proportionately with strength. Several sources present differing degrees of agreement.

Depending on the mix (especially the water-cement ratio) and the time and quality of curing, compressive strengths of concrete can be obtained up to 10,000 psi or more. Commercial production of concrete with ordinary aggregates is usually in the 3,000 to 7,000 psi range (15). In land-based buildings, concrete beams average 3,000 to 3,500 psi; prestressed concrete averages about twice these values (27). Another reference specifies that compressive strength for prestressed concrete should not be less than 4,500 psi (25). The British Standards Institution prescribes four grades of concrete specified for prestressed use (26); compressive strength varies from 30 to 50 Newtons per squared millimeter ( $N/mm^2$ ), or



(see Appendix A) from 4,350 to 7,250 psi. After aging for one year, these same compressive strengths have increased to a range varying from 5,365 to 10,150 psi.

As for permissible compressive stress, the British Code (26) allows a value between 40 and 50 percent of  $f'_c$ . The ACI Code (13) permits a value of  $0.6f'_c$  before losses, but at service loads (after losses) it allows only  $0.45f'_c$ . Similarly, Gerwick (23) also recommends a maximum permissible compressive stress of  $0.45f'_c$ . Interestingly enough, the specifications for the World War II concrete ships (with  $f'_c = 5,000$  psi) allowed a maximum compressive stress in the concrete of 2,250 psi, or exactly  $0.45f'_c$  (12).

The one obvious point of consensus, however, is the permissible tensile stress in traditional reinforced concrete: in accordance with standard practice, concrete tensile strength is neglected in reinforced concrete design calculations. Nevertheless, tensile strength becomes important in prestressed concrete. Since the prestressing force is of such magnitude that tensile stresses in the precompressed zone do not occur from creep and shrinkage alone, small tensile stresses are usually permitted in prestressed concrete under working loads.

Various equations have been proposed to relate modulus of rupture (an index of tensile strength) to compressive strength. One of the higher values for the







tensile strength of concrete is 10 to 15 percent of the compression strength, occasionally 20 percent (15).

Another range that is utilized is 7 to 11 percent (27).

The reinforced concrete ships of World War II, even though concrete tension was neglected in design, had a modulus of rupture ( $f_r$ ) varying from 600 to 800 psi, or 12 to 16 percent of the compressive strength (12). It was due to this relatively high concrete tensile strength that the formation of minute cracks in high tension regions was minimized.

The 1959 edition of reference (26) adopted a formula relating permissible concrete tensile stress to compressive stress ( $f_r = f'_c/20 + 100$ ). In the current version, however, stress limitations are based on cracking considerations, a topic to be deferred until Chapter III. The most frequently encountered equation is:

$$f_r = 7.5(f'_c)^{0.5} \quad (9)$$

whereas the formula adopted by the American Concrete Institute is:

$$f_r = 6.0(f'_c)^{0.5} \quad (10)$$

This permissible stress may be exceeded when it is shown experimentally or analytically that performance will not be impaired (13).

Figure 5 is a composite graph of several of the aforementioned relationships. Permissible tensile stresses are indicated by the crosshatched region within



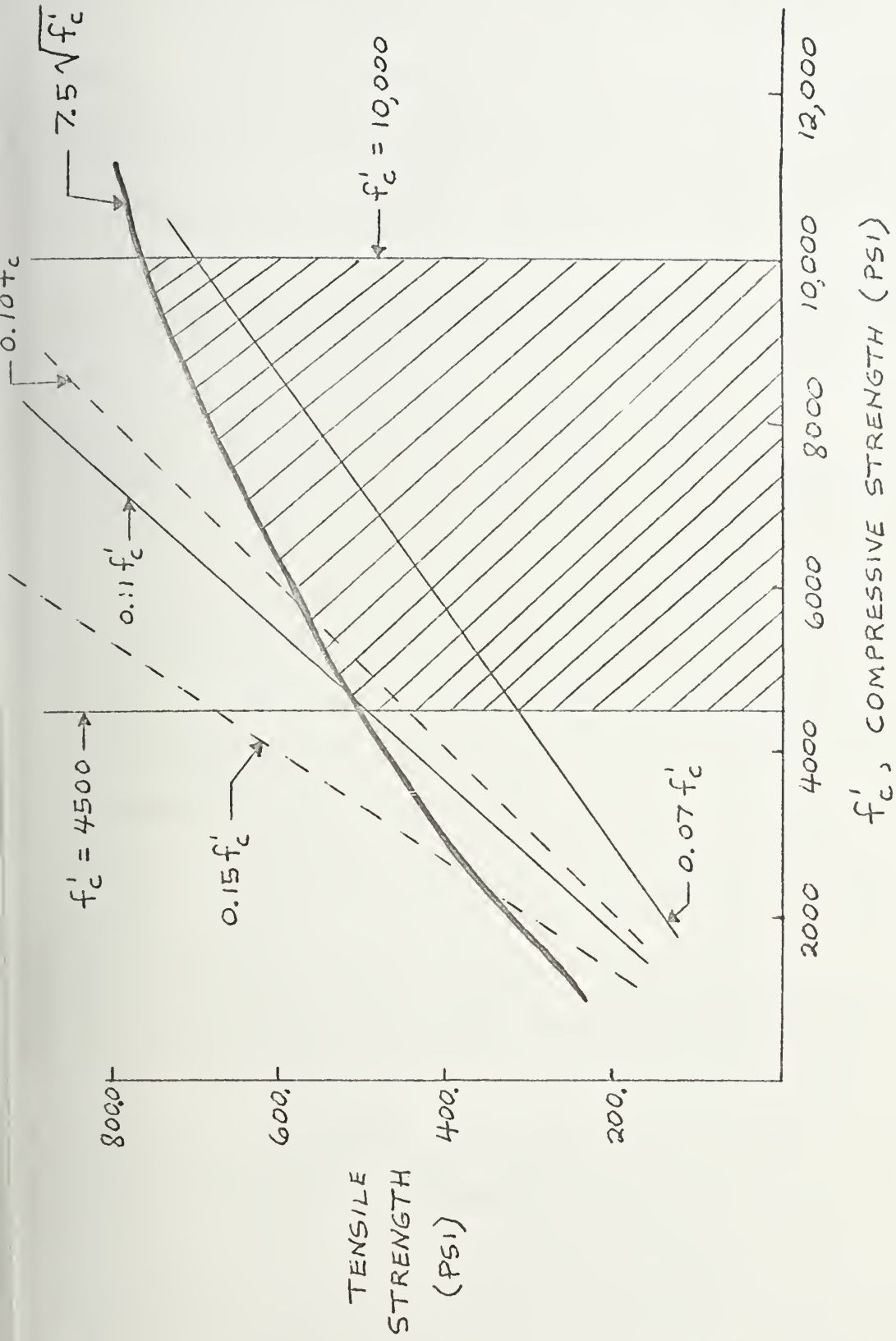


FIGURE 5  
PERMISSIBLE TENSILE STRESS IN CONCRETE



the typical concrete compressive strength range of 4,500 to 10,000 psi. Notice that the curve representing equation (9) is rather conservative (as compared with the other curves) in the range indicated.

#### D. Material Selection -- Theoretical Aspects

One of the first chronological steps in considering the feasibility of applying post-tensioned reinforced concrete to ship construction is that of material selection. Preliminary decisions to be made include the determination of the composition of all components in the tertiary system, namely: the type of steel for reinforcing rods, the type of steel for post-tensioned tendons, and the type of concrete. (Steel has been traditionally used as reinforcement rather than other materials, such as aluminum or titanium, for the simple reason of economics, namely, cost and availability. Some materials, particularly copper and aluminum, have been avoided because of the possibility of electrolytic corrosion and hydrogen embrittlement.)

The material selection process, appearing in this and the following section, will be divided into two aspects -- theoretical and economic. A preliminary selection will be made solely on technical considerations; and after the economic factors are weighed, a final decision will be made: either supporting or revising the



original choice.

1. Steel. Alternatives to choose from are:

(a) low carbon, or mild, steel, with a tensile yield strength ( $f_y$ ) of about 32,000 psi; (b) high-tensile-strength (HTS) steel, with a yield strength of about 50,000 psi; (c) HY-80, with a minimum tensile yield strength of 80,000 psi; (d) HY-100; and (e) HY-130 and other higher strength steels.

Material selection is basically a trade-off study, to determine which of various material characteristics are most suitable. Some of the more important properties materials must possess and which merit consideration are (28): strength-to-weight ratio, fracture toughness, fatigue strength, corrosion resistance, ease of fabrication, weldability, durability, maintainability, general availability, and cost.

In dealing with concrete ships, the weight factor deserves paramount attention, since the inherent disadvantage of concrete vessels is low deadweight-displacement ratio due to notoriously heavy structure. Thus, selection of a high strength steel (e.g., HY-80) would be logical, since steel cross-sectional area, and hence weight, decreases as steel yield strength increases. (Higher strength steels, such as HY-100 and above, are eliminated at this preliminary stage from further





consideration due to high cost, fabrication and/or joining problems, low ductility, relatively low fatigue life, and poor corrosion resistance (29)). This choice (HY-80) is more appropriate for the post-tensioned tendons than the reinforcing rods, as the purpose of the tendons is to induce compression in the concrete; furthermore, the greater the tensile strength of the tendon, the greater level of prestress (post-tensioning) can be applied (although this is also a function of the number of tendons).

This last statement implies that perhaps the higher strength steels (HY-100 and above) should not have been so hastily discarded, since more than 80,000 psi prestress may be desirable. Hence, final judgment will be deferred until the next section.

In addition to weight, cost certainly deserves to be a prime consideration. Cost reduction can be best applied to the selection of steel for reinforcing rods, since the largest (in total-number-of-rods sense) steel component in a post-tensioned reinforced concrete section is the reinforcement. Thus, in order to reduce cost, reinforcing rods should be composed of a lesser strength steel (e.g., mild steel). This, too, is a logical decision for another reason: since the reinforcement will be in compression (due to the post-tensioned tendons inducing compression in the concrete and hence in the



reinforcing rods), a high tensile strength will not be required to reduce tension in the concrete; under loading conditions, any tendency for tensile stress to develop will merely negate the applied prestress.

2. Concrete. The selection of concrete entails the consideration of factors somewhat different from those in choosing steel. Several of the properties listed previously are all inherent advantages of concrete: corrosion resistant, ease of fabrication, maintainability, availability, and low cost. Obviously, consideration of only these factors would be somewhat limited.

Other factors, integral aspects in the selection of concrete, are: type and size of aggregate, porosity, density, compressive strength, and water-cement ratio.

Concrete is a heterogeneous mixture of sand, gravel, cement and water, plus air, salts, fine inert materials, and other additives or admixtures which modify the characteristics of concrete. In brief, concrete for reinforced concrete consists of aggregate bonded together in a paste made from portland cement and water. The aggregate occupies roughly three-quarters of the entire volume of an average concrete; the remaining one-quarter is filled with cement paste and air voids (27).

It may be said that the properties of concrete are studied primarily for the purpose of mix design.



Mix design can be defined as the process of selecting suitable ingredients of concrete and determining their relative quantities with the object of producing as economically as possible concrete of certain minimum properties, notably strength and durability (31).

There are several methods of mix design, although in principle they are all basically similar. The traditional British method is summarized below (32):

(1) To satisfy a specified compressive strength and durability, a value of water-cement ratio is chosen, from data given, for the appropriate age and type of portland cement (see Figure 6).

(2) The level of workability of the concrete required is chosen, being based primarily on the degree of mix wetness desired.

(3) Tables are provided relating aggregate-cement ratio, workability, and water-cement ratio for aggregates of different particle shape and maximum particle size.

Therefore, knowing the available aggregates and having fixed the workability and water-cement ratio, the aggregate-cement ratio can be selected.

Referring to step (1), factors which affect compressive strength are water-cement ratio, cement type, aggregate type, and aggregate-cement ratio. Figure 6 (31) shows the relation between compressive strength and water-cement ratio for different cement types at various



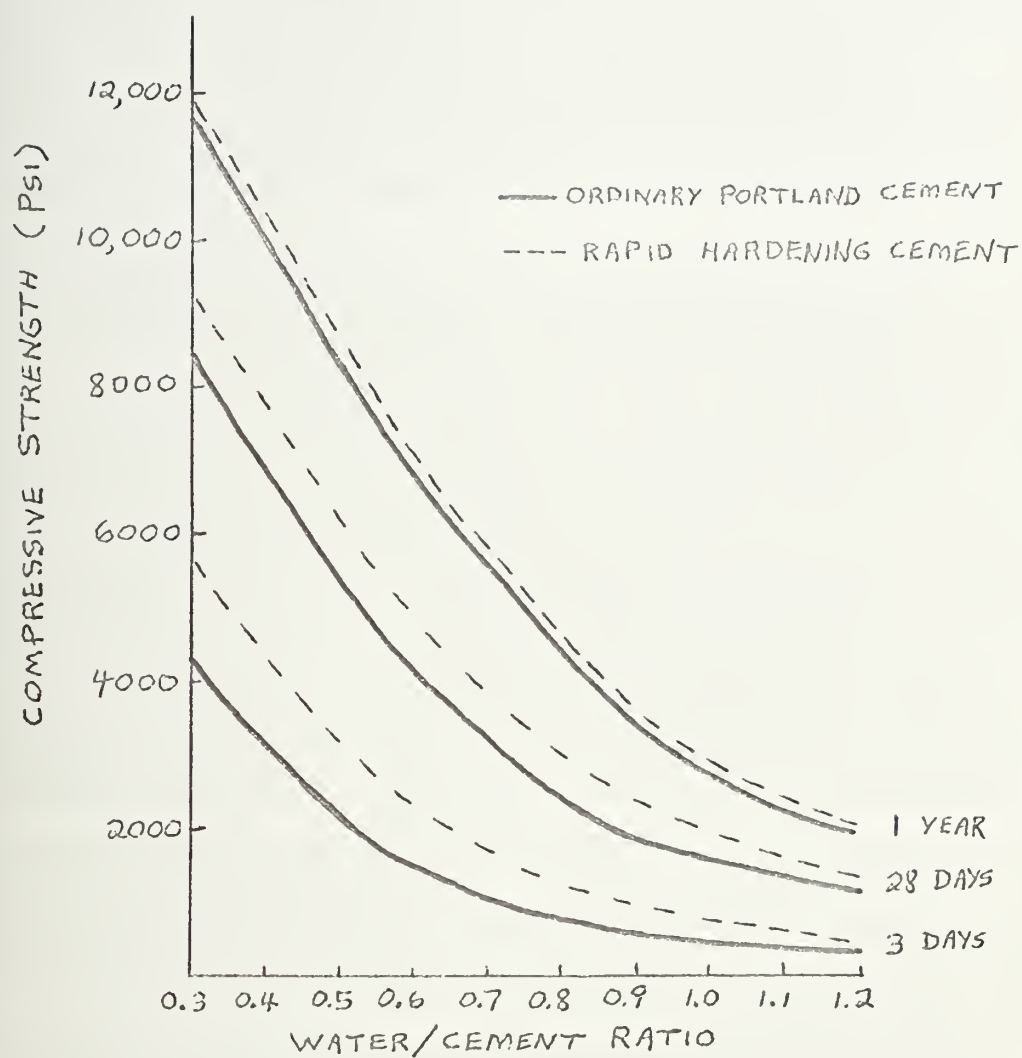


FIGURE 6

RELATION BETWEEN CONCRETE COMPRESSIVE STRENGTH  
AND WATER-CEMENT RATIO





ages. In essence, a lower water-cement ratio yields a greater compressive strength, and a Type III portland cement attains its strength sooner than ordinary Type I. (Note: The ratio of water to cement is expressed in U.S. gallons of water per 94-pound sack of cement.) Table 1 gives the five types of portland cement, as well as their approximate relative strengths, with normal portland cement used as the basis for comparison (33). The American Concrete Institute (ACI) specifies (13) that when concrete made with normal weight aggregate is intended to be watertight, it must have a maximum water-cement ratio of 0.48 for exposure to fresh water and 0.44 for exposure to sea water.

Aggregates, the next consideration enumerated above, should be selected with regard to the following (14): (a) strength (a strong aggregate, e.g., granite, makes for a strong concrete); (b) size (must be small enough to be worked in between and around all reinforcements); (c) particle shape (rounded aggregates require the smallest water-cement ratio); (d) surface texture (a rough surface gives a stronger concrete); (e) grading; and (f) cost.

Another consideration in selecting concrete is the water-cement ratio. The quantity of water relative to that of the cement is the most important item in determining concrete strength. In general, the lower the



TABLE 1

## TYPES AND STRENGTHS OF PORTLAND CEMENT

<u>Type</u>	Portland Cement <u>Name</u>	Compressive Strength (percent of Type I strength)		
		<u>3 days</u>	<u>28 days</u>	<u>3 months</u>
I	Normal	100	100	100
II	Modified	80	85	100
III	High-early- strength	190	130	115
IV	Low-heat	50	65	90
V	Sulfate- resistant	65	65	85



water-cement ratio, the greater the strength and water-tightness. Also, low permeability (low porosity or high water-tightness) is associated with high strength and high resistance to weathering. Thus, the three factors of strength, porosity, and water-cement ratio are inter-related.

Density, another property for consideration, depends on the grading, shape and maximum size of the aggregates, as well as the water-cement ratio. Actually, the size and grading of aggregates have an important influence on the water-cement ratio itself. So, in fact, all the factors mentioned so far are interrelated.

In reinforced concrete, the maximum size of aggregate that can be used is governed by the width of the section and, as just mentioned, the spacing of the reinforcement. With this proviso, it has generally been considered desirable to use as large a maximum size of aggregate as possible. However, it has been demonstrated (31) that the improvement in concrete properties with an increase in aggregate size does not extend beyond about 1-1/2 inches. Above the 1-1/2 inch maximum size, the gain in strength due to the reduced water requirement is offset by the detrimental effects of lower bond area and of discontinuities introduced by the very large particles. Therefore, from the point of view of strength, there is no advantage in using aggregate with a maximum size



greater than about 1-1/2 inch. Table 2(a) presents the general range in unit weight of common natural aggregates (27), while Table 2(b) summarizes the basic aggregates and their approximate 28-day compressive strength (3).

For a given water-cement ratio, the higher the aggregate-cement ratio the higher the compressive strength tends to be, for mixes of the same aggregate type. Thus, a leaner mix will give a higher strength than a rich one.

So far only the requirements for the concrete to be satisfactory in the hardened state have been considered -- step (1). However, properties when being handled and placed are equally important; one essential at this stage is a satisfactory workability -- step (2).

The workability that is considered desirable depends on two factors. The first of these is the size of the section to be concreted and the amount and spacing of reinforcement; the second is the method of compaction used (e.g., for very low workability -- too dry a mix -- intensive vibration is required, since it cannot be sufficiently worked by hand; for high workability -- too wet a mix -- vibration should not be used, as segregation may result).

The most important influences affecting workability are water content of the mix, aggregate properties, and cement content. For given materials and proportions,





TABLE 2  
AGGREGATES COMMONLY USED IN CONCRETE

(a) Weight of Aggregates

<u>Material</u>	<u>Unit Weight (pcf)</u>
sand	95 to 115
gravel: 3/4 inch	99 to 107
1-1/2 inch	104 to 112
crushed stone: 3/4 inch	95 to 103
1-1/2 inch	100 to 108

(b) Strength of Aggregates

<u>Aggregate type</u>	<u>Concrete Density (pcf)</u>	<u>Maximum 28-day Compressive Strength (psi)</u>
lightweight	100	8,000-10,000
sand and gravel, or crushed stone	150	12,000-15,000
heavy aggregates	200-300	9,000-11,000



the workability increases with increase in water content per cubic yard of concrete. If the water content and the other mix proportions are fixed, workability is governed by the maximum size of aggregate, its grading, shape and texture. As the aggregate size decreases, more water must be added to maintain workability, and the corresponding aggregate-cement ratio increases. As an aggregate progresses in shape from angular to irregular to rounded, the aggregate-cement ratio also increases. Grading refers not only to the percentage of sand, but also to the overall range of particle sizes; in general, an increase in sand content at the low end of the workability range may cause a more noticeable drop in workability than at the higher end of the range. The final influence on workability, cement content, is negligible and may be ignored for normal mixes (when cement content is less than  $24 \text{ lb/ft}^3$ ); in very rich mixes, however, (richer than 28 lb of cement per cubic foot of concrete), there is an apparent drop in workability (32).

It must be noted that predicting the influence of mix proportions on workability requires care, since of the three factors, namely, water-cement ratio, aggregate-cement ratio, and water content, only two are independent. For instance, if the aggregate-cement ratio is reduced, but the water-cement ratio is kept constant, the water



content increases, and consequently the workability also increases. If, on the other hand, the water content is kept constant when the aggregate-cement ratio is reduced, then the water-cement ratio decreases but workability is not seriously affected.

All the factors considered up to now, including water-cement ratio, will determine between them the aggregate-cement ratio of the mix -- step (3). The choice of the aggregate-cement ratio is made either on the personal experience of the mix designer or alternatively from charts and tables prepared from comprehensive laboratory tests. The latter course is frequently followed, use being made of tables of Road Note No. 4 (32); these tables are reproduced in reference (31). As an example, Table 3 presents the aggregate-cement ratio (by weight) required to give four degrees of workability with different gradings of rounded, 3/4 inch aggregates. As the grading number increases from 1 to 4, the aggregate grading varies from coarse to fine. Knowing the water-cement ratio and the aggregate-cement ratio, there is little difficulty in determining the proportions of cement, water, and aggregate -- the major components of concrete.

One other consideration, endemic to concrete ships, is the minimization of weight. So overriding was this factor in the World War II concrete ship program that



TABLE 3

AGGREGATE-CEMENT RATIO (BY WEIGHT) REQUIRED TO GIVE FOUR DEGREES OF WORKABILITY  
WITH DIFFERENT GRADINGS FOR ROUNDED 3/4 INCH AGGREGATE

Degree of workability	Very low				Low				Medium				High			
	1	2	3	4	1	2	3	4	1	2	3	4	1	2	3	4
Grading																
Water- cement ratio																
0.35	4.5	4.5	3.5	3.2	3.8	3.6	3.2	3.1	3.1	3.0	2.8	2.7	2.8	2.8	2.6	2.5
0.40	6.6	6.3	5.3	4.5	5.3	5.1	4.5	4.1	4.2	4.2	3.9	3.7	3.6	3.7	3.5	3.3
0.45	8.0	7.7	6.7	5.8	6.9	6.6	5.9	5.1	5.3	5.3	5.0	4.5	4.6	4.8	4.5	4.1
0.50	-	-	8.0	7.0	8.2	8.0	7.0	6.0	6.3	6.3	5.9	5.4	5.5	5.7	5.3	4.8
0.55	-	-	-	8.1	-	-	8.2	6.9	7.3	7.3	7.4	6.4	6.3	6.5	6.1	5.5
0.60	-	-	-	-	-	-	-	7.7	-	-	8.0	7.2	X	7.2	6.8	6.1

- Indicates that the mix was outside the range tested.

X Indicates that the mix would segregate.





heavy aggregates (200 to 300 pcf) and natural sand and gravel aggregates (150 pcf) were not even considered. Lightweight aggregates (110 pcf) were used solely to lighten the hull structure, despite its disadvantages.

Some of the disadvantages of lightweight aggregate concrete just alluded to are: lightweight aggregates are relatively weak (27), and tensile strength is lower than ordinary weight concrete in many cases (15); lightweight aggregates are more costly, they present greater difficulty in handling, mixing, and controlling the concrete mixes, and they are more porous (12). All concretes made with lightweight aggregate exhibit a higher moisture movement than is the case with normal weight concrete. Many lightweight aggregates are angular and have a rough surface, producing harsh mixes and hence decreasing workability. If lightweight aggregate is to be used in reinforced concrete, a greater cover will be required than if ordinary aggregates were employed (31). Creep and drying shrinkage (the latter a cause of cracking) are likely to be perhaps twice the magnitude of that of comparable normal concrete (32). It is, thus, doubtful whether the weight advantage of lightweight aggregate outweighs all the disadvantages enumerated here. Furthermore, even a  $33\frac{1}{3}$  percent savings in weight by using 100 pcf vice 150 pcf aggregates would be nullified by a corresponding increase in cover thickness from say,



1-1/2 to 2 inches. (The figures are arbitrary, but they emphasize the point.)

Thus, a preliminary selection of concrete would indicate usage of an ordinary weight (150 pcf) aggregate, Type III portland cement for its high-early-strength, and a low (about 0.45) water-cement ratio.

The definition of mix design given at the beginning of this section stressed two points: that the concrete is to have certain specified minimum properties, and that it is to be produced as economically as possible. The following section will consider the economic aspects of material selection.

#### E. Material Selection -- Economic Aspects

Having arrived at a quasi-theoretical determination of material selection, it is necessary to approach the subject from a practical standpoint. In other words, what materials are physically available (i.e., "off-the-shelf")? And which are the optimum economically-speaking?

1. Steel. In general, the price of reinforcing steel depends upon the quantity in pounds purchased, the size of the bars, and the number of bends and hooks. The base price is the price per 100 pounds of reinforcing bars. The size of the bars available for ordinary steel reinforcement are indicated in Table 4 (34).



TABLE 4

## SIZE AND WEIGHT OF ORDINARY REINFORCING BARS

<u>Bar number</u>	<u>Diameter (in)</u>	<u>Area (in<sup>2</sup>)</u>	<u>Weight (lb/ft)</u>
3	3/8	0.110	0.376
4	1/2	0.196	0.668
5	5/8	0.307	1.043
6	3/4	0.442	1.502
7	7/8	0.601	2.044
8	1	0.785	2.670
9	1-1/8	1.000	3.400
10	1-1/4	1.2656	4.300
11	1-3/8	1.5625	5.310
14	1-3/4	2.405	8.180
18	2-1/4	3.976	13.520



It is trivial, yet significant, to point out that steel reinforcing bars cost more per unit weight than structural steel (due to fabrication and formation). For example, a 20-cities' average cost of structural steel (average 3 mills) in September 1974 was \$10.80 per hundredweight (cwt); the cost of reinforcing bars per cwt at the same time was \$18.83. To indicate the effect of inflation, the percentage change of these two prices from September 1973 was + 27.1 and + 84.4, respectively (35).

As a comparison with 1974 prices in Europe (36), the same reinforcing steel bars cost 179 Pounds per metric ton in England (vice 110 Pounds in 1973), and 845 Deutschemarks per metric ton in West Germany (vice 700 Deutschemarks in 1973). With the latest exchange rates of 2.55 Deutschemarks per U.S. Dollar and 0.425 Pounds per U.S. Dollar, these figures translate into \$421 per metric ton in England and \$331 per metric ton in West Germany; or, compared with the 1974 U.S. price of \$18.83 per cwt, the English cost is \$19.10 per cwt and the West German cost is only \$15 per cwt. Interestingly, the U.S., English and West German prices per cwt in 1973 were \$10.21, \$11.74, and \$12.43, respectively.

The \$18.83 per cwt average quotation is for ASTM A-615 Grade 40 reinforcing bars, with a minimum order of 20 to 25 tons. The price varies from a low of \$14.50 in





Los Angeles to a high of \$25 in Pittsburgh (Boston is \$21); a 6 percent sales tax in California and Pennsylvania is not included.

Extra orders (i.e., over the minimum) average \$0.87 per cwt for bar size numbers 6 through 11, \$1.10 per cwt for number 5, \$2 per cwt for number 4, and \$2.70 per cwt for number 3. Charges for extra orders of different quality bars are: \$0.38 per cwt for A-615 Grade 60, and \$1.13 per cwt for A-615 Grade 75 (37). The three grades in which reinforcing bars are commercially available (40, 60, and 75) have minimum yield strengths of 40,000 psi, 60,000 psi and 75,000 psi, respectively. Reinforcing bars of Grades 40 and 60 are available in all bar sizes shown in Table 4, whereas Grade 75 comes only in size numbers 11, 14 and 18 (38).

It thus appears from available price quotations that, in practice, only one grade of steel is used for reinforcing bars in the majority of cases. This is buttressed by the fact that the 1971 ACI Code is intended specifically for the use of standard Grade 60 reinforcement ( $f_s = 36\text{ksi}$ ), although provision is also made for the use of Grades 40 and 75 (39). The latter are available under the reference ASTM specifications, up to a maximum limit of 80 ksi yield strength, except for prestressing steels.

The price differential for the different available



grades of reinforcing steel is actually not very significant. Taking A-615 Grade 60 as the standard, its cost is  $\$18.83 + \$0.38 = \$19.21$  per cwt. The most expensive commercial reinforcement, A-615 Grade 75, costs  $\$19.96$  per cwt, or just 3.9 percent more than Grade 60. The least expensive commercial reinforcement, A-615 Grade 40, costs  $\$18.83$  per cwt, or only 1.9 percent less than Grade 60. Hence, varying the grade of steel reinforcing bars will not have a tremendous economic effect.

A significant conclusion, for steel reinforcing bars, is that the greatest price differential is not for the various qualities of steel, but rather for the size of the bars. Hence, the selection of mild steel (Grade 40) is a valid and logical choice for reinforcing steel, confirming the preceding section.

For post-tensioned tendons, the three types of steel used are bars, strands, and wires. Bars vary from  $3/4$  inch to  $1-3/8$  inch diameter; indeed, the leading importer (40) of prestressed concrete strand and wire sells post-tensioned steel bars in four sizes: 18 mm (0.71 in), 24 mm, 27 mm, and 33 mm (1.3 in). Tendons with up to 168 wires are available. Table 5 summarizes the costs, both material and labor, of various tendons available for post-tensioning (41). Labor cost consists of preparation and placing cables, stressing cables, and



TABLE 5

## COST OF STEEL USED FOR POST-TENSIONING TENDONS

Type of steel	Bars		Wires		Strand	
Diameter (in)	3/4	1-3/8	1/4		1/2	
Number	1	1	12-20	24-42	6	12
Force (kips)	42	143	84-140	168-294	140	298
Labor cost/lb	\$0.25	\$0.20	\$0.31	\$0.25	\$0.31	\$0.31
Prestressing steel weight (lb/ft)	1.533	5.066	2-3.35	4-7.0	3.25	6.4
Material cost/lb	\$0.35	\$0.30	\$0.55	\$0.45	\$0.55	\$0.45



grouting; labor cost per pound goes down as the size and length of the tendon increases. The primary economic consideration is the cost per Kip (1,000 psi) for the member.

From an economic viewpoint, it can be seen from Table 5 that bars are far cheaper than both wires and strands for post-tensioning tendons, even though labor costs are similar. In comparison with ordinary reinforcing bars (\$18.83 per cwt), however, post-tensioning tendons (\$30 to \$35 per cwt) are considerably more expensive.

Thus, as predicted in the preceding section, a high strength steel bar is the optimum choice for the tendon; as also suspected, an even higher strength bar (i.e., 143,000 psi) appears to be a better selection. (Note, however, the increased weight as indicated in Table 5.)

2. Concrete. The price of concrete depends, in general, upon the type of aggregate and cement. The cost of portland cement seems to be rather standard, regardless of the variety (42): the 20-cities' average cost of portland cement in September 1974 was \$32.25 per ton, ranging from \$30.20 in Atlanta to \$37.40 in Boston. Since the price differential between Types I and III portland cement is negligible, Type III should be





selected for post-tensioned work due to its high-early-strength. The average 1974 cost of portland cement in West Germany was 106 Deutschemarks per metric ton (\$37.70 per ton), and was only 11.17 Pounds per metric ton (\$23.84 per ton) in England.

As for aggregates, Table 6 summarizes the 20-cities' average costs of sand, gravel (3/4" and 1-1/2"), and crushed stone (3/4" and 1-1/2"). It is seen that the price differential between types and even sizes of aggregates is inconsequential.

Another way to compare prices is by looking at the cost of ready-mixed concrete at a specified compressive strength. For example, the 20-cities' average cost per cubic yard (September 1974 prices) of 3,000 psi concrete is \$23.98, ranging from \$20.60 in Detroit to \$27.95 in Baltimore. The average cost per cubic yard of 5,000 psi concrete is \$27.57, ranging from \$23.45 in St. Louis to \$33.25 in Baltimore (42).

The price can also be correlated to relative density of aggregate (i.e., heavy, medium, lightweight). The average cost per cubic yard of 3,000 psi concrete with regular heavyweight aggregates is \$23.98 (as above), with medium-weight (150 pcf) aggregates is \$25.58, and with all lightweight (110 pcf) aggregate is \$34.08. The average cost per cubic yard of 5,000 psi concrete with heavy-weight aggregates is \$27.57, with medium-weight



TABLE 6

## AVERAGE COST OF AGGREGATES

<u>Aggregate</u>	<u>Average cost per ton</u>	<u>Low cost</u>	<u>High cost</u>
sand	\$3.66	\$1.15 (Detroit)	\$5.90 (Pittsburgh)
gravel:			
3/4 inch	\$4.06	\$1.75 (Birmingham)	\$5.80 (Pittsburgh)
1-1/2 inch	\$3.89	\$1.75 (Birmingham)	\$5.80 (Pittsburgh)
crushed stone:			
3/4 inch	\$3.97	\$1.55 (St. Louis)	\$6.75 (Minneapolis)
1-1/2 inch	\$3.92	\$1.55 (St. Louis)	\$6.75 (Minneapolis)



aggregates is \$29.87, and with all lightweight aggregate is \$38.30. To determine the cost of concrete at other strengths, it is assumed that the above figures can be linearly extrapolated (41).

Thus, it can be seen that a great financial penalty will be paid if lightweight aggregates are employed; coupled with all other disadvantages of lightweight aggregate concrete mentioned in the last section, the evidence appears to be overwhelmingly in favor of selecting ordinary medium-weight (150 pcf) aggregates.

#### F. Selection of Concrete Mix for a Ship

An interesting application of the preceding two sections is to determine an appropriate concrete mix for a specific ship. The hypothetical oil tanker mentioned previously will be considered.

With the great magnitude of alternating loads experienced by a prestressed concrete ship in a seaway, materials of high strength are necessary for good performance. This is true not only for the post-tensioning steel, but also for the concrete. Although strengths of concrete in the range of 3500 to 5000 psi have been traditionally used, actual experience with concrete strengths of 6000 to 7000 psi has been very satisfactory. In fact, the Fédération Internationale de la Précontrainte (F.I.P.) has a commission investigating



the techniques and evaluating the potential of concrete in strength ranges above 12,000 psi.

The importance of using a high-strength concrete in ship construction is readily apparent. The modulus of elasticity of concrete increases approximately as the square root of the strength; thus deflection characteristics are improved. The tensile strength of concrete also increases approximately as the square root of the strength, thus improving behavior under overload conditions. As will be seen in Chapter III, a greater tensile strength reduces the likelihood of cracking -- a serious consideration for concrete ships. Another factor of especial importance to ships, and which is also increased with strength, is durability. Durability is generally proportional to strength in that the same factors that improve strength also improve durability by reducing porosity and permeability.

Concrete can be reliably produced with strengths of 7000 to 9000 psi (and even 10,000 psi), using conventional materials and techniques (43). This last phrase is important, since in order for a prestressed concrete tanker to be economically feasible (and competitive with steel tankers), materials and techniques must be in the state-of-the-art. Thus, it is not unreasonable to assume a concrete compressive strength of 7000 psi for the





hypothetical oil tanker.

Since the oil tanker is to be constructed with post-tensioned reinforced concrete, Type III portland cement is preferred. Referring to Figure 6, the required water-cement ratio for 7000 psi Type III portland cement at 28 days is 0.45. This low water-cement ratio has the added beneficial effect of yielding a mix with a high cement density and a low porosity.

The maximum size of aggregate is next chosen, based on the size of the tanker midship section and the spacing of rods. Actually, for most structural members, 3/4 inch is the optimum maximum diameter (43). It has already been shown that aggregate size has minimal influence on cost.

The proportions of sand and aggregate are then selected for workability and surface finish; so that a good finish can be readily obtained, about 40 percent sand is chosen (32). This corresponds approximately to a grading number "3" in Table 3. Using rounded aggregates (which are needed for high strength), Table 3 can finally be consulted with all the aforementioned information to yield an aggregate-cement ratio (assuming medium workability) of 5.0.

It is customary to calculate the quantities of ingredients to produce one cubic yard of concrete. Then if W, C, S, and A are the required weights of water,



cement, sand, and aggregate, respectively, the following formula results (31):

$$W/62.4 + C/d_c + S/d_s + A/d_a = 27$$

where d with the appropriate suffix represents the density of each material. Since water density is expressed in pounds per cubic foot, the total volume (1 cubic yard) has also to be expressed in cubic feet; hence the numbers 62.4 and 27, respectively.

Since  $W/C = 0.45$ ,  $W = 0.45C$ ; since the aggregate-cement ratio  $(S + A)/C = 5.0$ , and  $S = 40$  percent of  $(S + A)$ , then  $S = (0.4)(5.0)C = 2.0C$ ; since  $A = 60$  percent of  $(S + A)$ , then  $A = (0.6)(5.0)C = 3.0C$ . From Table 2(a), the average density of sand (fine aggregate) is 105 pcf, and that of 3/4 inch crushed stone (coarse aggregate) is 99 pcf; and assuming the density of cement is 196.6 pcf (31), the cement content,  $C$ , in pounds per cubic yard for the oil tanker can be found from the expression:

$$0.45C/62.4 + C/196.6 + 2.0C/105 + 3.0C/99 = 27$$

Hence,  $C = 438 \text{ lb/yd}^3$ , and the weights of the ingredients per cubic yard of concrete are:

Cement	=	438 lb
Water = $(0.45)(438)$	=	197 lb
Sand = $(2.0)(438)$	=	876 lb
3/4 inch aggregate = $(3.0)(438)$	=	<u>1,314 lb</u>
Total	=	2,825 lb



Thus, the density of concrete for the oil tanker is  $2,825/27 = 105 \text{ lb/ft}^3$ . This result is considerably below the medium-weight (150 pcf) concrete recommended in the last two sections. However, another reference (31) gives different values for aggregate densities, namely, 162 pcf for fine aggregate (sand) and 156 pcf for coarse aggregate. Carrying through the preceding calculations for these densities yields an overall concrete density of 146 pcf.

Averaging these two results (105 pcf and 146 pcf) yields a value of 125.5 pcf for the concrete density of the oil tanker. This is a compromise between the two extremes of lightweight and medium-weight concrete, and thus combines the advantages of both.



## CHAPTER III

### DESIGN CONSIDERATIONS

Implicit in the establishment of permissible stresses is the consideration of what may be dubbed the "Cardinal C's": cracking, corrosion, and cover. Sufficiently deep tensile cracking in a ship hull may result in salt water gaining access to the reinforcing rods. This would cause corrosion of the steel reinforcement and perhaps seepage into the cargo. A greater cover of concrete might generally tend to preclude tensile cracks from reaching the reinforcing bars (but, unfortunately, would also augment the size and weight of the hull). Thus, a compromise must be reached.

#### A. Cracking of Concrete

European specifications place considerable emphasis on the cracking load, requiring that no cracks be formed for a given (usually small) overload. American practice places greater emphasis on ultimate strength. Each of these methods is an attempt to provide an adequate factor of safety, the first indirect, the second direct.

The need for both working stress and ultimate strength calculations lies in the radical change in beam behavior when cracks form. Prior to cracking, the





gross area of the beam is effective; as a crack develops, all the tension from the concrete must be picked up by the steel. If the percentage of steel is small, there may be very little added capacity between cracking and failure (21). Cracking may be assumed to occur when the calculated tensile strength reaches  $7.5(f'_c)^{0.5}$ .

Before discussing the design considerations of such cracking, it will prove beneficial to comprehend the mechanisms of crack formation in concrete. A brief review of Fracture Mechanics is an appropriate starting point.

1. Fracture Mechanics. Fracture Mechanics theories all begin with the assumption of an initial flaw, which was first treated by Inglis (44). The flaw is assumed to be an elliptical hole in an infinite sheet, with the imposed stresses being applied at the external boundaries of the sheet.

Griffith (45) determined a technique for predicting the behavior of brittle materials by establishing an energy balance between the strain energy released by a given movement of an initial flaw and the irrecoverable energy required to generate the new fracture surface resulting from this crack extension. Whenever the energy released by a crack's growth exceeds the energy required, Griffith postulated that the crack would grow



in an unstable manner.

Griffith assumed that the initial flaw was a line crack of length  $2c$ . He also considered two contributions to the energy of the system: the elastic strain energy ( $U$ ), and the surface energy ( $T$ ). Griffith calculated the decrease in strain energy per unit thickness due to the formation of the crack to be (for plane stress):

$$U = \pi c^2 \sigma^2 / E \quad (11)$$

and the corresponding increase in the surface energy of the system is:

$$T = 4Sc \quad (12)$$

where  $S$  is the specific surface energy, or that energy required for the formation of unit area of fracture surface.

Griffith postulated that the system would become unstable and the crack would increase in size if the partial derivative with respect to crack length of the change in total energy ( $T - U$ ) equals zero. Applying this criterion, the critical stress for failure is:

$$\sigma_c = (2ES/\pi c)^{0.5} \quad (13)$$

Irwin (46) adopted a slightly different approach to the flaw hypothesis: he considered the stress field in the immediate vicinity of the flaw tip, and assumed the flaw to be a line crack of zero thickness. Irwin derived the stress at any point to be of the form:



$$\sigma = (EG/2\pi r)^{0.5} f(\theta) \quad (14)$$

where  $r$  is the radius from the crack tip to the point where the stress is being considered, and  $\theta$  is the angle between  $r$  and the abscissa; the quantity  $G$  is designated the "strain energy release rate" or crack extension force.

The parameter  $K$  is called the "stress intensity factor" and is defined such that:

$$G = dU/dc = \pi K^2/E \quad (15)$$

It is related only to the loading and geometry of the system, and corresponds to the strain energy derivative in the Griffith theory. Irwin designated the strain energy release rate at onset of unstable crack propagation as  $G_c$ , the critical strain energy release rate; the corresponding value of  $K$  is  $K_c$ , the critical stress intensity factor.

The final aspect of this Fracture Mechanics review in-a-nutshell is the work of Orowan (47). He observed that the physically minimum radius of curvature ( $\rho$ ) at the tip of a crack is of the same order of magnitude as the interatomic spacing ( $a$ ). The theoretical or "true" strength of the material is then equal to  $(2ES/a)^{0.5}$ . For fracture to occur, this expression must be equivalent to  $2\sigma(c/\rho)^{0.5}$ , the latter being Inglis' expression for the stress concentration due to a flaw. Thus, for



fracture:

$$\sigma = (SE/2c)^{0.5} \quad (16)$$

Recall from Griffith's theory that the stress required for fracture is

$$\sigma = (2SE/\pi c)^{0.5} \quad (13)$$

Hence, Orowan's derivation verifies the theories of Griffith and Irwin, since the difference between equations (13) and (16) is relatively small and is well within the accuracy of assumptions made by Griffith.

## 2. Application of Fracture Mechanics to Concrete.

Kaplan (48) suggested that the Griffith theory might be extended to concrete even though concrete is a heterogeneous composite. Two assumptions are necessary (49): (a) the laws of elasticity for homogeneous continuous materials can be applied to the case of microscopic cracks at which level concrete is both heterogeneous and discontinuous, and (b) the values of the elastic modulus (E) and the specific gravity are constant throughout the material. It is assumed that the concrete has average values of Young's Modulus and Poisson's Ratio (u) to satisfy the second criterion.

Using the Griffith equation modified for beam flexure, the critical strain energy release rate can then be calculated from the following:

$$G_c = \sigma_n^2 h (1 - u^2) \pi c (1 - c/d_o)^3 / (E d_o) \quad (17)$$





where  $\sigma_n$  = nominal stress at root of the notch,  
 $d_o$  = overall depth of beam,  $c$  = depth of notch, and  
 $h$  = net depth =  $(d_o - c)$ . Theoretical calculations  
 agreed closely enough with experimental determinations  
 of  $G_c$  to verify that Griffith fracture mechanics could be  
 modified and applicable to concrete (48). Kaplan (48)  
 reported  $G_c$  values in the range of 0.07 to 0.10 inch-psi  
 (or, pound-inch per squared inch) and Romualdi and  
 Batson (50) measured values as low as 0.03 inch-psi.

The critical stress intensity factor has also been  
 obtained for concrete (51):

$$K_c = 6M_b(2d_o h(c/d_o)/\pi)^{0.5}/d_o^2 \quad (18)$$

where  $M_b$  = bending moment at the notched section per unit  
 width of the beam, and

$$h(c/d_o) = 10.08(c/d_o)^2 - 1.225(c/d_o) + 0.1917 \quad (18a)$$

Glucklich (52) suggested that the increased energy  
 requirement for crack propagation in cement paste is  
 caused by the formation of a microcracking region near  
 the tip of the crack. When a notched cement paste  
 specimen is subjected to an increasing tensile stress,  
 the stress-strain curve will be nearly linear up to a  
 point when it departs from linearity. This marks the  
 onset of microcracking near the crack tip. The condi-  
 tion is attained when the surface energy required for the  
 main crack and the microcracks is balanced by the strain  
 energy released, and the main crack begins to propagate.



As the main crack slowly propagates, the size of the microcracking region and the energy required to form it increases. This slow crack growth continues until the zone of microcracking reaches a limiting size, and rapid crack propagation occurs. The stress intensity factor and the strain energy release rate at onset of rapid crack propagation are denoted by  $K_c$  and  $G_c$ , respectively. For a given loading and geometry, these values can be found from equations (17) and (18).

3. Application of Fracture Mechanics to Reinforced Concrete. As a flaw in concrete tends to enlarge to a crack, displacements develop in the material ahead of the crack as a result of the stress field singularity at the crack edge. The greater rigidity of steel reinforcement, however, opposes these displacements, and forces are exerted on the concrete by the reinforcement. These forces can be interpreted in fracture mechanics terms as being a reduction in the crack extension force, or in other words, a crack arresting force. It has been found (50) that the stress required to extend a crack beyond the area enclosed by reinforcing rods is inversely proportional to the square root of the rod spacing.

The surface cracking phenomena of a reinforced concrete member that is gradually subjected to axial tension occurs in three stages (53). The first stage of cracking



is concerned with primary cracks that form at random critical sections; steel stresses during this stage are usually well below 14,000 psi. The secondary stage of cracking is concerned with the formation of secondary cracks between the random primary cracks; these cracks are due to the difference of extensibility between the concrete and the reinforcement and to the bonding that occurs between the two. The steel stresses during the second stage of cracking are usually greater than 14,000 psi. The third stage of cracking, also referred to as the equilibrium stage, occurs when no additional surface cracks form during further increases in the axial load, and existing secondary cracks continue to widen. Steel stresses are usually greater than 30,000 psi during the equilibrium stage.

A cracking mechanism for reinforced concrete based on fracture mechanics concepts has been postulated (54). The length of a crack is a function of crack width at the reinforcement, length of the member, fracture toughness and modulus of elasticity of the concrete. The crack width, in turn, is a function of the elongation of the steel and the ability of the concrete to deform with it. New cracks will form and propagate to the surface when the spacing between adjacent cracks is large; however, crack growth will be arrested within the concrete when the spacing is small compared to the concrete cover.





4. Cracking as a Design Factor. It is now appropriate to apply the preceding theory to the consideration of cracking in the construction of concrete ships. The importance of crack minimization becomes vividly apparent if one considers a concrete tanker: the prospect of an oil spill or, in the case of an LNG tanker, cryogenic vapor escaping to the atmosphere, is enough to cause the Coast Guard to shudder. The possibility of seawater corroding the reinforcement has been alluded to previously.

In ferro-cement boatbuilding, it is assumed that the mortar is cracked (although perhaps not visibly so) before the steel reaches yield and that failure is due to failure of the reinforcement and not due to failure of the bond between the mortar and reinforcement. Under tensile loadings, cracks develop in the mortar when the strains in the reinforcement become sufficiently large, or when the reinforcement slips through the mortar. Steel strains can be reduced by increasing the steel's sectional area, or, if in the yield zone, by increasing the yield strength. Resistance to slippage of the reinforcement through the mortar is increased by increasing the bond area (by dispersing the reinforcement via many smaller rods rather than fewer, larger diameter rods). However, too fine a dispersion of reinforcement will resist mortar penetration during construction, and may





consequently reduce strength (7).

This practice is commensurate to that of reinforced concrete in which compressive bending stresses are carried by concrete and tensile bending stresses are carried entirely by steel reinforcing bars. Except in post-tensioned reinforced concrete, when the steel stress reaches about 6,000 psi the tensile concrete starts to crack and the steel soon thereafter must pick up essentially all the tension necessary to provide for the applied moment. Hence, in ordinary reinforced concrete beams, the tensile concrete is not assumed to assist in resisting the moment because of its relatively low tensile strength and brittle nature. However, tension is of importance with regard to cracking, which is a tensile failure; most cracking (aside from that due to loading) is due to restraint of contraction induced by drying or by lowering of temperature (27).

By looking at some of the other causes of cracking in concrete, perhaps some insight may be gained germane to the minimization of cracks. Initiation of discontinuities or microcracks occur in concrete even before external loads are applied. These initial cracks are due to nonuniform volume changes resulting from shrinkage of the cement paste, build-up of corrosion products around reinforcement or expansion of deleterious aggregates. Cracks initiate at critical locations where the



limiting tensile properties of the concrete have been exceeded due to weak material or high stress and strain (53).

The Army Corps of Engineers has listed a number of environmentally induced mechanisms that can cause cracking in concrete (55): unsound cement (internal expansion caused by reaction of moisture with unhydrated calcium oxide or magnesium oxide that was introduced into the concrete as a part of the cement); alkali-silica reaction (internal expansion caused by reaction of alkalies in solution in the concrete with soluble silica in the aggregates); plastic shrinkage; sulfate attack; and corrosion of embedded metal. The latter problem is especially acute in an environment where chlorides are present.

In essence, there are two major causes of cracking in concrete: shrinkage and load. Shrinkage cracking of reinforced concrete structural members can be controlled by proper design of the concrete mix, proportioning the member to minimize differential shrinkage stresses, using curing procedures which minimize concrete shrinkage, and proper use of control joints (56). Atmospheric steam curing, typically used with prestressed concrete, has been found to reduce shrinkage 25 to 40 percent for Type III portland cement when compared to moist cured samples (25).

Flexural (load) cracking, however, is inherent to



some degree in all reinforced concrete flexural members and is always present in efficiently designed structures utilizing steels with yield strengths of 60,000 psi or higher (56). Despite the fact that flexural cracking cannot be prevented, it can be controlled.

One method of controlling flexural cracking is by proper material selection. The higher the strength of steel, the more brittle it usually is. High-strength steel has a slightly lower elastic modulus and therefore elongates more at a given stress than mild steel. These characteristics contribute to formation of wider cracks and to larger deflections than would occur if mild steel reinforcement were used (in ordinary reinforced concrete). Hence, here is further justification for selecting mild steel as ordinary reinforcement. For concrete, higher strength is customarily associated with increased brittleness and smaller ultimate strain; furthermore, unless proper care is exercised, shrinkage and creep are increased. For these reasons, high-strength concrete is not specified for reinforced concrete in building codes and full advantage cannot be taken of high-strength steel because of a code limitation on allowable stress (19).

On the other hand, in prestressed concrete, materials of high strength are necessary for good performance. High-strength steel is necessary to absorb losses of prestress; concrete must have adequate bond strength to





adhere to steel and adequate tensile strength to resist cracking and shear. Ideally, it is arranged that no net tension stresses occur under working-load conditions: the very high tension stress from the tendons induces compression into the concrete, so that applied tension effects do no more than relieve the compressive prestress. The merits of prestressed concrete therefore include almost complete absence of cracking, shallower concrete sections, and reduced quantities of steel.

Herein lies a significant difference between reinforced concrete, prestressed concrete, and post-tensioned reinforced concrete. In reinforced concrete, the reinforcement resists the whole of the tension as the concrete cracks. In prestressed concrete, theoretically there is almost no cracking since no net tensile stresses occur. In post-tensioned reinforced concrete, a certain amount of net tension is allowed, thereby increasing the amount of loading that can be experienced; alternatively, the amount of reinforcement or perhaps post-tensioning tendons could be reduced.

Another method of controlling cracking is rather basic (57): the modulus of rupture ( $f_r$ ) of concrete should not be exceeded under service loads, where  $f_r = 7.5(f'_c)^{0.5}$ . As further insurance against unsightly cracking, reinforcement should be provided. The cross-sectional area of non-prestressed reinforcement ( $A_s$ )





required is:

$$A_s = M/(a^*d) \quad (19)$$

where  $M$  = design moment (ft-kips),  $a^*$  is a constant determined from Table 7,  $d$  = depth to the reinforcement, and  $A_s$  is area in squared inches. Values of  $a^*$  are given for  $f'_c = 5,000$  psi, which is a typical concrete strength under service loads.

TABLE 7

CONSTANTS FOR USE IN DETERMINATION  
OF REQUIRED AREA OF NONPRESTRESSED  
REINFORCEMENT (Equation 19)

<u>Calculated tensile bending stress (psi)</u>	<u><math>a^*</math></u>
0 to 300	1.44
301 to 500	0.98
over 500	Excessive stress; cracking cannot be controlled by reinforcement.

Another possible means of minimizing the effects of cracking is to apply the techniques of ferro-cement. The addition of closely spaced wire reinforcement in the form of mesh, close to the concrete surface and outside the steel reinforcing bars, can increase the tensile strength of the concrete (58). It has also been shown how this increases the modulus of rupture of portland



cement concrete (50). Investigations also show that steel fibrous reinforcement enhances fatigue and impact characteristics of concrete (59).

This last point is of particular interest when one realizes that the U.S. Navy has eliminated concrete from consideration as a ship hull material, solely on the basis of poor shock and impact resistance (60). It must be recognized, however, that the Navy is looking at this from a warship perspective. Nevertheless, substantial evidence and test data demonstrate that prestressed (as opposed to reinforced concrete which the Navy has ruled out) concrete ships will behave excellently under impact (e.g., collision) provided it has employed grouted tendons, multiaxial prestress, closely spaced grid of mild steel reinforcement, and embedded fibers or closely spaced wire mesh (23).

In this same vein, "WIRAND" concrete has been recently developed by the Battelle Development Corporation. The concrete matrix contains a random dispersion of small metallic filaments which act as crack arrestors. This increases the usable tensile strength by a factor of two or more. It also decreases the modulus of elasticity, and greatly increases the impact and abrasion resistance, thermal-spall index, durability, and fatigue strength (43).

Recent research into the subject of proper crack control has isolated a few of the important variables



that must be examined. One important consideration is the maximum permissible crack width before corrosion of the reinforcement becomes a problem. Only a few investigators have studied this relation (61).

The American Concrete Institute (13) limits crack width to a maximum of 0.01 inch for exterior members and 0.015 inch for interior members. Satisfactory service performance is expected under the more conservative CEB Code (62) limitations of 0.008 inch and 0.012 inch for the corresponding environments. The British (26) have by far the most practical standards, as they relate permissible crack width to concrete cover thickness: for seawater environments, the surface widths of cracks at points nearest the main reinforcement should not exceed 0.004 times the nominal cover to the main reinforcement. Thus, for a cover of (say) 2 inches, the limitation coincides with that of the CEB Code for exterior members. The above figures, however, are for reinforced concrete.

For prestressed concrete, and assuming it can be extended to post-tensioned reinforced concrete, the British Standards Institution has different limits on flexural tensile stress depending on the class under which a structure is categorized. They are as follows (26):



Class 1: No tensile stresses.

Class 2: Tensile stresses, but no visible cracking.

Class 3: Tensile stresses, but surface width of cracks not exceeding 0.1 mm (0.004 inch) for structures exposed to seawater.

Whether these limits are indeed suitable for post-tensioned reinforced concrete can be questioned. Two contradictory considerations could supervene: (a) it could be considered that the requirements can be made less stringent than in the case of reinforced concrete, since the cracks are only temporary; (b) on the contrary, it could be considered that the requirements should be more stringent, since a higher standard is required. This is a question of judgment which can be influenced by the frequency of application of the loads which provoke or can provoke cracking (63).

It is significant to observe that the "Class 3" limitation is at least twice as stringent (regarding crack width) as those in the preceding paragraphs. Consequently, it is deemed acceptable to adopt this criterion to post-tensioned reinforced concrete ship construction.

Table 8 summaries the allowable flexural tensile stresses for "Class 2" post-tensioned members. The





TABLE 8

ALLOWABLE TENSILE STRESSES FOR  
CLASS 2 POST-TENSIONED MEMBERS

<u>Concrete Grade</u>	<u>Characteristic Strength</u>		<u>Cube Strength at 2 months</u>		<u>Allowable Tensile Stress</u>	
	<u>N/mm<sup>2</sup></u>	<u>psi</u>	<u>N/mm<sup>2</sup></u>	<u>psi</u>	<u>N/mm<sup>2</sup></u>	<u>psi</u>
30	30.0	4350	33.0	4785	2.1	305
40	40.0	5800	44.0	6380	2.3	334
50	50.0	7250	54.0	7830	2.55	370
60	60.0	8700	64.0	9280	2.8	406



stress in this table may be increased by up to  $1.7 \text{ N/mm}^2$  (247 psi) if such enhanced stress does not exceed 75 percent of the tensile stress when the first crack appears (26).

For "Class 3" members in which cracking is allowed, it may be assumed that the concrete section is uncracked and that hypothetical tensile stresses exist at the maximum size of cracks. Table 9 presents these tensile stresses for grouted post-tensioned tendons. The cracking in prestressed concrete flexural members is dependent on the member depth; the stress given by Table 9 should thus accordingly be modified by multiplying by the appropriate factor from Table 10 (26).

When additional reinforcement is contained within the tension zone and positioned close to the tension faces of the concrete, as is the case for post-tensioned reinforced concrete, the stresses in Table 9 may be increased. The amount to be increased is proportional to the cross-sectional areas of the additional reinforcement expressed as a percentage of the cross-sectional area of the concrete. For one percent of additional reinforcement, the stresses in Table 9 may be augmented by  $4.0 \text{ N/mm}^2$  (580 psi). For other percentages of additional reinforcement, the stresses may be increased proportionately, but not to exceed 25 percent of the concrete characteristic strength (26). In cases of



TABLE 9

ALLOWABLE TENSILE STRESSES FOR  
CLASS 3 POST-TENSIONED MEMBERS

<u>Concrete Grade</u>	<u>Tensile Stress for Limiting Crack Width</u>			
	<u>0.1 mm</u>		<u>0.2 mm</u>	
	<u>N/mm<sup>2</sup></u>	<u>psi</u>	<u>N/mm<sup>2</sup></u>	<u>psi</u>
30	3.2	464	3.8	551
40	4.1	595	5.0	725
over 50	4.8	696	5.8	841

TABLE 10

FACTORS TO BE MULTIPLIED BY ALLOWABLE  
TENSILE STRESSES IN TABLE 9

<u>Depth of Member</u>			<u>Depth Factor</u>
	<u>mm</u>	<u>in</u>	
under	200	7.87	1.1
	400	15.75	1.0
	600	23.62	0.9
	800	31.50	0.8
over	1000	39.35	0.7



severe loading (e.g., ships acting in a seaway), it may be desirous to further augment the amount of reinforcement with the addition of transverse, or shear, reinforcement.

It has been recently recommended (64) that the three "classes" just discussed be eliminated. This is due to an undesirable side-effect, namely, that many people have considered the three classes as a differentiation of qualities and, consequently, have demanded only Class 1 criteria (no tensile stresses). Actually, Class 1 structures cost much more, and have a greater risk due to higher stresses and a larger number of closely spaced tendons that reduce the effective concrete cross-section. Furthermore, the tensile stresses due to temperature effects alone, especially in moderate and cold climates (e.g., North Atlantic ship routes), can easily reach values which exceed the tensile strength of concrete. Thus, the risk exists, and cracking can actually be experienced, in Class 1 structures.

For these reasons it has been suggested (64) that we should rather use "partial prestressing" (Class 3) with bonded mild steel reinforcement, and base our design on crack width considerations. Tables 9 and 10, as well as the comments immediately following them, are thus still applicable. Since "Class 3" members are limited to surface crack widths of 0.1 mm (0.004 inch), a discussion of





factors effecting crack width calculations is necessary.

As a parenthetical aside, it is only for "Class 3" members that probable crack widths need be checked. Unfortunately, the more rational approach to crack width calculations, given on the next pages for nonprestressed members, has not yet been extended to their prestressed counterparts, primarily for lack of test data (65). However, the design of post-tensioned reinforced concrete is in accordance with the methods appropriate to non-prestressed reinforced concrete in combined bending and compression (63).

The major design requirement for the limit state of local damage is that crack widths should be limited to acceptable magnitudes. As these limits have already been discussed, it remains to determine how these crack widths can be calculated.

The mean width of the cracks in a member depends mainly on: the mean strain of the reinforcement ( $e_s$ ), mean strain of the concrete, the spacing between cracks, the proximity to the point considered of reinforcing bars perpendicular to the cracks ( $a_{cr}$ ), and the proximity of the neutral axis to the point considered ( $x$ ).

Several equations have been proposed to determine the maximum crack width ( $w_{max}$ ) on the concrete tensile surface. By far the simplest is (54):

$$w_{max} = 4e_s a_{cr} \quad (20)$$



Another researcher (56) obtained the formula:

$$w_{\max} = 0.715 R f_s (A)^{0.25} \times 10^{-6} \quad (21)$$

where  $R$  = ratio of distances from the neutral axis to the tension face and to the centroid of the reinforcement,  $A$  = average area of concrete surrounding each bar, and  $f_s$  = reinforcement stress.

Equations (20) and (21) are for tensile cracks on the top surface of a beam in hogging. In a sagging condition, the most probable maximum crack width on the bottom face of a beam, with  $f_s$  as the variable, is (66):

$$w_{\max} = 0.076 (A c_{\min})^{0.33} R f_s \times 10^{-6} \quad (22)$$

where  $c_{\min}$  = the minimum cover to the tension steel.

A more complex expression is propounded by the British, and is valid provided the strain in the tension reinforcement is limited to  $0.8 f_y / E_s$ . A simplified version of this formula gives a crack width with an acceptably small chance of being exceeded (26):

$$w_{\max} = 3 a_{cr} e_m / (1 + 2(a_{cr} - c_{\min}) / (d - x)) \quad (23)$$

where  $e_m$  = the average strain at the point in question.

Another researcher (65) has derived an expression for the average crack width. It has been shown that if the maximum width is taken as twice the average, the probability is only about 0.01 that the calculated maximum will be exceeded. Thus, for plain round bars:

$$w_{\max} = 4 a_{cr} y f_s / (d - x) E_s \quad (24)$$

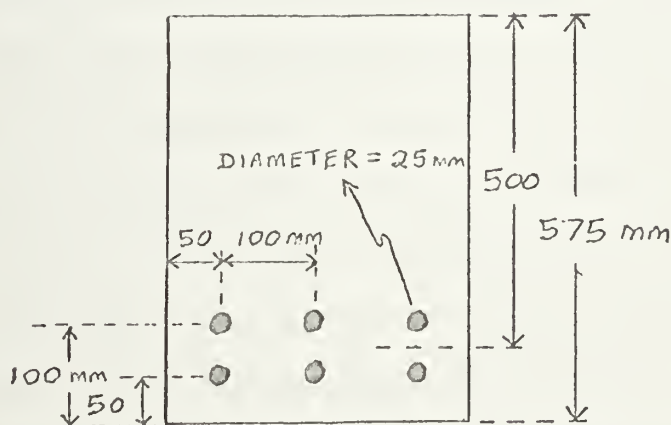
where  $y = d_o - x$ , and other terms are as defined earlier.



Equation (23) is similar to equation (24), but slightly less conservative; i.e., equation (23) corresponds to a slightly higher probability of any given crack exceeding the width calculated for it.

It can be seen from equation (24) that there are two basic ways of controlling crack widths: (a) using low working stresses for the main steel, and (b) distributing the bars so that  $a_{cr}$  is kept to a minimum. The former alternative is generally uneconomical, and the latter should be adopted. For a given area of steel, the use of smaller diameter bars increases the maximum permissible bar stress for a fixed crack width (65).

An interesting exercise is to calculate the maximum crack width, for a given member, from the five preceding equations and compare the results. Suppose a cross-sectional area is configured as follows:



Considering that the widest cracks are at the bottom corners of the beam and referring to the sketch, it can be observed that:  $d_o = 575$  mm;  $d = 500$  mm;  $x = 225$  mm;



$$y = d_o - x = 350 \text{ mm}; a_{cr} = 50\sqrt{2} - 12.5 = 58.2 \text{ mm};$$

$$c_{min} = 50 - 12.5 = 37.5 \text{ mm}; R = 225/150 = 1.5;$$

$$6A = (300)(150) - 6\pi(25)^2/4 = 42,055 \text{ mm}^2, \text{ or}$$

$A = 7,009 \text{ mm}^2$ . Letting  $f_s = 213 \text{ N/mm}^2$  (30,885 psi) and  $e_s = 0.0013$ , and assuming that  $e_m = e_s$  (since concrete strain is small compared to steel strain), substitution into equations (20-24) yields:

<u>equation</u>	<u>w<sub>max</sub></u>
(20)	0.3mm
(21)	0.3mm
(22)	0.26mm
(23)	0.197mm
(24)	0.31mm

Equation (23), a simplified version of the British formula, appears to be the best for design purposes.

While many expressions for maximum crack width have been proposed, few investigators have agreed on even the significance of fundamental variables. Recent investigations in the United States have indicated that bar spacing (54) and concrete area about the reinforcing bars (56) have important influences on crack spacing and width, while bar size and reinforcement percentage are considered significant in Europe (62). Another American (66) considers steel stress as the most important variable affecting crack width, with other major factors including





the number of bars and the cover thickness.

Another difficulty is the large variation of crack widths. It has been shown (67) that the range of crack width within the same specimen, because of variation in crack spacing, can be as high as  $\pm 50$  percent. Thus, the prediction of an absolute maximum width is not possible.

It is in this perspective that post-tensioned reinforced concrete becomes a viable and attractive option. With a combination of reinforcing rods and post-tensioning tendons, a greater amount of tensile stresses can be encountered before any net tension in the concrete results, and therefore before there arise any tendencies to crack.

#### B. Corrosion and Concrete

The paramount incentive of precluding (or at least minimizing) crack formation in concrete is to prevent corrosion of the underlying steel rods. (Of course, in the words of that trite expression, there are two sides to the proverbial coin. One investigator (68) has theorized that cracks are generally not as important a factor in the corrosion mechanism as commonly believed; he offers evidence that cracks at the concrete surface narrower than 0.2 mm (0.008 inch) will not necessarily lead to serious corrosion.)



The two categories of rods in a post-tensioned reinforced concrete system are inhibited from corroding in dissimilar fashion. Reinforcing rods are protected by a "sufficient" cover of concrete (see next section). The tendons, on the other hand, are protected by grouting: after the steel tendons have been post-tensioned and anchored, the ducts which contain the tendons are filled completely with grout; this protects the steel against corrosion and prevents any free water in the ducts from freezing with consequent expansion and cracking; the grout also enables proper bond to be developed, and this reduces deformation under conditions of over-loading.

Corrosion has traditionally been a prime design factor when new materials are considered for marine applications. Such has been the case for aluminum-magnesium alloys, titanium alloys, and glass reinforced plastics. In this sense, concrete thus becomes an ideal candidate for a marine structural (i.e., ship) material. Its corrosion resistant attributes have already been mentioned in the first section of Chapter II. Accrued monetary benefits also occur: lower maintenance and life-cycle costs result from the virtual absence of corrosion. For example, drydocking time and costs would be practically eliminated as constant scraping, chipping, and painting for both appearance and function would no longer be necessary. It has even been demonstrated that



concrete ship hulls exhibit reduced fouling from barnacles. Furthermore, tests on the World War II concrete ships confirmed what had been experienced with the World War I vessels, namely, that dense, strong concrete is immune to attack or disintegration by seawater (12). As a result, no paint, either anti-fouling or protective, need be applied to the hull underbody; this obviously also reduces lifecycle costs.

In the case of ordinary reinforced concrete, seawater used in the mixing process with cement is believed to increase the risk of corrosion of the reinforcement, although there is no experimental evidence that the use of seawater in mixing leads to attack on the reinforcing steel. The danger appears to be greater in tropical climates. In practice, however, it is generally considered inadvisable to use seawater for mixing unless this is unavoidable. On the other hand, in prestressed concrete the use of seawater is definitely not permitted, since the small cross-section of the tendon means that the effects of corrosion are relatively more serious (31).

In the case of a concrete ship, the concrete in the splash zone, subjected to alternating wetting and drying, is severely attacked; permanently immersed concrete, however, is attacked least. In addition to the seawater itself, there is ample oxygen for corrosion of the reinforcement. Chlorides may be deposited by evaporation in



permeable concrete and lead to salt-cell electrolytic corrosion. In some cases the action of seawater on concrete in the splash zone is accompanied by the destructive agencies of frost, wave impact and abrasion, and all these tend to aggravate the damage of the concrete.

Concrete for prestressed structural elements that are to be exposed to freezing and thawing in a moist condition should contain entrained air. Air-entraining cements are designated as Types IA, IIA, and IIIA, and correspond to Types I, II and III. Air entrainment can also be obtained by adding a suitable admixture to the concrete during the mixing process. In Western Norway, up to 8 percent entrained air is used with success in combatting the combination of freeze-thaw and marine environment (43).

The mechanism of corrosion in reinforced concrete does not neatly fall into one of the standard categories of corrosion: uniform attack, pitting, dezincification and parting, intergranular corrosion, or stress corrosion cracking (69). Rather, the deleterious effects begin as the seawater evaporates, creating concentrated solutions of magnesium sulfate which usually attack most of the constituents of the hardened cement paste matrix in the concrete. The sodium chloride concentrations promote corrosion of the steel reinforcement. The alkalies (sodium and potassium) present in the concentrated







solutions may react with the aggregate in the concrete. The reaction between calcium hydroxide crystals, formed in the hydration of portland cement, and the magnesium sulfate (from the seawater) results in the formation of calcium sulfate and magnesium hydroxide. The insoluble products of this reaction occupy a greater volume than do the calcium hydroxide crystals that are replaced; consequently, these products are the cause of disruptive forces which are evidenced by cracking of the concrete cover over the steel and subsequent spalling (70).

In reinforced concrete, the absorption of salt establishes anodic and cathodic areas; the resulting electrolytic action leads to an accumulation of the corrosion products on the steel with a consequent rupture of the surrounding concrete, so that the effects of seawater are more severe on reinforced concrete than on plain concrete.

In the case of prestressed concrete, it is essential that tendons be protected from substantial corrosion. Corrosion may affect the ductility of the tendons or may simply reduce the cross-section of tendons and thus reduce both the prestress and the ultimate strength. Corrosion may also reduce the fatigue strength.

To minimize these problems, the concrete must incorporate a sulfate-resistant portland cement (ASTM Type V or Type II) and the steel reinforcement must be covered



with an adequate amount of watertight concrete (i.e., low permeability). For post-tensioned work, however, Type III is preferred due to its high early strength through rapid hardening. Watertight concrete can be achieved with a low water-cement ratio; this can be accomplished by reducing the water content or by increasing the cement content. The former has the effect of reducing workability, and the latter has the effect of increasing shrinkage and plastic flow; a compromise of these two should be used.

To minimize the possible adverse effect of chlorides present in the seawater, not only is a watertight concrete mandatory but supplementary alkalinity is needed to protect the embedded steel. This protection can be attained by using lime-saturated freshwater in the concrete mixture; 5 grams of calcium hydroxide per liter of water is known to prevent corrosion of steel in concrete (70). A pozzolan, as partial replacement of the cement, is another precautionary measure. The pozzolanic silicate combines, in the presence of moisture, with any excess calcium hydroxide present in the concrete. This reaction precludes any leaching of the lime, due to evaporation at the concrete surface, since additional cementitious compounds (calcium silicates) are created within the mass of concrete. These additional silicates strengthen the concrete to resist cracking; they improve its durability



by increasing its resistance to the effects of the sulfates present in seawater.

There remain a couple other considerations when dealing with corrosion of post-tensioned reinforced concrete. Stress corrosion cracking is an extremely rare phenomenon but, unfortunately, the occurrence of the word "stress" in both stress corrosion and prestress has led to unwarranted fear and trepidation. Stress corrosion is usually associated with minute traces of chlorides or sulfides occurring in a humid atmosphere.

Hydrogen embrittlement, while extremely serious, also appears to be rare. The International Federation of Prestressing (F.I.P.) Commission on Durability warns against the use of dissimilar materials, other than steel, in prestressed concrete, because of the possibility of electrolytic corrosion and hydrogen embrittlement. Aluminum and copper are particularly to be avoided.

Another consideration, attributable exclusively to post-tensioned construction, is that the anchorages must be protected from corrosion. The wires at the anchorages are under higher stress than anywhere else. This matter is especially important when high-capacity tendons are used. When the anchorage is seated in a pocket, and the encasement consists of filling the pocket with epoxy concrete flush with the ends, performance should be excellent, with no cracking, rust-staining, or other evidence of



corrosion (43).

In an attempt to establish serviceability criteria to the design and construction of prestressed concrete vessels, it has been suggested (23) that the following be adhered to, most of which have already been mentioned. For corrosion protection, there should be: (1) rigid watertight ducts; (2) grouted tendons; (3) maximum water-cement ratio = 0.45; (4) recessed anchorages, with pockets filled with epoxy mortar; (5) strict limitations on chloride and sulfide contents in concrete mix; and (6) a certain minimum cover of concrete. The latter point logically brings us to the next section.

#### C. Cover of Concrete

The section on corrosion is a natural transition between the design factors of cracking and cover of concrete. Cracking must be minimized to preclude corrosion of the steel rods; and one way to guard against such corrosion is by having an adequate concrete cover over the rods. This "sufficient" cover has been qualitatively alluded to several times, and it now remains to attach to it some quantitative relevance.

A few general design considerations should be looked at first. The optimum cover of concrete must be enough to prevent seawater from seeping through any surface tensile cracks and attacking corrosively the reinforcement;







however, the cover must not be so thick as to impede the reinforcement from reducing tension in the concrete (i.e., reinforcing rods at the neutral axis are pointless). It is also important to recognize that increasing the thickness of concrete cover causes considerable increase in cost as well as in weight. Cost and weight are two primary characteristics that must be minimized (to the greatest extent that is structurally feasible) in order to achieve a post-tensioned reinforced concrete ship that is competitive with traditional steel hulls.

Comparison with steel ships poses a potential problem. In order to certify a steel oil tanker, United States Coast Guard (USCG) Regulations require that all tankers be constructed with a double hull. No USCG regulations have as yet been adopted for concrete tankers; but it is apparent that a similar requirement for concrete double hulls would eliminate concrete ships as a viable competition for steel ships, mainly due to the excessive amount of concrete cover necessary for a double hull, and the fact that concrete ships are already heavier than corresponding steel ships.

The concrete cover protects the steel by creating a passive condition of high pH at the surface of the steel. Too thin a cover allows carbonation to proceed, usually around the surface of the coarse aggregate particles; carbonation lowers the pH.



Oxygen is necessary to the corrosion mechanism; a thicker cover minimizes the movement of oxygen to the steel surface. In seawater, chloride ion movement is also inhibited by thicker covers.

The cover should properly be related to the density and cement content. The exact relationships have not been thoroughly established, so arbitrary values are usually used as guides or standards. Thicker covers make it possible to achieve better compaction, fewer voids, and less permeability (43).

Recommended thicknesses of concrete cover tend to range rather widely. At one end of the spectrum are the reinforced concrete ships of World War II: specifications called for the outer layer of steel to have a minimum concrete coverage of  $3/4$  inches for those portions of the shell in contact with the water, and  $1/2$  inch coverage elsewhere (12). On the other hand, the "adequate amount" of watertight concrete referred to in the last section is 3 inches (70). As stated though, increasing the concrete cover results in considerable cost increases; thus, Gerwick (71) considers a 2-inch cover adequate in marine structures. However, Gerwick has recently altered his figures (23) such that the minimum cover over tendon ducts should be 2 inches, but the minimum cover over mild reinforcing steel need only be  $1-1/2$  inches.



The American Concrete Institute (13) specifies that the minimum concrete cover over reinforcing bars and post-tensioned tendons shall be 1-1/2 inches for members exposed to earth or weather. If tensile stresses exceed  $6(f'_c)^{0.5}$ , cover must be increased 50 percent. No specific coverage is given for "corrosive atmospheres or severe exposure conditions" (i.e., seawater) other than that the amount of concrete protection "shall be suitably increased."

The British Standards Institution (26) is a little more specific on this last point. They claim that the concrete cover to both ordinary reinforcement and post-tensioning tendons will generally be governed by considerations of durability and fire resistance. For post-tensioning systems in particular, a dense concrete cover is recommended. The nominal cover should always be at least equal to the diameter of the bar. Specifically, the nominal cover for "very severe" conditions of exposure (i.e., seawater) is 60 mm (2.36 inches) for concrete of grade 40, and 50 mm (1.97 inches) for concrete of grades 50 and over.

The fire resistance of reinforced concrete and prestressed concrete is dependent primarily on the protective concrete cover of the steel. For ordinary reinforced concrete beams, the fire rating improves from 1 to 4 hours as the concrete cover increases from 3/4 inch to



1-1/2 inches (27). Prestressed concrete requires a thicker cover for a given fire rating since prestressing steel, which is usually cold-drawn to increase its strength, is weakened more by high temperatures than ordinary reinforcement steel is. Excluding fire resistance, however, the required cover for prestressed concrete is less than that for nonprestressed concrete (39).

The CEB Code (62) actually recommends a maximum (vice minimum) permissible distance between reinforcement and concrete surface. This amount is 4 cm (1.57 inches), and is remarkably close to Gerwick's 1-1/2 inches recommended cover over mild reinforcing steel. Similarly, the BSI nominal cover of 50 mm (1.97 inches) is almost identical to Gerwick's 2 inches cover over ducts. Another reference (39) indicates that beyond about 2 inches, increases in cover do not provide proportional increases in protection against penetration of seawater. Thus, it seems that Gerwick's recommendations may be reasonable.

#### D. Spacing of Rods

As indicated in the section on cracking, reinforcing bar spacing has an important influence on crack width. It has been shown (63) that because of the reinforcement, which prevents concentrations of tensile strain (if the reinforcement is "suitably spaced"), cracks will remain







very small -- on the order of 0.01 mm. An adequate definition of "suitably spaced", however, remains to be seen.

Intuitively, reinforcement rods must be spaced far enough apart to allow maneuvering room for the largest aggregate. The American Concrete Institute (13) specifies that the maximum size of the aggregate shall not be larger than three-fourths of the minimum clear spacing between individual reinforcing bars or post-tensioning ducts. As to what this minimum spacing is, it is also specified that the clear distance between parallel reinforcing bars in a layer shall be not less than the nominal diameter of the bars, nor 1 inch. Where parallel reinforcement is placed in two or more layers, the bars in the upper layers are to be placed directly above those in the bottom layer, with the clear distance between layers not less than 1 inch.

The British Code (26) requires that the horizontal distance between bars should not be less than  $h_{agg} + 5$  mm, where  $h_{agg}$  is the maximum size of the coarse aggregate. For two or more rows, the vertical distance between bars should be not less than  $2/3h_{agg}$ . Thus, for a 1-1/2 inch aggregate, the British regulation coincides with its American counterpart regarding distance between layers.

The CEB Code (62), recommendations for an international code of practice, suggests that the free distance



between two neighboring bars in the same plane must be equal at least to: (a) 1 cm; (b) the diameter of the thicker bar; or (c) 1.2 times the maximum size of the aggregate.

The British Code also specifies the minimum area of reinforcement. The area of tension reinforcement in a beam should not be less than 0.15 percent of  $bd$  when using high yield reinforcement, or 0.25 percent of  $bd$  when mild steel reinforcement is used, where  $b$  = the breadth of the section and  $d$  = the effective depth.

Bar size and reinforcement percentage, factors considered significant in Europe, give rise to the terms under-reinforced and over-reinforced. An under-reinforced cross-section is one in which ultimate failure is characterized by large deflections and cracking on the tensile face. An over-reinforced cross-section is one where ultimate failure is characterized by cracking of the compressive side and rapid collapse; there are no known flexural failures in this over-reinforced mode (7).

The size, number, and spacing of reinforcing bars and post-tensioning tendons should be such that cracking of the concrete would precede failure of the beam (26). This requirement will be satisfied for under-reinforced beams where failure would be due to fracture of the tendons, if the percentage of reinforcement, calculated on an area equal to  $bd$ , is not less than 0.25. For



over-reinforced beams, where failure would be due to crushing of the concrete, the maximum number and size of tendons will be governed by strain compatibility considerations.

An equation for the maximum diameter (mm) of mild steel reinforcement has been proposed (63), and is dependent upon the effective percentage of reinforcement ( $p = A_s/bd$ ), tensile stress in the steel ( $f_s$  in  $\text{kg/cm}^2$ ), and  $k$  -- a factor which is dependent on the consequences of cracking. This equation is:

$$\text{maximum diameter} = kp/f_s(10 + p) \quad (25)$$

where  $k$  has the value 150,000 or 100,000 or 50,000 depending on whether the effects of the crack are slight, undesirable, or very serious, respectively. The percentage,  $p$ , should not be less than 2 percent. A possible synthesis with the section on cracking is to use equation (19) to solve for the required area of reinforcement,  $A_s$ , and then use that result to find the percentage of reinforcement,  $p$ , for use in equation (25).

There is no requirement for minimum diameters of reinforcing bars. Diameters which are too small, however, should not be used in an attempt to reduce the opening of cracks because of the risks of corrosion (low cover protection).

All these empirical rules can be considered only as indicative, however; and the distribution of the



reinforcement, both as regards position and diameter, is primarily a question of good judgment.

#### E. Cost Considerations

The economic and durable properties required of marine structural materials are (8): low cost, easy to fabricate and handle, easy to repair, low maintenance requirement, high resistance to corrosion, waterproof, and high fire resistance. As has been previously stated, post-tensioned reinforced concrete possesses most of these properties. What remains to be demonstrated is whether such a concrete ship-as-a-whole is economically feasible and comparable to a steel ship.

The economic advantage that post-tensioned reinforced concrete ships would have over steel ships, particularly regarding maintenance costs, has already been mentioned. Periodic maintenance drydocking for steel ships, though very expensive in terms of labor and material, is also costly from the standpoint of revenue loss due to the hulls being out of service during drydocking.

The first economic comparison between concrete and steel ships was undoubtedly that done on the World War II reinforced concrete ship program. Unfortunately, the construction cost was higher than had originally been estimated; this was due, in part, to (12): lack of background knowledge and experience; the thin shell (to save







weight) with many closely spaced reinforcing bars was difficult to form and presented many concrete pouring problems; the use of lightweight aggregates introduced problems already well-documented; shipyard facilities and equipment were inadequate; and labor costs ran high.

A recent comparison has been made between prestressed concrete tankers and steel tankers having the same cargo capacity (22). This study corrected the invalidity of the World War II study, in that the latter compared steel tankers to concrete tankers with only one-half the capacity of its steel counterpart. The more current report presents an economical evaluation of the total cost (building cost and operating expenses) of the two tankers.

Before discussing the results, two diametrically opposed facts of prestressed concrete should be understood. On one end of the spectrum, prestressed concrete has resulted in substantial economies in marine structures; these economies are due to two causes (43): greater structural efficiency and economies in production. On the other hand, prestressed concrete requires more hardware, e.g., end anchorages and ducting. Including all these extra costs, prestressed concrete is approximately three times more expensive than reinforced concrete (63).

The study just alluded to (22) concludes that the building cost of concrete tankers is about 90 percent of the building cost of steel tankers with corresponding



speed, draft, and cargo capacity. Furthermore, the life of a concrete ship will probably exceed the 20 years assumed for a steel ship, consequently decreasing its annual cost. Therefore, it appears that prestressed concrete tankers may be competitive with steel tankers.

It, thus, follows that post-tensioned reinforced concrete ships are also competitive with steel ships, if not more so. This is apparent since fewer of the more expensive prestressing tendons are used, the balance consisting of less expensive ordinary reinforcing bars.



## CHAPTER IV

FLEXURAL ANALYSIS OF CONCRETE BEAMS

As a prelude to Chapter V, it is necessary to understand the mechanics of flexural analysis as applied to concrete members, or, in other words, the bending behavior of concrete beams. This is particularly important when one realizes that a ship has traditionally been analytically approximated -- in a gross sense -- as a simple beam. The principles of bending analysis apropos of simple reinforced concrete beams will first be considered; they will then be extended to the bending of prestressed concrete beams. Finally, a synthesis of the two cases will be made in an attempt to examine the bending of post-tensioned reinforced concrete beams.

A. Bending of Reinforced Concrete Members

In a homogeneous elastic beam subjected to a bending moment (M), one can calculate the bending stresses (f) from:

$$f = Mc/I \quad (26)$$

where c is the distance from the face in question to the neutral axis, and I is the moment of inertia. The extreme fiber on one face carries compression, while the opposite face carries tension. If the beam is rectangular (or of any shape symmetrical about the centroidal



axis), the maximum tensile stress equals the maximum compressive stress. In concrete construction, it is not economical to accept the low tensile strength of plain concrete as a limit on beam strength (15). It is generally more economical to make up a beam with compressive bending stresses carried by concrete and tensile bending stresses carried entirely by steel reinforcing bars.

#### 1. Reinforced Concrete Beam Bending Analysis.

Certain general assumptions must be made prior to analysis of reinforced concrete beam bending (72): (a) The tensile load is carried by the reinforcement alone. (b) Perfect adhesion exists between reinforcement and surrounding concrete; in other words, the reinforcing material must be properly bonded to the concrete so that the beam acts as a single unit. (c) Sections which are plane before bending remain so during bending. (d) The stress-strain diagram of concrete, when compressed, is in reality not a straight line but a curve. However, for purposes of design calculation, Hooke's law is assumed to be valid, or, strain is proportional to stress. (e) As a result of assumptions (c) and (d), the stress distribution follows the linear law.

At this time, only the bending stresses in reinforced concrete beams will be considered and the discussion will be limited to "simple reinforced rectangular beams,"





i.e., beams having reinforcement only on the tension side of the neutral axis. Since such beams are composed of two materials having different moduli of elasticity, the simple bending formula (equation 26) is not applicable, because the neutral axis does not pass through the centroid of the section.

Figure 7(a) shows a cross-section of a rectangular reinforced concrete beam with steel reinforcement on the tension side. The deformation (Fig. 7b) is assumed to be linear (assumptions d and e), with zero deformation at the neutral axis of the beam. The steel portion of the beam is assumed to deflect the same amount as it would if it were concrete (assumption b), but the stresses in the steel will exceed the stresses in the concrete by a factor of  $n$ , where from equation (1),  $n = E_s/E_c$ .

There are several approaches to the analysis of a reinforced concrete beam (16, 17, 72, 73), albeit they are all similar in principle. The first step is to transform the steel area ( $A_s$ ) into equivalent concrete area ( $A_t$ ):

$$A_t = nA_s \quad (27)$$

This area is assumed to be located at the centerline of the steel and to be so narrow as to have a uniform stress distribution. Therefore, the total tensile force ( $T$ ) is given by:

$$T = f_s A_s \quad (28)$$



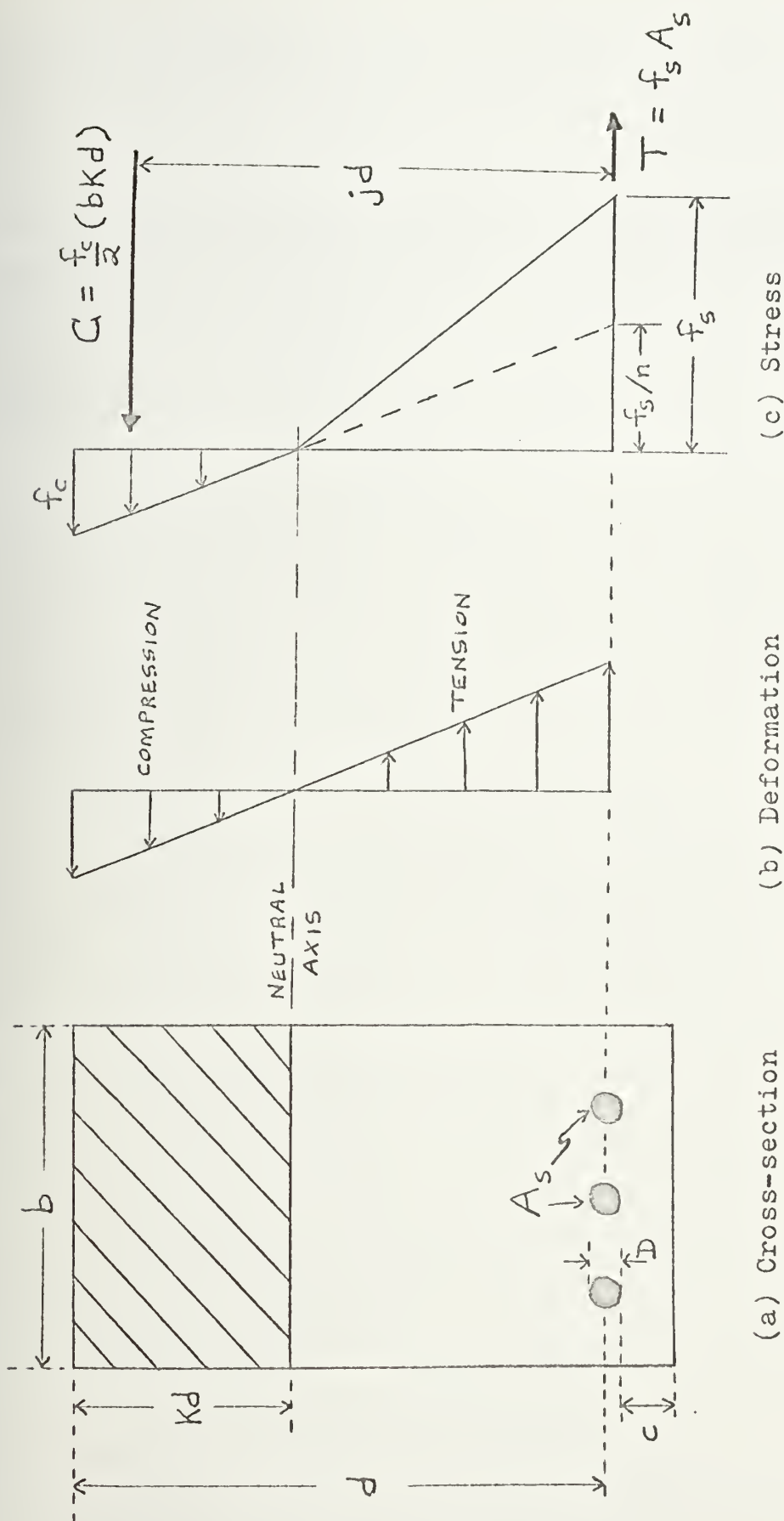


FIGURE 7

RECTANGULAR REINFORCED CONCRETE BEAM



Rewriting this equation as  $T = (f_s/n)(nA_s)$ , and substituting equations (4) and (27), yields:

$$T = f_c A_t \quad (29)$$

The total compressive force in the beam, using only the portion above the neutral axis, is given by the average compressive stress ( $f_c/2$ ) multiplied by the area in compression:

$$C = (f_c/2)(bkd) \quad (30)$$

where  $b$  is the width of the beam,  $d$  is the depth of the beam from top to the center of steel reinforcement,  $k$  is the ratio of location of neutral axis to the depth, and  $f_c$  is the maximum concrete stress at service loads.

However, the condition for equilibrium requires that  $C = T$ , and a couple thus exists with a moment arm of  $jd$ , where  $j$  is the ratio of moment arm of C-T couple to the depth. Figure 7(c) portrays the results propounded thus far in this section. (Notice that the depth ( $d$ ) of the beam, as indicated in the figure, is the "effective" depth; the extra cover of concrete ( $c$ ) under the steel serves only as protection to the steel and has no structural function -- this is so since the concrete is in tension and is supposed to have lost its tensile stresses by cracking.)

The bending moment of the concrete force is thus:

$$C(jd) = (f_c/2)(bkd)(jd) \quad (31)$$



and the bending moment of the steel is:

$$T(jd) = f_s A_s (jd) \quad (32)$$

It must now be further assumed that both the steel and concrete reach their maximum stresses simultaneously: this condition is referred to as "balanced reinforcement." For balanced reinforcement, the resisting moment ( $M$ ) must equal either or both of the moments given by equations (31) and (32). Thus

$$M = (f_c/2)(bkjd^2) = f_s A_s (jd) \quad (33)$$

Two useful relations can be obtained from this equation. Equating the two furthest left terms yields the following expression for the depth of the beam:

$$d = (2M/f_c bkj)^{0.5} \quad (34)$$

The second relation results from equating the two furthest right terms, namely, an expression for the steel area:

$$A_s = f_c bkd/(2f_s) \quad (35)$$

A more simplified version of equation (35), and one which is equivalent, is obtained by equating the extreme left and right terms of equation (33):

$$A_s = M/(f_s jd) \quad (36)$$

It is necessary to know the values of the two ratios,  $k$  and  $j$ , for usage in the above equations. The neutral axis can be easily located by similar triangles; referring to Figure 7(c),  $(kd)/d = f_c/(f_c + f_s/n)$ . Therefore,

$$k = 1/(1 + f_s/nf_c) \quad (37)$$

Since the centroid of the upper triangle in Figure 7(c)





is equal to  $(kd)/3$ , then the moment arm of the couple is  $jd = d - (kd)/3$ . Hence,

$$j = 1 - k/3 \quad (38)$$

Equations (34) through (38) are actually sufficient for the design of a beam for bending when balanced reinforcement is assumed. For example, given the maximum tensile stress in steel ( $f_s$ ), maximum compressive stress in concrete ( $f_c$ ), modular ratio ( $n$ ), width of the beam ( $b$ ), and bending moment ( $M$ ), then the following can be determined in the sequence below: (a)  $k$  from equation (37); (b)  $j$  from equation (38); (c) depth ( $d$ ) of beam from equation (34); and (d) steel area ( $A_s$ ) from either equation (35) or (36).

2. Applications. An interesting exercise is to determine the effect on beam depth ( $d$ ) by varying the modular ratio ( $n = E_s/E_c$ ). For example, as Young's modulus of elasticity for concrete ( $E_c$ ) increases, the beam becomes more homogeneous, and  $n$  decreases. Values of  $n$  typically range from about 6 to 15.

Appendix B carries out the calculations of this exercise. It is found that, for a given breadth and bending moment, as the modular ratio decreases, steel area also decreases, but the depth increases. Thus, the moment arm ( $jd$ ) increases, and the neutral axis gets closer to the top of the beam.



Another exercise is to hold  $n$  constant (along with breadth and bending moment), vary the stress in the steel reinforcement ( $f_s$ ), and again determine the effect on beam depth. Appendix C presents the results. In summary, as steel stress ( $f_s$ ) increases, steel area ( $A_s$ ) decreases, but beam depth also increases.

The decrease in steel area with increasing steel stress is in agreement with preliminary material selection remarks in Chapter II. But the increase of beam depth in both exercises is a somewhat surprising result, and the question arises as to whether the weight increases as well. Appendix D considers this question. In brief, it is discovered that as the depth increases, concrete area increases, and the weight of the beam likewise increases.

A general conclusion to be drawn from this is that in order to minimize weight (a prime consideration in concrete ships), either the depth or the concrete area must be decreased. Appendix E is an attempt to determine an analytical expression for the minimum weight of a reinforced concrete beam. It is obvious, however, that the search for such an expression, without any stress limitations imposed, is purely academic, in that it results in the trivial solution of zero depth.

Appendix F addresses this particular problem by adopting the following stress limitations: (a) maximum



concrete stress (compression):  $f_c = 0.45f'_c$ ; (b) maximum concrete stress (tension):  $f_t = 6.75(f'_c)^{0.5}$ ; and (c) maximum steel stress (tension):  $f_s = 0.8f_y$ .

Notice that the concrete tensile stress limitation is the average of equations (9) and (10).

Summarizing the key results, it is found that as the depth decreases, the moment of inertia (and hence also the section modulus) likewise decreases. It is further shown that as the beam depth decreases, the stresses in the beam's outer fibers increase; hence, a limit is reached (i.e., the maximum concrete tensile stress), beyond which it is not structurally practicable to further reduce the depth. It is, thus, this solution which is the optimum "minimum weight", namely, when both concrete and steel attain their maximum permissible stresses simultaneously.

Appendix G considers the additional effect of varying the reinforcement area and distribution. For a constant beam depth, it is found that the moment of inertia increases with increasing steel reinforcement area.

### 3. Use of Codes in Reinforced Concrete Bending.

The American Concrete Institute (ACI) Code specifies a few assumptions different from those in the first section. The strength design of reinforced concrete members for



flexural loads is based on these assumptions (13):

- (a) Strain in the reinforcing steel and concrete is assumed directly proportional to the distance from the neutral axis.
- (b) The maximum usable strain at the extreme concrete compression fiber is assumed equal to 0.003 (the British Code uses  $e_c = 0.0035$ ).
- (c) Stress in reinforcement below the specified yield strength,  $f_y$ , for the grade of steel used is taken as  $E_s$  times the steel strain. For strains greater than that corresponding to  $f_y$ , the stress in the reinforcement is considered independent of strain and equal to  $f_y$ .
- (d) Tensile strength of the concrete is neglected in flexural calculations of reinforced concrete.

The reinforcement ratio,  $p$ , was defined in Chapter III as  $p = A_s/bd$ . The ACI Code requires that, for flexural members, this reinforcement ratio must not exceed 0.75 of that ratio which would produce balanced conditions (13). "Balanced reinforcement" was discussed in the preceding section; in terms of the present discussion, balanced conditions exist at a cross-section when the tension reinforcement reaches its specified yield strength,  $f_y$ , just as the concrete in compression reaches its assumed ultimate strain of 0.003. These regulations represent an attempt to assure the ductile failure produced by yielding of steel as compared to the brittle type of failure occurring when the failure is in compression.





It is possible to establish relationships for both the balanced reinforcement ratio ( $p$ ) and the balanced moment. Referring to Figure 8(a), the steel strain will be  $f_y/E_s$  and the maximum concrete strain 0.003. The neutral axis can be located from the strain triangles; for  $E_s = 29 \times 10^6$  psi:

$$\begin{aligned} kd &= 0.003d / (0.003 + f_y/E_s) \\ &= 87,000d / (87,000 + f_y) \end{aligned} \quad (39)$$

Note the similarity to equation (37), which was derived by considering the stress triangles and which utilized  $f_s$  vice  $f_y$ .

Figures 8(b) and 8(c) are based on the ACI Code, in which the stress distribution of Figure 8(b) is treated as the equivalent rectangular concrete stress distribution of Figure 8(c), the latter of which is defined as follows: "A concrete stress of  $0.85f'_c$  shall be assumed uniformly distributed over an equivalent compression zone bounded by the edges of the cross-section and a straight line located parallel to the neutral axis at a distance  $a = B_1(kd)$  from the fiber of maximum compressive strain. The fraction  $B_1$  shall be taken as 0.85 for strengths,  $f'_c$ , up to 4000 psi and shall be reduced continuously at a rate of 0.05 for each 1000 psi of strength in excess of 4000 psi" (13). In the case of the concrete mix selected in Chapter II ( $f'_c = 7,000$  psi), it follows



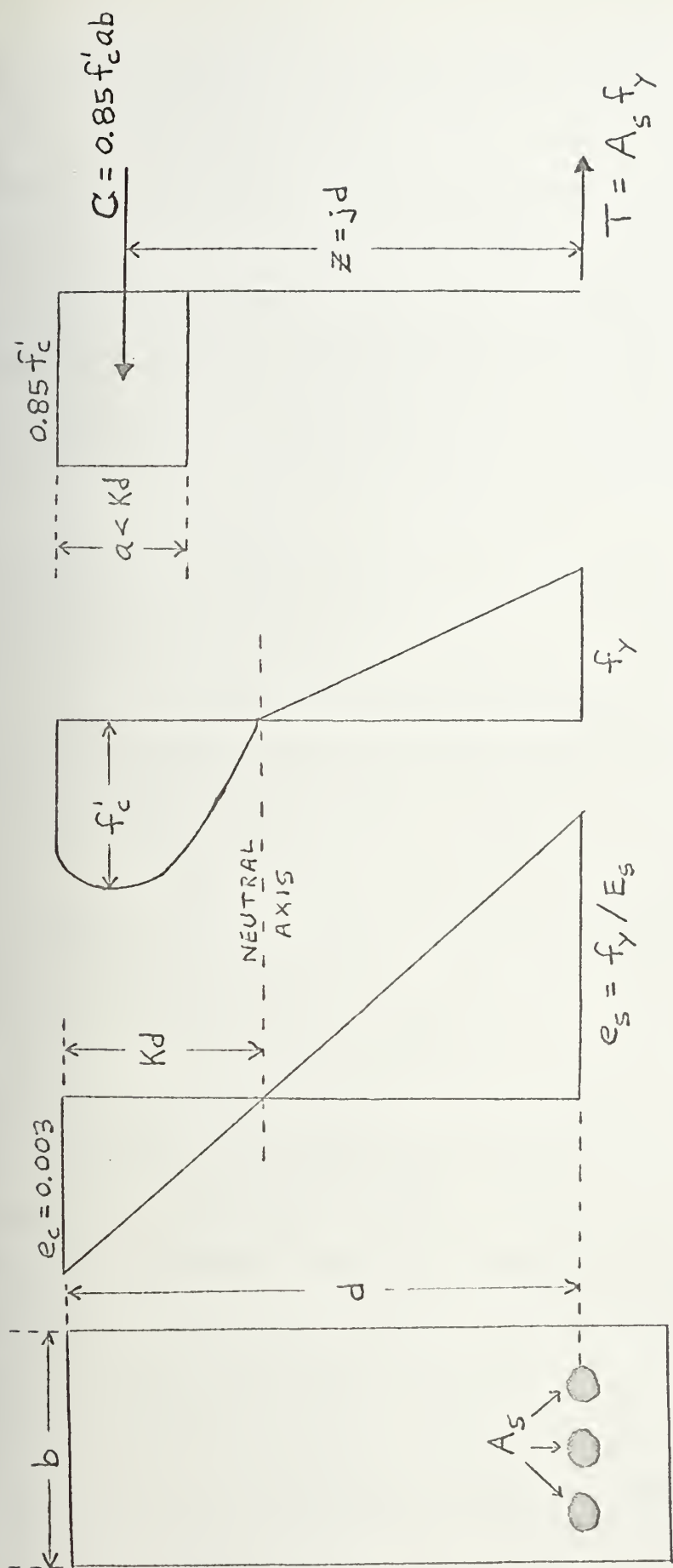


FIGURE 8  
RECTANGULAR REINFORCED CONCRETE BEAM (ACI CODE)



that the fraction  $B_1$  would be equal to  $0.85 - 3(0.05) = 0.70$ . Thus, as concrete strength increases above 4,000 psi, the depth of the equivalent rectangular concrete stress distribution decreases.

The reinforcement ratio ( $p$ ) can now be established by equating compressive force ( $C$ ) and tensile force ( $T$ ). From Figure 8(c), it is seen that

$$\begin{aligned} T &= A_s f_y \\ &= p b d f_y \end{aligned} \quad (40)$$

$$\begin{aligned} \text{and } C &= 0.85 f'_c a b \\ &= 0.85 f'_c B_1 k d b \\ &= 0.85 f'_c B_1 b d (87,000) / (87,000 + f_y) \end{aligned} \quad (41)$$

Equating equations (40) and (41) yields the following expression for reinforcement ratio:

$$p = 0.85 f'_c B_1 (87,000) / (87,000 f_y + f_y^2) \quad (42)$$

Equation (42) is valid for a rectangular beam with tension reinforcement only. The ACI Building Code Commentary (74) derives a similar expression for a rectangular beam with both tension and compression reinforcement; this situation is a closer approximation to what is experienced in a ship hull girder. Figure 9 presents the pertinent notation. From the strain triangle at balanced conditions, the stress in the compression steel ( $f'_s$ ) is:

$$\begin{aligned} f'_s &= E_s e'_s \\ &= E_s ((k d - d') / k d) (0.003) \end{aligned} \quad (43)$$



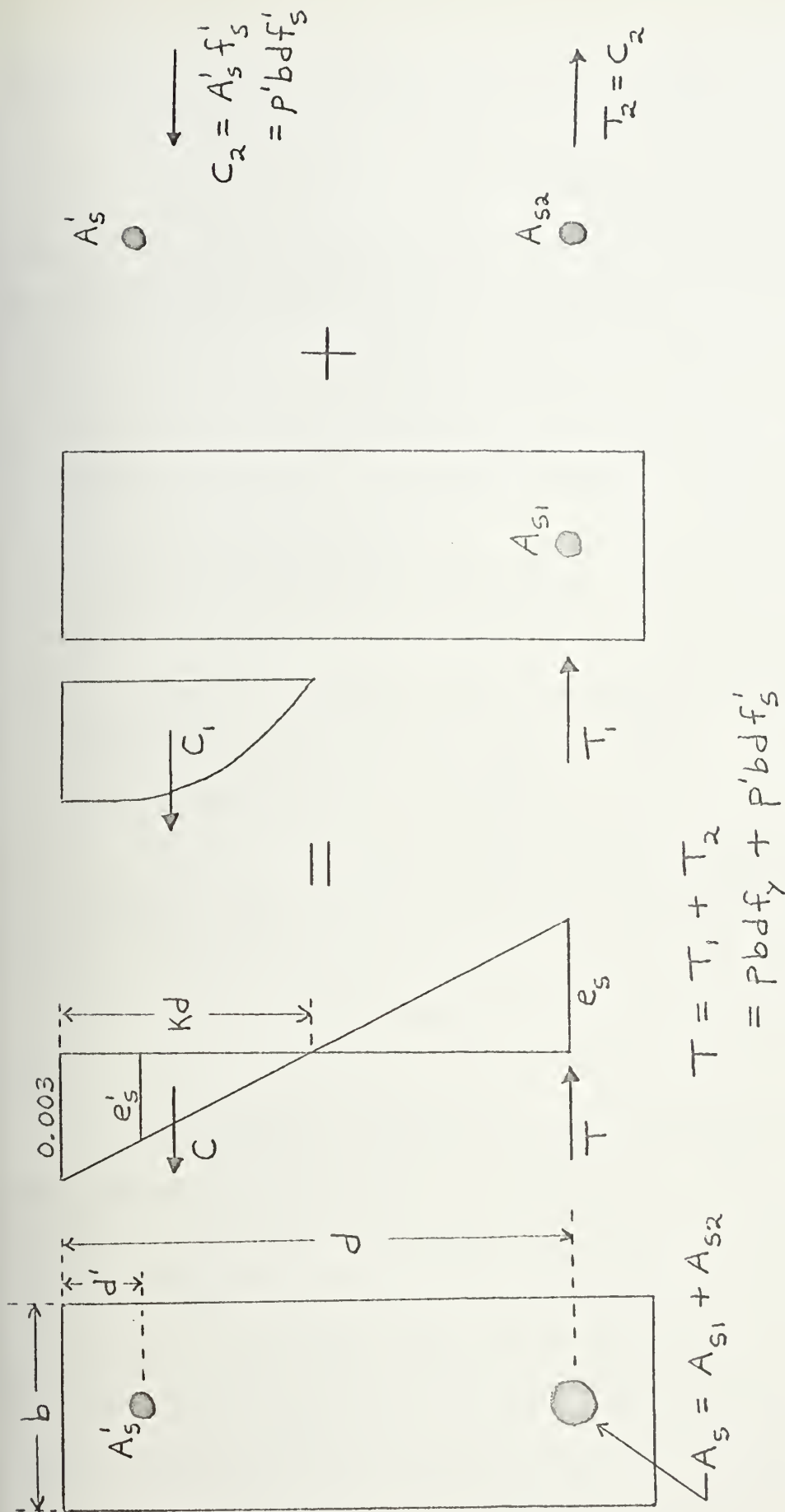


FIGURE 9

RECTANGULAR BEAM WITH BOTH TENSION AND COMPRESSION REINFORCEMENT





Equation (43) can be rewritten as:

$$\begin{aligned} f'_s &= 87,000 (1 - d'/kd) \\ &= 87,000 (1 - (d'(87,000 + f_y)/87,000d)) \quad (43a) \end{aligned}$$

where  $f'_s$  is less than or equal to  $f_y$ . The total reinforcement ratio ( $p_t$ ) is then equal to:

$$p_t = p + p'f'_s/f_y \quad (44)$$

where  $p'$  is the reinforcement ratio ( $A'_s/bd$ ) of the compression steel, and  $p$  is the reinforcement ratio of the tension steel as calculated from equation (42).

The ACI Code further specifies that the strength of a member or cross-section, whether in terms of load, moment, shear, or stress, must be calculated with a "capacity reduction factor" ( $\phi$ ) included. For bending in reinforced concrete, the value of  $\phi = 0.90$  is to be used. Thus, to be precise, the expressions for  $T$  and  $C$  in equations (40) and (41) should be multiplied by a factor of 0.90; however, in the solution for  $p$  in equation (42), the two  $\phi$ -factors would cancel each other out.

In determining the moment, on the other hand, the capacity reduction factor is essential. It is rather simple to establish the moment from the resisting couple. Referring again to Figure 8, the moment arm is given by:

$$z = jd = d - a/2 = d - B_1kd/2 \quad (45)$$

The moment is equivalent to either of the forces,  $C$  or  $T$ , multiplied by both the moment arm and the capacity



reduction factor:

$$\begin{aligned}
 M &= \phi Tz \\
 &= \phi (p b d f_y) (d - B_1 k d / 2) \\
 &= 0.9 p f_y b d^2 (1 - B_1 k / 2) \quad (46)
 \end{aligned}$$

where  $k$  and  $p$  can be calculated from equations (39) and (42), respectively.

Two interesting comparisons with the foregoing developments can be made. The first concerns the reinforcement ratio, which has been shown elsewhere (22) to equal:

$$p = 1 / (f_s / f'_c - E_s / E_c + 1) \quad (47)$$

A comparison between equations (42) and (47) can be demonstrated by assigning some hypothetical values, say,  $f'_c = 3,000$  psi and  $f_s = 40,000$  psi. From equation (5a), the concrete modulus of elasticity is calculated to be  $E_c = 3.32 \times 10^6$  psi (assuming medium-weight concrete). Substitution into equations (42) and (47) leads to values of  $p = 0.0371$  and  $p = 0.1775$ , respectively. The significance of this difference lies in the fact that the value of 3.71 percent reinforcement is more of a minimum requirement, whereas the 17.75 percent figure is a typical value of reinforcement percentage encountered in the aforementioned Norwegian study (22).

A second comparison is between moment equations. The British Code (26) defines the ultimate moment of resistance, for rectangular beams without compression reinforcement, as the lesser of the values obtained from



equations (48) and (49).

$$M = 0.87 f_y A_s z \quad (48)$$

$$M = 0.15 f'_c b d^2 \quad (49)$$

Significantly, equation (48) is identical to its American counterpart in equation (46), except for the reduction factor 0.87 as opposed to 0.90.

For rectangular reinforced concrete beams with both tension and compression reinforcement, the British Code adopts the following formula, where notation is as defined in Figure 9:

$$M = 0.15 f'_c b d^2 + 0.72 f_y A'_s (d - d') \quad (50)$$

#### B. Bending of Prestressed Concrete Members

As seen from the preceding section, the uncracked stage of a reinforced beam is very short lived, because of the low tensile strength of the concrete. However, if some external or internal reaction can be applied to produce a state of compressive stress in the section prior to the application of external load, then before the section can crack, these initial compressive stresses must first be overcome. Thus the uncracked stage of the beam can be extended considerably. Such a procedure is termed "prestressing" and the resulting construction material "prestressed concrete".

#### 1. Flexural Analysis of Prestressed Concrete. In



the case of grouted post-tensioned beams, the strength of the section in flexure at the ultimate limit state can be calculated in a manner similar to that for reinforced concrete beams. This is so since all the assumptions in the latter case apply equally to the former, with the exception that the initial strain of the steel due to prestressing has to be taken into account in working out the force in the tendon.

It must be appreciated, however, that calculations relating to prestressed concrete, even in the so-called "elastic phase", can only be considered to be approximate. As in the case of all other materials, they are based on the twin hypotheses that sections that are plane before bending remain plane after bending, and on the proportionality of stress and strain.

The flexural analysis of a member prestressed by any method (pre- or post-tensioning) for all stages of loading, from fabrication through full design service loads, is built around the combined stress formula:

$$f = P/A \pm Mc/I \quad (51)$$

where  $f$  is stress in concrete,  $P$  is applied load,  $A$  is gross cross-sectional area of concrete,  $M$  is applied moment,  $c$  is distance from neutral axis to extreme fiber, and  $I$  is moment of inertia of the gross concrete section.

Normally, the use of this formula involves only externally applied direct loads and moments; however, the





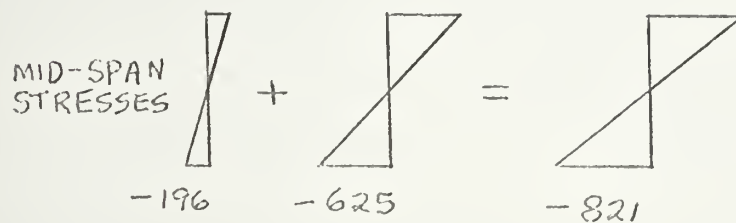
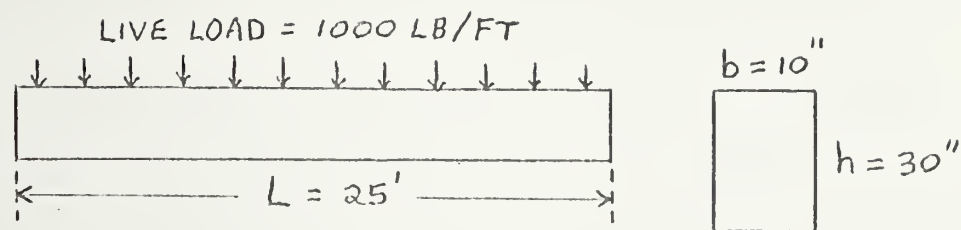
internal loads and moments created by the prestressing tendons become fundamental features of the analysis and design of prestressed concrete. The following example is illustrative (25): Figure 10 portrays two different beams -- one of plain concrete and the other of prestressed concrete. The bottom fiber stress at mid-span under the loaded concrete beam of Figure 10(a), with compressive strength of 5000 psi, is:

$$\begin{aligned} f_b &= -M_d/S - M_l/S \\ &= -(w_d L^2/8)/(bh^2/6) - (w_l L^2/8)/(bh^2/6) \\ &= -196 - 625 = -821 \text{ psi} \end{aligned}$$

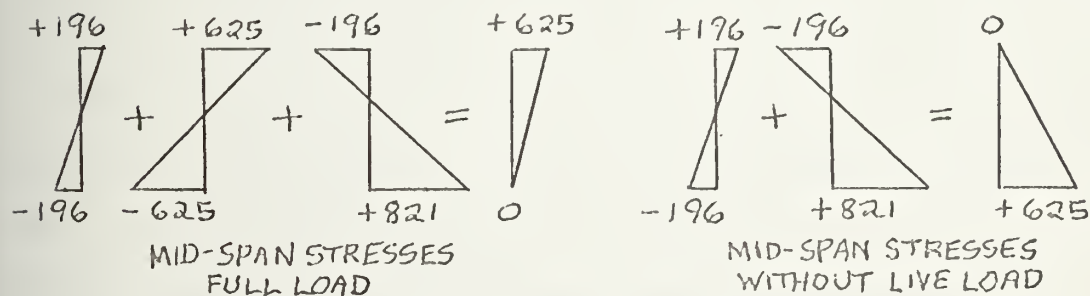
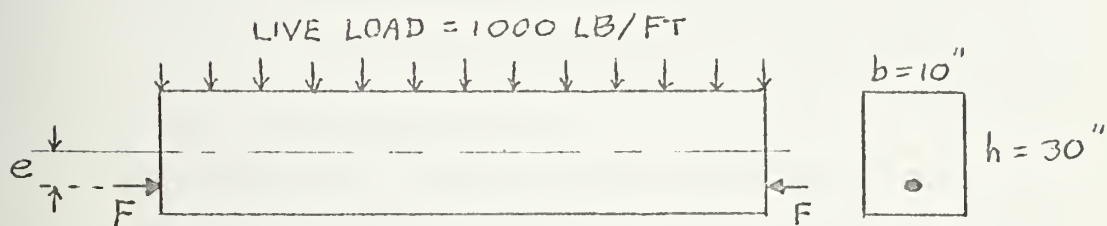
where  $S = I/c = bh^2/6$  is the section modulus, and subscripts d and l refer to "dead" and "live" loads.

This stress would likely exceed the tensile strength of the concrete. Recall that the maximum concrete compressive stress is limited to 0.45 times the cube strength at transfer, as indicated in Chapter II. The maximum tensile stress is limited to  $1.0 \text{ N/mm}^2$  (145 psi) for Class 1 structures (65), and to the values given in Tables 8 or 9 for Class 2 or 3. If an eccentric load were applied to the ends of the beam so that the resulting stress in the bottom fiber at mid-span equals 821 psi or greater, no tension would likely be expected to exist in the concrete at mid-span, as shown in Figure 10(b). In order to achieve the greatest compression in the bottom fibers with the least force,  $F$ , it must be applied with





(a) Plain Concrete Beam



(b) Prestressed Concrete Beam

FIGURE 10

DETERMINATION OF STRESSES



the greatest eccentricity possible. Allowing 2 inches to the center of the prestressing steel for concrete cover, the eccentricity ( $e$ ) becomes 13 inches. Solution of the following expression yields the force required to produce a final bottom fiber stress of zero.

$$\begin{aligned} f_b &= 0 = F/A + Fe/S - M_d/S - M_l/S \\ &= F/300 + 13F/1500 - 294,000/1500 \\ &\quad - 938,000/1500 \end{aligned} \quad (52)$$

Solving yields  $F = 68,500$  psi.

However, if the live load is not acting, the top fiber stress at mid-span is:

$$\begin{aligned} f_t &= F/A - Fe/S + M_d/S \\ &= -170 \text{ psi} \end{aligned} \quad (53)$$

In order to have no tensile stresses under any conditions of loading (Class 1 criterion), the eccentricity must be reduced and the prestress must be increased. Setting  $f_t = 0$  in equation (53), the simultaneous solution of equations (52) and (53) for  $F$  and  $e$  yields:

$$\begin{aligned} F &= 94,000 \text{ lb} \\ \text{and} \\ e &= 8.1 \text{ inches} \end{aligned}$$

Between the stage of transfer and the working condition, there occur various losses of prestress. These losses must be taken into account in determining the effective prestressing force for use in subsequent calculations. As indicated in Chapter II, steel stress losses are usually assumed to be 25,000 psi in



post-tensioned structures. An illustrative example is to determine the allowable uniform load that a 12" by 26" rectangular beam can carry over a simple span of 36 feet, given that  $f'_c = 5000$  psi,  $f_{pu} = 250,000$  psi, and the post-tensioning steel consists of ten 1/2" strands in 2 rows of 5 strands each, with 2" between rows and a 2" concrete cover. Assume also that the allowable bottom fiber tension  $= 6(f'_c)^{0.5} = -425$  psi, using equation (10).

Taking into account prestressing losses, the prestressing force can be determined as follows:

$$\begin{aligned} F &= (\text{steel area})(\text{steel stress}) \\ &= (10)(0.144)(250,000(0.7) - 25,000) \\ &= 216,000 \text{ lb} \end{aligned}$$

where the area of 1/2" diameter 250 ksi ASTM A-416-68 strand is 0.144 in<sup>2</sup> as per reference (75), and the stress in prestressing tendons immediately after transfer is  $0.7f_{pu}$ , as noted in Chapter II. Since  $A = (26)(12) = 312$  in<sup>2</sup>,  $e = 13 - 3 = 10$  in, and  $S = (12)(26)^2/6 = 1352$  in<sup>3</sup>, the total load ( $w$ ) can be solved from the following:

$$\begin{aligned} f_b &= F/A + Fe/S - wL^2/8S = -425 \\ &= 216,000/312 + (216,000)(10)/1352 \\ &\quad - w(36)^2(12)/(8)(1352) \end{aligned}$$

or,  $w = 1,888$  lb/ft. Assuming a medium-weight concrete (150 lb/ft<sup>3</sup>), the weight of the beam  $= (150)(312)/(144) = 325$  lb/ft. Thus, the allowable superimposed load





is:

$$w_1 = 1888 - 325 = 1563 \text{ lb/ft.}$$

## 2. Use of Codes in Prestressed Concrete Bending.

Formulae for the ultimate moment of ordinary reinforced concrete beams were presented in equations (46), (48), (49) and (50). Determination of the ultimate flexural capacity of prestressed concrete is also an important part of design procedure. The Prestressed Concrete Institute (25) adopts the following ultimate flexural strength formula:

$$M_u = bd^2 f'_c q (1 - 0.59q) \quad (54)$$

where  $M_u$  is the ultimate moment, and  $q$  is the reinforcement percentage index,  $p_p f_{pu} / f'_c$ .

The American Concrete Institute (74) presents this formula in a slightly different manner, and currently refers to ultimate flexural strength as "design strength":

$$M_u = \phi (A_{ps} f_{ps} d (1 - 0.59q')) \quad (55)$$

where  $A_{ps}$  is area of prestressed reinforcement in the tension zone,  $f_{ps}$  is calculated stress in prestressing steel at design load, and  $q' = p_p f_{ps} / f'_c$ , where

$p_p = A_{ps} / bd$ . In lieu of a more precise determination of  $f_{ps}$  based on strain compatibility, the following approximate value may be used:

$$f_{ps} = f_{pu} (1 - 0.5 p_p f_{pu} / f'_c) \quad (56)$$

The British Code employs a less complicated formula



for calculation of the ultimate moment:

$$M_u = f_{pb} A_{ps} (d - 0.5x) \quad (57)$$

where  $f_{pb}$  is the tensile stress in the tendons at failure, and  $x$  is the neutral axis depth. Table 11 presents values of  $f_{pb}$  and  $x$  for post-tensioned members with effective bond between the concrete and tendons. Notice that the left-hand column heading is identical to the index  $q$  in equation (54), and the right-hand column is equivalent to  $k$  in equation (37). If prestressing tendons and additional (nonprestressed) reinforcement are in the compression zone, as would be the case in a ship hull girder, they should be ignored in strength calculations when using this method (26).

### C. Bending of Post-Tensioned Reinforced Concrete Members

The addition of nonprestressed reinforcement to a post-tensioned member offers even further advantages over the latter. Complementary reinforcement tends to restrict the opening of cracks, if they occur, and it spreads them out so that they take the form of closely spaced fine fissures, or microcracks (63, 76). Also, if the tensile stress in a prestressed concrete member exceeds the allowable stress given in Tables 8 or 9, the stress can be kept within permissible limits by reducing the prestress force to about 60 percent of the original value and providing the remaining tensile resistance by



TABLE 11

STRESS IN POST-TENSIONING TENDONS FOR  
 DETERMINATION OF ULTIMATE MOMENT  
 (EQUATION 57)

$(f_{pu}A_{ps})/(f'_c b d)$	Stress in tendons as a proportion of design strength, $f_{pb}/0.87f_{pu}$	Ratio of depth of neutral axis to that of the centroid of the tendons in the tension zone, $x/d$
0.025	1.0	0.054
0.05	1.0	0.109
0.10	1.0	0.217
0.15	1.0	0.326
0.20	0.95	0.414
0.25	0.90	0.488
0.30	0.85	0.558
0.40	0.75	0.653



supplementary nonprestressed reinforcement (65). This additional non-tensioned reinforcement is also helpful in reducing creep deformations under dead load, for crack control under full live load, and for reducing tensile forces in the webs of girders due to shear (64).

The disadvantage, however, is that there has been a lack of sufficient understanding of the behavior of prestressed concrete beams containing non-tensioned steel. The use of non-tensioned steel in prestressed concrete has been referred to as partial prestressing (64), which, in general, is taken to mean either or both of the following conditions:

- (1) Tensile stresses are permitted under working loads.
- (2) Non-tensioned steel is used in addition to tensioned prestressing steel.

Some work on partial prestressing has been done in the last twenty years (76, 77, 78, 79, 80), but most of it deals with the form of partial prestressing defined under item (1) above. Abeles (78) mentions that "with more non-tensioned steel of lower strength, as compared to less non-tensioned steel of higher strength, the loss of prestress will be directly more. However, as better control on cracking is likely, a vital need for research in this direction exists."





# 1. Synthesis of Reinforced and Prestressed Concrete.

As can be observed from the preceding section, the presence of non-prestressed tensile and compressive reinforcement in prestressed concrete beams is not taken systematically into account by the Codes in the formulae for ultimate moment capacity. A recent attempt has been made (81) to arrive at a general procedure for the design of ultimate moment capacity of prestressed concrete beams in which auxiliary non-prestressed reinforcement is automatically accounted for.

In order to compute the ultimate resisting moment, it is first necessary to determine the stress in the prestressing steel at ultimate capacity of the beam ( $f_{ps}$ ). When the effective stress in the prestressing steel after all losses ( $f_{se}$ ) is greater than or equal to half its ultimate strength ( $f_{pu}$ ), equation (56) may be used to calculate  $f_{ps}$ . On the other hand, if  $f_{se}$  is less than  $0.5f_{pu}$ , then a compatibility check is required.

Once the stress in the steel at ultimate capacity of the beam has been determined, equilibrium of the forces in the section and the corresponding ultimate moment are easily computed. If there is prestressed reinforcement only, the percentage index is as given in section B:

$$\begin{aligned} q' &= p_p f_{ps} / f'_c \\ &= A_{ps} f_{ps} / b d f'_c \end{aligned} \quad (58)$$



However, if there is non-prestressed tension and/or compression reinforcement as well, equation (58) is modified as follows:

$$q' = A_{ps}f_{ps}/bdf'_c + A_s f_y / bdf'_c - A'_s f'_y / bdf'_c \quad (59)$$

where  $f'_y$  is the yield strength of non-prestressed conventional reinforcement in compression.

The ACI Code (13) recommends the use of  $q'_{max} = 0.3$  as a practical design limit between normally and over-reinforced members. Hence, for over-reinforced beams ( $q'$  exceeds 0.3), the ultimate moment is given by:

$$M_u = \phi (0.25f'_c b d^2 + A'_s f'_y (d - d')) \quad (60)$$

For normally or under-reinforced beams ( $q'$  is less than or equal to 0.3), the ultimate moment is a modification of equation (55):

$$M_u = \phi (A_{ps} f_{ps} d (1 - 0.59q') + A_s f_y d (1 - 0.59q')) \quad (61)$$

It can be seen that when prestressing steel is nonexistent, equation (61) is the same as for a reinforced concrete beam.

Once the ultimate resisting moment of a beam has been calculated, it must be compared to the cracking moment ( $M_{cr}$ ) and to the ultimate design or service moment ( $M_s$ ). Both the ACI (13) and AASHTO (82) Codes specify that the ultimate resisting moment must be at least equal to 1.2 times the cracking moment, in order to ensure ductile (non-brittle) behavior. However, they



differ on the value to assign to the ultimate service moment. For example, the ACI Code suggests the value of:

$$M_s = 1.4M_d + 1.7M_l + 1.4M_f \quad (62a)$$

whereas the corresponding AASHTO formula is:

$$M_s = 1.3(M_d + 5M_l(1 + I)/3) \quad (62b)$$

where  $M_d$ ,  $M_l$ , and  $M_f$  are moments due to dead loads, live loads, and hydrostatic forces, respectively, and  $I$  is the impact coefficient.

Gerwick (23) is slightly more conservative than the ACI Code in that he recommends that the ultimate moment must exceed the cracking moment by a factor of 1.3 (as opposed to 1.2). Furthermore, when impact is applicable, he adds a factor of  $2.0I$  to equation (62a). In the case of ships, the design wave produces hogging and sagging in the vessel; hence, a factor of  $1.0M_w$  is also included to cover the effect of the design wave bending moment. Thus, equation (62a) becomes:

$$M_s = 1.4M_d + 1.7M_l + 1.4M_f + M_w + 2I \quad (63)$$

2. Calculation of Section Properties. One problem in dealing with concrete members consisting of both prestressing and non-tensioned steel is that of calculating the section properties. A convenient method employed in Germany (83) is to combine the respective cross-sectional areas of both the post-tensioned tendon



ducts and of the prestressing steel itself as rectangular areas with the centroid located at the appropriate level in the section, as shown in Figure 11(a). Figure 11(b) denotes the terminology for the respective centroids and distances. For clarification of the forthcoming equations, the symbols are defined below:

$A_g$  = total (gross) cross-sectional area of concrete,  
without deducting steel areas

$A_d$  = cross-sectional area of duct(s)

$A_{ps}$  = cross-sectional area of prestressing steel

$A_s$  = cross-sectional area of non-tensioned steel  
(can usually be neglected)

$A_n$  = net cross-sectional area of concrete

=  $A_g - A_d$  (or  $A_g - A_s - A_d$ )

$A_e$  = effective cross-sectional area of concrete

=  $A_g + (n - 1)A_{ps}$ , or,  $A_g + (n - 1)(A_{ps} + A_s)$

$I_e$ ,  $I_g$ , and

$I_n$  = effective, gross, and net moments of inertia

$I_{ps}$  and

$I_d$  = moment of inertia of the prestressing steel areas and of the duct areas, taken about their own centroidal axes (these moments of inertia are generally very small and are neglected)

$S_{tn}$  and

$S_{bn}$  = net section modulus at top and bottom

$e$  = distance to centroid of  $A_g$





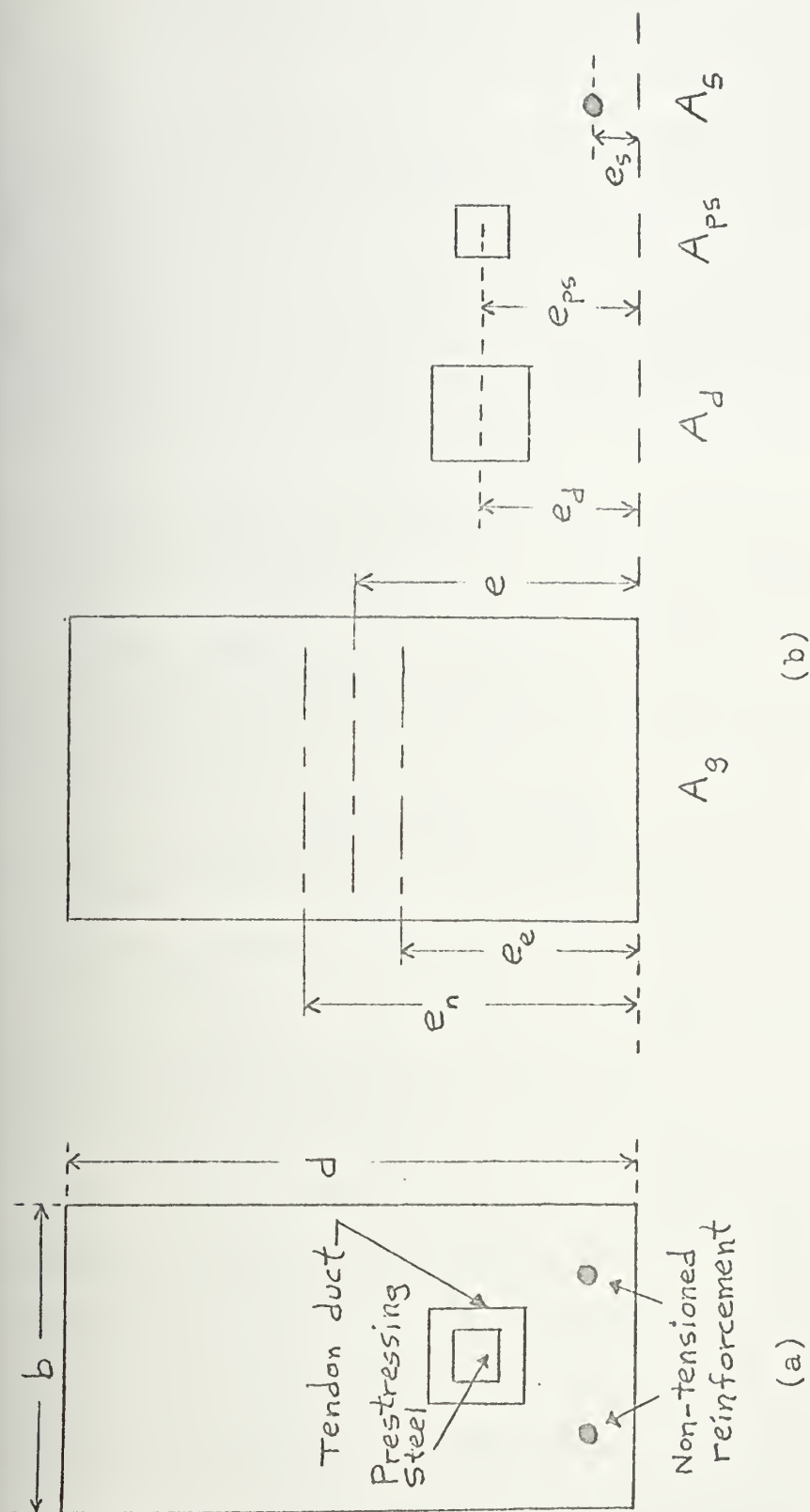


FIGURE 11  
POST-TENSIONED REINFORCED CONCRETE BEAM



$e_d$  = distance to centroid of duct  $A_d$

$e_{ps}$  = distance to centroid of prestressing steel  $A_{ps}$

$e_s$  = distance to centroid of non-tensioned steel  $A_s$

$e_n$  = distance to centroid of net section  $A_n$

$e_e$  = distance to centroid of effective section  $A_e$ .

The calculations of the section properties can then be carried out in the following sequence:

#### Net Values

$$A_n = A_g - A_d \quad (64)$$

$$e_n = (eA_g - e_d A_d) / A_n \quad (65)$$

$$I_n = I_g + A_g (e_n - e)^2 - A_d (e_n - e_d)^2 \quad (66)$$

$$S_{tn} = I_n / (d - e_n) \quad (67)$$

$$S_{bn} = I_n / e_n \quad (68)$$

#### Effective Values

$$A_e = A_g + (n - 1)A_{ps} \quad (64a)$$

$$e_e = (eA_g + (n - 1)e_{ps} A_{ps}) / A_e \quad (65a)$$

$$I_e = I_g + A_g (e - e_e)^2 + (n - 1)A_{ps} (e_e - e_{ps})^2 \quad (66a)$$

$$S_{te} = I_e / (d - e_e) \quad (67a)$$

$$S_{be} = I_e / e_e \quad (68a)$$

The longitudinal stresses can finally be determined, given the axial force (component of prestressing force  $N_p$ ), and bending moments due to prestress ( $M_p$ ), dead load ( $M_d$ ) and live load ( $M_l$ ). The stress at the top of a post-tensioned reinforced concrete beam is thus:

$$f_t = N_p / A_n - (M_d + M_p) / S_{tn} - M_l / S_{te} \quad (69)$$



and the stress at the bottom of the beam is:

$$f_b = N_p/A_n + (M_d + M_p)/S_{bn} + M_l/S_{be} \quad (70)$$

3. Applications. In anticipation of designing the midship section of a ship, a beneficial tool would be a closed form solution for the required amounts of ordinary reinforcing steel ( $A_s$ ) and post-tensioning steel tendons ( $A_{ps}$ ). The required reinforcing steel area is simply calculated from equation (36):

$$A_s = M/(f_s j d) \quad (36)$$

where depth ( $d$ ) is assumed,  $j$  is found from equation (38) in conjunction with equation (37), and the moment is given by equation (49):

$$M = 0.15f'_c b d^2 \quad (49)$$

The required post-tensioning steel tendon area can then be calculated as below, the derivation of which appears in Appendix H:

$$A_{ps} = F/f_{ps} \quad (71)$$

where the prestressing force ( $F$ ) equals:

$$F = (\max f_c + \max f_t)A/2 \quad (71a)$$

and  $A$  is the gross cross-sectional area. With the stress limitations adopted in Appendix F, equation (71) becomes:

$$A_{ps} = 2585A/2f_{ps} \quad (71b)$$

An alternative method of determining the area of post-tensioning steel, given the area of nonprestressed reinforcement from equation (36), is by utilizing a



modification of equation (59):

$$q' = A_{ps}f_{ps}/bdf'_c + A_sf_y/bdf'_c \quad (72)$$

Since the ACI Code recommends the use of  $q'_{\max} = 0.3$  as the division between normally and over-reinforced members in land-based structures, it is not unreasonable to adopt a slightly higher value (e.g.,  $q'_{\max} = 0.35$  or  $0.40$ ) for use in ocean-going structures, due to the more severe loading conditions inherent in the latter. Hence, equation (72) can be solved for  $A_{ps}$ , and, as Appendix H demonstrates, yields results remarkably similar to equation (71b).

Appendix I is yet another method for determining  $A_s$  and  $A_{ps}$ . This particular technique is based on the formulae presented in the preceding section, and deals with both non-prestressed and prestressed reinforcement simultaneously. However, since it is necessary to assume the location of both the  $A_s$  and  $A_{ps}$  centers of gravity, as well as that of the net section, this method is not deemed as accurate as the method of Appendix H.

A general conclusion to be drawn from Appendix H is that as the gross cross-sectional area increases (specifically as depth increases), the required area of non-prestressed reinforcement ( $A_s$ ) decreases (for constant moment); on the other hand, the required area of prestressed tendons ( $A_{ps}$ ) increases, if the gross area increases. Results also confirm equation (72) in that,





for a constant  $q'_{\max}$  and gross cross-sectional area, as the area of nonprestressed reinforcement increases, the required area of post-tensioned tendons decreases. The amounts of steel calculated from equations (36), (71) and/or (72) can, thus, be employed in the preliminary stages of designing the midship section for a post-tensioned reinforced concrete ship.



## CHAPTER V

APPLICATION TO THE DESIGN OF  
A TANKER MIDSHIP SECTION

There is currently a widespread interest in the application of prestressed concrete to sea structures. Prestressed concrete barges have recently been built in Hawaii (24), Russia (84), and even Fiji (85). The International Federation of Prestressed Concrete (F.I.P.) has published recommendations for the design of concrete sea structures (86), albeit they are not applicable to ships. Perhaps one of the most promising prospects for applying prestressed concrete to ships is in the construction of liquified natural gas (LNG) carriers (87, 88, 89). Indeed, having discussed the principles, permissible stresses, material selection, design considerations, and flexural analysis of post-tensioned reinforced concrete, it is now fitting to apply this knowledge to the design of a ship.

A crucial aspect in the design of a post-tensioned reinforced concrete ship is establishing its structural feasibility; and the most important structural problem is undoubtedly the design of the midship section. It has been said (90) that "since the hull scantlings for a vessel's full length are generally derived from those obtained amidships, a correctly conceived and developed



midship section insures, to a large degree, adequate strength for the whole vessel."

#### A. Calculation of Section Modulus

It is an easy task to determine the moment of inertia (I) or section modulus ( $S = I/c$ ) of a simple, homogeneous beam; however, the bookkeeping becomes a bit more complicated when dealing with a post-tensioned reinforced concrete structure. Therefore, before proceeding to the calculation of section modulus for a midship section, the procedure will first be illustrated by considering a post-tensioned reinforced concrete beam.

Before continuing, however, a preliminary step is the determination of concrete modulus of elasticity. Recall from equation (5a) that

$$E_c = 33(W^3 f'_c)^{0.5}$$

for values of W between 90 and 155 pcf. For the concrete mix selected in Chapter II ( $f'_c = 7,000$  psi and  $W = 125.5$  pcf), the value of  $E_c$  is calculated to be  $3.88 \times 10^6$  psi.

Since the modulus of elasticity of nonprestressed steel reinforcement,  $E_s$ , is taken as  $29 \times 10^6$  psi (13), the modular ratio is found to be  $n = E_s/E_c = 29/3.88 = 7.47$ . The ACI Code specifies that the modular ratio can be rounded off to the nearest whole number; hence,  $n = 7$  for the concrete mix selected.



# 1. Post-Tensioned Reinforced Concrete Beam.      Suppose

a post-tensioned reinforced concrete beam consists of rods on both the tension and compression sides, as indicated in Figure 12(a). Assume that this beam represents a portion of the transverse section of a ship hull, with the lower side coinciding with the outer skin of the ship; hence, notice that the concrete cover is greater on that side of the beam which will come in contact with water forces. As a result, the neutral axis will not lie at mid-plane.

To calculate the section modulus, the location of the neutral axis and the moment of inertia about the neutral axis must be determined. It is necessary to first divide the cross-section into several sub-sections, preferably arranging boundaries such that each sub-section has its center of gravity at its midpoint. Figure 12(b) is one such division of Figure 12(a).

The standard method of calculation (91) will be employed, with the following modifications:

$$A_g = \text{gross area of a sub-section} = bh$$

$$h = \text{depth of sub-section}$$

$$A_s = \text{steel area}$$

$$A_{eq} = \text{equivalent concrete area}$$

$$= A_g - A_s + nA_s \quad (73)$$

The remaining terminology is standard, i.e.:

$$d_n = \text{distance from the sub-section center of}$$





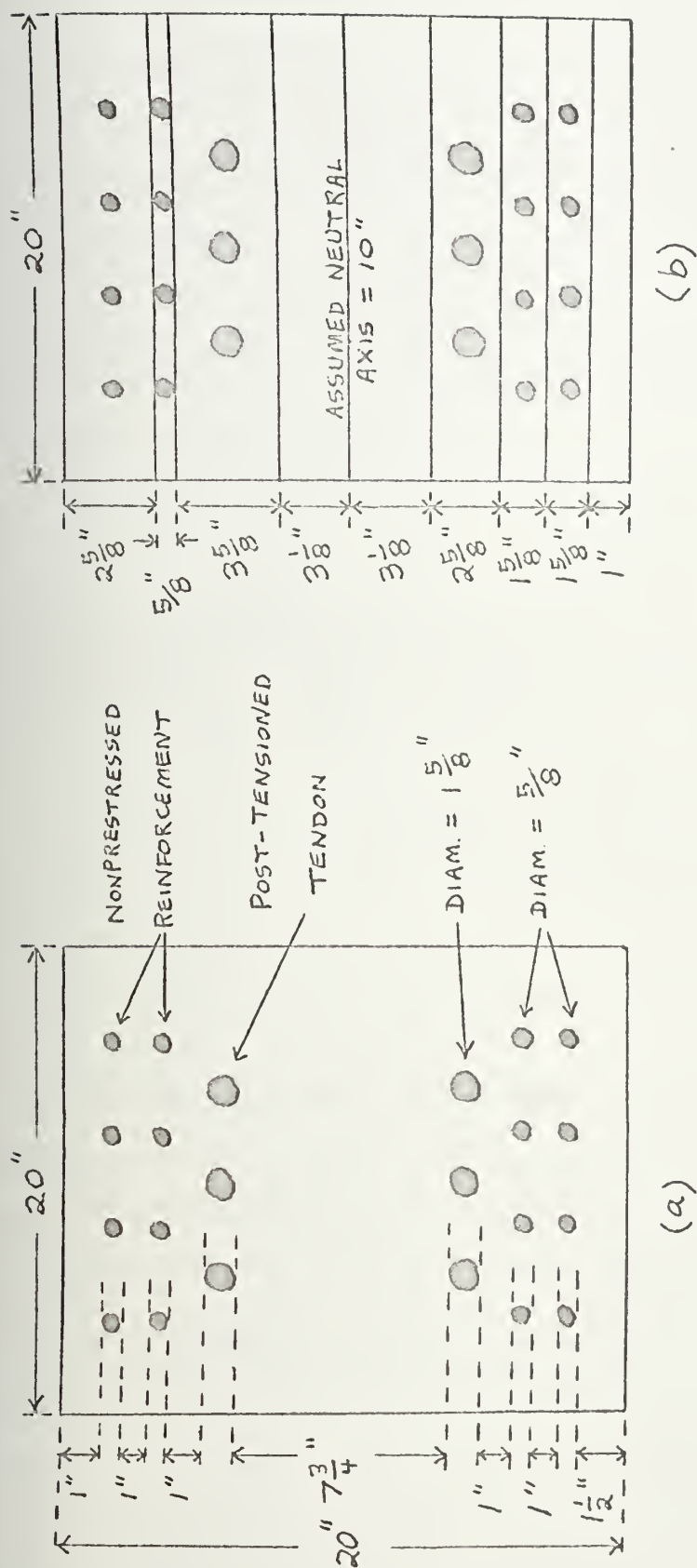


FIGURE 12  
POST-TENSIONED REINFORCED CONCRETE BEAM WITH  
BOTH TENSION AND COMPRESSION REINFORCEMENT



gravity to the assumed neutral axis

$$\text{and } i_o = bh^3/12$$

The moment of inertia about the neutral axis is thus:

$$I = \sum(A_{eq}d_n^2 + i_o) \quad (74)$$

and the neutral axis is situated  $(d/2 + d_g)$  inches above the base, where:

$$d_g = \sum(A_{eq}d_n)/\sum A_{eq} \quad (75)$$

Table 12 summarizes the method of calculation and the results.

For the example in Figure 12, the neutral axis is found, using equation (75), to be located 10.05 inches above the base; from equation (74), the moment of inertia is 15,094 in<sup>4</sup>. Hence, the section modulus at the bottom of the beam, is, from equation (68):

$$S_b = 15,094/10.05 = 1,502 \text{ in}^3$$

and, from equation (67), the section modulus at the top of the beam is:

$$S_t = 15,094/9.95 = 1,517 \text{ in}^3$$

## 2. Computerized Extension to a Tanker Midship

Section. A computer program has been written (92) to extend the aforementioned procedure in order to calculate the midship section modulus of a post-tensioned reinforced concrete liquified natural gas (LNG) tanker. In essence, the method divides the midship section into numerous thin slices, where each slice is approximated as a trapezoid;



TABLE 12

CALCULATION OF NEUTRAL AXIS LOCATION AND  
MOMENT OF INERTIA FOR EXAMPLE IN FIGURE 12

Sub- Section	<u>h</u>	<u>A<sub>g</sub></u>	<u>A<sub>s</sub></u>	<u>A<sub>eq</sub></u>	<u>d<sub>n</sub></u>	<u>A<sub>eq</sub>d<sub>n</sub></u>	<u>A<sub>eq</sub>d<sub>n</sub><sup>2</sup></u>	<u>i<sub>o</sub></u>
1	2.625	52.5	1.23	59.88	8.688	520.24	4,519.8	30.15
2	0.625	12.5	1.23	19.88	7.063	140.41	991.7	0.41
3	3.625	72.5	6.22	109.82	4.938	542.29	2,677.8	79.39
4	3.125	62.5	0.0	62.50	1.563	97.69	152.7	50.86
5	3.125	62.5	0.0	62.50	-1.563	-97.69	152.7	50.86
6	2.625	52.5	6.22	89.82	-4.438	-398.62	1,769.1	30.15
7	1.625	32.5	1.23	39.88	-6.563	-261.73	1,717.8	7.15
8	1.625	32.5	1.23	39.88	-8.188	-326.54	2,673.7	7.15
9	1.0	20.0	0.0	20.0	-9.5	-190.0	180.5	1.67
				<u>504.16</u>		<u>+26.05</u>	<u>14,835.8</u>	<u>257.8</u>



this extensive subdivision accounts for the curvature of the hull cross-section. By reading in the dimensions and distance from the baseline of each slice, as well as the number, area, and distance from the baseline of both reinforcing rods and post-tensioning tendons in each slice, the methodology of the preceding section is basically followed to calculate the section modulus.

The only significant departure lies in the determination of section modulus for hogging and sagging conditions; in each case, the supplemental transverse reinforcement is neglected and deducted from the tension side. For example, to find the section modulus in the sagging condition, the amount of transverse reinforcement is deducted from the net concrete area of each slice below the neutral axis; for the hogging condition, the amount of transverse reinforcement is deducted from the net concrete area of each slice above the neutral axis.

#### B. Effect on Tanker Midship Section Modulus of Varying Key Parameters

As observed in the first section of Chapter IV and documented in Appendix F, the addition of reinforcement to an ordinary reinforced concrete beam increases the section modulus, whereas the reduction of cross-section depth tends to decrease the section modulus. In a post-tensioned reinforced concrete tanker midship section, many





parameters are involved, for example: (a) concrete cover thickness, (b) post-tensioning tendon strength, (c) tendon diameter, (d) tendon area (i.e., number of tendons), (e) ordinary reinforcement strength, (f) reinforcing bar diameter, (g) reinforcement area, (h) modular ratio,  $n$ , and (i) overall midship section dimensions, namely, depth and breadth.

#### 1. Selection of Parameter Range of Values. By

letting these parameters vary, the effect on a tanker midship section modulus can be determined with recourse to the aforementioned computer program. Utilizing the knowledge gleaned in Chapters II and III, realistic ranges of values can be assigned to the above parameters:

(a) Concrete cover thickness. Reference (63) states that "whatever the nature of the steel, a minimum cover of 2 cm (0.787 in) to the bare steel is necessary." Reference (39) mentions the impracticality and lack of benefits accrued in employing cover thicknesses exceeding 2 inches. Hence, a reasonable range of values would logically be 1 inch to 2 inches.

(b) Tendon strength. Table 5 shows tendon strength varying from 42,000 to 298,000 psi, although Gerwick (43) gives the typical strength of post-tensioning bars (as opposed to strands and wires) as 140,000 to 165,000 psi.

(c) Tendon diameter. There is less speculation in



pinpointing the range of this parameter, since post-tensioning steel bars are commercially available in only four sizes: 18 mm (0.71 in), 24 mm, 27 mm, and 33 mm (1.3 in).

(d) Tendon area. There exists no standard upon which to base a typical range of values, hence, the method of Appendix H will be employed to determine the required area. Rod spacing guidelines of Chapter III must, of course, be adhered to.

(e) Ordinary reinforcement strength. Once again the choice is limited, as reinforcing bars are available in only three grades: 40, 60, and 75 ksi.

(f) Reinforcement diameter. Table 4 summarizes the reinforcing bar sizes, which range from 3/8 to 1-3/8 inch in diameter.

(g) Reinforcement area. The comments under tendon area are applicable here.

(h) Modular ratio. As indicated in Appendix B,  $n = E_s/E_c$  typically ranges from 6 to 15.

(i) Overall midship section size. In actual ship design, the principal ship dimensions (length, breadth, and depth) have already been determined by the time the midship section is to be designed. Thus, the overall midship section dimensions have, in fact, actually been established. However, since the effect of varying depth



was rather extensively discussed in Chapter IV, it will likewise be a parameter in the present consideration.

Summing up, it is apparent that there are six key parameters (excluding depth and breadth) which may have a significant effect on section modulus: concrete cover thickness, tendon diameter, tendon area, ordinary reinforcement diameter and area, and modular ratio.

2. Application of Computer Program. The computer program previously alluded to has been modified (see Appendix J) to permit all the preceding key parameters to be input data. The program is also simplified in two ways: (a) a box girder midship section is considered, which obviates the necessity of subdividing the cross-section into an excessive number of slices; Figure 13 is such a midship section for a post-tensioned reinforced concrete ship; and (b) rather than deducting the amount of transverse reinforcement from the net concrete area of each slice and using that result to in turn calculate the moment and moment of inertia of each slice, a percentage of total steel area (219 percent for sagging and 235.5 percent for hogging) is deducted from the sum of the areas; a similar factor is subtracted from both the sum of the moments and the sum of the moments of inertia.

Despite these seemingly over-simplifying assumptions, results of the two computer programs are quite compatible.



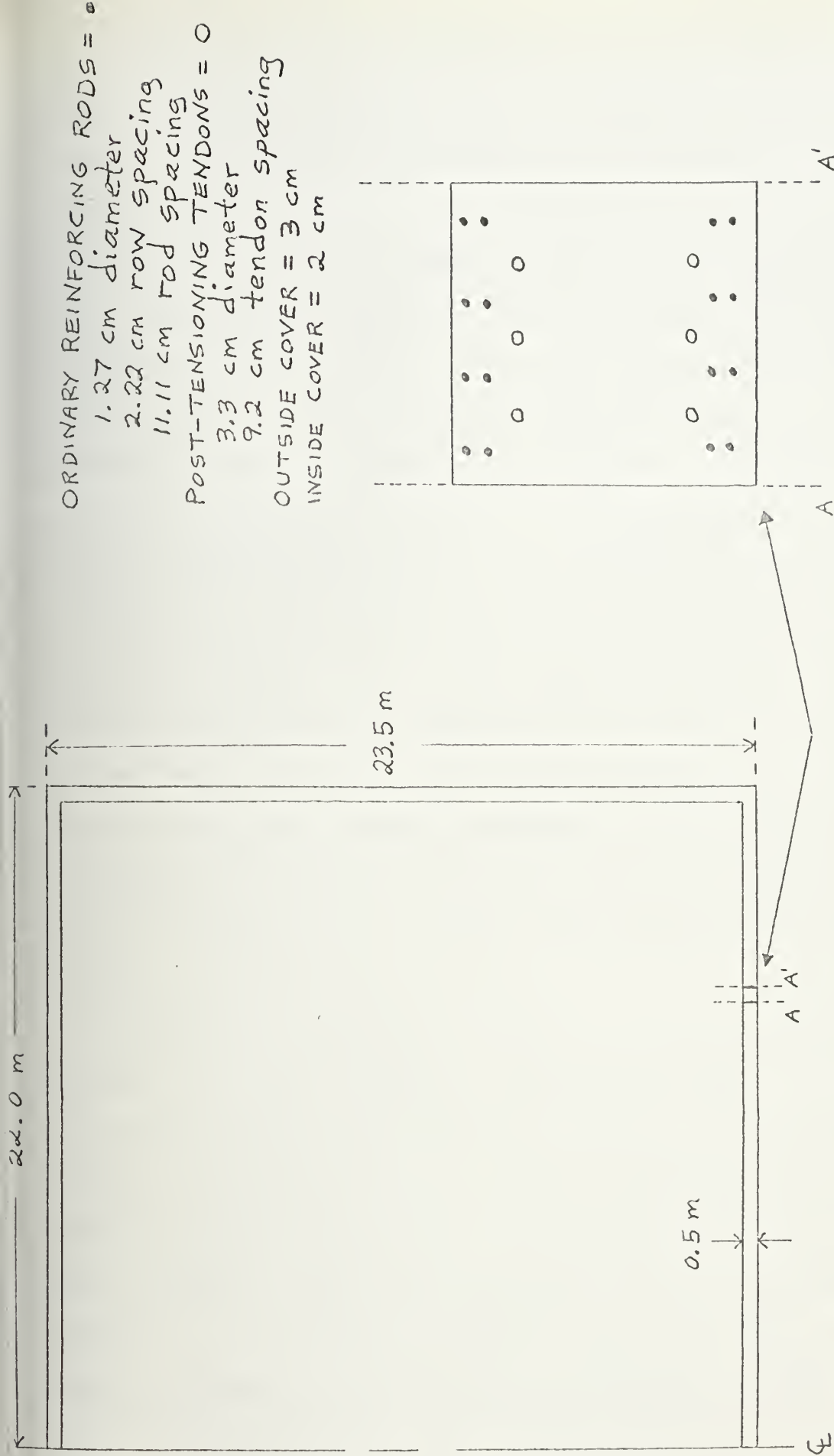


FIGURE 13: POST-TENSIONED REINFORCED CONCRETE RECTANGULAR MIDSHIP SECTION





The program of reference (92) determined the section modulus of an elliptical-shaped post-tensioned reinforced concrete LNG tanker by subdividing the midship section into thirty-nine trapezoidal slices; in the sagging condition, the section modulus at deck and bottom were  $626 \text{ m}^3$  and  $596 \text{ m}^3$ , respectively, while the corresponding values were  $573 \text{ m}^3$  and  $637 \text{ m}^3$  in the hogging condition. The modified computer program, which appears in Appendix J, calculated the section modulus of a rectangular midship section with the same depth and breadth as above by subdividing the cross-section into only three rectangular slices (see Figure 13); in the sagging condition, the section modulus at deck and bottom are  $691 \text{ m}^3$  and  $653 \text{ m}^3$ , respectively, while the corresponding values were  $650 \text{ m}^3$  and  $692 \text{ m}^3$  in the hogging condition. Thus, this grossly approximated rectangular midship section nevertheless yields results with an accuracy averaging within ten percent.

Appendix J contains not only the revised computer program, but also a typical input/output page. It is thus seen that the key parameters selected in the preceding section are all input data to this modified program, namely: modular ratio (YR), total reinforcing rod steel area (RDARSM), total post-tensioning steel area (TDARSM), reinforcing rod diameter (RDDIA), post-tensioning tendon diameter (TDNDIA), concrete cover thickness (COVER), ship



depth (DEPTH) and breadth (BREDTH).

By maintaining depth and breadth constant, and by choosing two different values for each of the remaining five parameters (excluding modular ratio), there exist thirty-two distinct combinations for investigation (twice this number, of course, when both hogging and sagging are considered). Limiting the number of parameter values to two is based solely on computer economics, as the increase of distinct combinations with increasing number of parameter values is exponential.

The following values of the five key parameters are selected:

- (a) reinforcing rod diameter (RDDIA):  
3/8" (0.95 cm); 3/4" (1.90 cm)
- (b) tendon diameter (TDNDIA):  
0.945" (2.4 cm); 1.3" (3.3 cm)
- (c) concrete cover thickness (COVER):  
1.25" (3.175 cm); 1.75" (4.445 cm)
- (d) total reinforcing rod area (RDARSM):  
1704 in<sup>2</sup> (1.1 m<sup>2</sup>); 2014 in<sup>2</sup> ( 1.3 m<sup>2</sup>)
- (e) total tendon area (TDARSM):  
1394 in<sup>2</sup> (0.9 m<sup>2</sup>); 1084 in<sup>2</sup> (0.7 m<sup>2</sup>)

The choice of the first three parameter values is self-explanatory. It should be noted, however, than an increase in concrete cover can be realized either by  
(a) increasing RODIST and TNDIST in the bottom slice, and



by decreasing same in the top slice (i.e., by merely shifting the steel towards the center of the slices); or (b) by physically increasing the depth of both top and bottom slices as well as the breadth of the side shell. In both cases, the overall depth is to remain unchanged.

The values of RDARSM and TDARSM are determined with the aid of formulae for  $A_s$  and  $A_{ps}$ , respectively, in Appendix H. It is first assumed that the concrete used has a compressive strength of 7,000 psi ( $500 \text{ kg/cm}^2$ ) as determined in Chapter II; the stress limitations are those in Appendix F;  $f_y = 60,000 \text{ psi}$  ( $4,219 \text{ kg/cm}^2$ );  $f_{pu} = 165,000 \text{ psi}$  ( $11,605 \text{ kg/cm}^2$ ); and the tanker cross-sectional dimensions and maximum moment are:

$$\text{depth} = 23.5 \text{ m}$$

$$\text{breadth} = 44.0 \text{ m}$$

$$M_{\max} = 700,000 \text{ tonne-meter.}$$

Hence, from equation (36):

$$\begin{aligned} A_s &= M/(f_s j d) \\ &= (700,000)/(0.8)(4,219)(0.83)(23.5) \\ &= 10,635 \text{ cm}^2 \end{aligned}$$

after multiplying by the conversion factor 1,000 kg/t, and assuming that the neutral axis is at half-depth (which gives a value of  $j = 0.83$ ). Substituting  $q' = 0.35$  into equation (72) yields:

$$\begin{aligned} A_{ps} &= (q' b d f'_c - A_s f_y)/f_{ps} \\ &= ((0.35)(691,000)(500) - (10,633)(4,219))/8,124 \end{aligned}$$



Or,  $A_{ps} = 9,365 \text{ cm}^2$

where  $f_{ps} = 0.7f_{pu} = 8,124 \text{ kg/cm}^2$ , and  $691,000 \text{ cm}^2$  represents the "bd"-term. (Note: In a solid beam, the gross area is given by bd; whereas in a rectangular ship hull girder, the gross area is equal to:

$$A_g = 2bt + 2(d - 2t)t \quad (76)$$

where  $t$  is the thickness of the top, bottom, and side shells. Thus, assuming a uniform hull thickness of 20.5 inches (0.52 m), the gross area of the tanker midship section is:

$$\begin{aligned} A_g &= 2(44.0)(0.52) + 2(23.5 - 1.04)(0.52) \\ &= 69.1 \text{ m}^2 = 691,000 \text{ cm}^2. \end{aligned}$$

From the given information, the required steel area is  $A_s + A_{ps} = 10,635 + 9,365 = 20,000 \text{ cm}^2$ , or,  $2.0 \text{ m}^2$ ; in other words, the required steel percentage is 2.9 percent. Consequently, two sets of values which satisfy this criterion are:

$$\begin{aligned} \text{and} \quad A_s &= 1.1 \text{ m}^2; A_{ps} = 0.9 \text{ m}^2 \\ A_s &= 1.3 \text{ m}^2; A_{ps} = 0.7 \text{ m}^2 \end{aligned}$$

### C. Results and Conclusions

Several different applications of the computer program were conducted. The principal results and conclusions of the various investigations are summarized herein.

#### 1. Treatment of Cover Thickness. A preliminary





decision to be made concerns the method of treating concrete cover. As previously indicated, there are basically two different ways to realize an increase in concrete cover: (a) keep the concrete area constant, but shift the steel towards the center of each slice; or (b) physically augment the gross area of the cross-section, although still maintain the same overall depth. Considering the original situation (before changing the cover) as Case 1, and alternatives (a) and (b) as Cases 2 and 3, respectively, the input data is as follows:

depth = 23.5 m

breadth = 44.0 m

rod area =  $0.55 \text{ m}^2$

tendon area =  $0.45 \text{ m}^2$

rod diameter = 0.0095 m

tendon diameter = 0.024 m

cover = 0.0317 m (for Case 1)

= 0.0381 m (for Cases 2 and 3)

The output of this preliminary computer run is summarized on the next page. It is apparent from Case 3 that increasing the concrete area results in a larger moment of inertia and a concomitant increase in section modulus. This is as anticipated; hence, alternative (b) -- physically increasing both sides of each slice by the amount of increased concrete thickness -- will be the method employed in forthcoming computer runs.



Case Number	1	2	3
Concrete area ( $m^2$ )	38.37	38.37	39.02
Moment of Inertia about the neutral axis ( $m^4$ )	3942.2	3941.2	4005.7
Neutral axis above base (m)	12.09	12.09	12.08
Section Modulus at deck ( $m^3$ )	345.37	345.27	350.76
Section Modulus at keel ( $m^3$ )	326.20	326.11	331.61

As a sidelight, however, Case 2 presents an interesting conclusion. With the identical concrete area and even steel area as in Case 1, Case 2 nevertheless has a slightly smaller moment of inertia and section modulus. This is attributed to the fact that in Case 1 the steel is located closer to the outer fiber and, thus, results in a larger moment about the neutral axis.

2. Effect of Varying Depth and Breadth. From the equation defining moment of inertia, it is readily apparent that by merely increasing either the depth or breadth of the midship section, the moment of inertia will likewise increase, since the area obviously increases. A more meaningful approach would be to hold the gross area constant: an increase in depth or breadth is hence partially counteracted by a decrease in section thickness.



The situations investigated were the following:

<u>Case</u>	<u>Depth (m)</u>	<u>Breadth (m)</u>	<u>Section Thickness (m)</u>
1	23.5	44.0	0.52
2	23.5	49.4	0.48
3	28.9	44.0	0.48

where the gross area in each case was  $69.1 \text{ m}^2$ . The resulting values for moment of inertia (I), with steel area of  $1.0 \text{ m}^2$ , concrete cover of  $0.0317 \text{ m}$ , and modular ratio = 7, are:

<u>case</u>	<u>I (<math>\text{m}^4</math>)</u>
1	3942.
2	4053.
3	5733.

The unsurprising result is that an increase in depth significantly increases (by 45.4 percent) the moment of inertia. An increase in breadth, on the other hand, only slightly increases (by 2.8 percent) the moment of inertia.

3. Effect of Five Key Parameters. Utilizing the foregoing method of increasing concrete cover thickness, the computer program was then run for the thirty-two distinct combinations of the five key parameters. Values of the parameters were those enumerated in the preceding section.

An easy way to visualize the thirty-two combinations



is to assign symbols to the five parameters: let A, B, C, D, and E represent cover, tendon diameter, total tendon area, reinforcing rod diameter, and total reinforcing rod area, respectively. The values of these main parameters are then:

$A_1 = 0.0317 \text{ m}$	$A_2 = 0.0444 \text{ m}$
$B_1 = 0.024 \text{ m}$	$B_2 = 0.033 \text{ m}$
$C_1 = 0.45 \text{ m}^2$	$C_2 = 0.35 \text{ m}^2$
$D_1 = 0.0095 \text{ m}$	$D_2 = 0.019 \text{ m}$
$E_1 = 0.55 \text{ m}^2$	$E_2 = 0.65 \text{ m}^2$

Notice that values for tendon and rod areas are for half the midship section. Table 13 presents the thirty-two distinct combinations of these parameter values.

Table 13 is prepared such that the effect of concrete cover thickness can be readily examined. Hence, Cases 1 and 2 represent an increase in cover thickness while the other four parameters remain constant at their lower values; so, too, for Cases 3 and 4, except that the other four parameters remain constant at their higher values. To investigate the effect of the other parameters Table 13 can still be used. For example, to observe the effect of increasing tendon diameter while all other parameters hold constant, it suffices to look at Cases 1 and 5, 2 and 6, 7 and 21, 13 and 3, etc. The effect of increasing reinforcing rod area can be visualized by comparing Cases 1 and 11, 2 and 12, 5 and 25, etc. All five parameters





TABLE 13

POSSIBLE COMBINATIONS OF THE FIVE KEY PARAMETERS

<u>Case</u>	<u>Combination</u>	<u>Case</u>	<u>Combination</u>
1	$A_1 B_1 C_1 D_1 E_1$	17	$A_1 B_2 C_2 D_1 E_2$
2	$A_2 B_1 C_1 D_1 E_1$	18	$A_2 B_2 C_2 D_1 E_2$
3	$A_1 B_2 C_2 D_2 E_2$	19	$A_1 B_2 C_2 D_2 E_1$
4	$A_2 B_2 C_2 D_2 E_2$	20	$A_2 B_2 C_2 D_2 E_1$
5	$A_1 B_2 C_1 D_1 E_1$	21	$A_1 B_2 C_2 D_1 E_1$
6	$A_2 B_2 C_1 D_1 E_1$	22	$A_2 B_2 C_2 D_1 E_1$
7	$A_1 B_1 C_2 D_1 E_1$	23	$A_1 B_2 C_1 D_2 E_1$
8	$A_2 B_1 C_2 D_1 E_1$	24	$A_2 B_2 C_1 D_2 E_1$
9	$A_1 B_1 C_1 D_2 E_1$	25	$A_1 B_2 C_1 D_1 E_2$
10	$A_2 B_1 C_1 D_2 E_1$	26	$A_2 B_2 C_1 D_1 E_2$
11	$A_1 B_1 C_1 D_1 E_2$	27	$A_1 B_1 C_2 D_2 E_1$
12	$A_2 B_1 C_1 D_1 E_2$	28	$A_2 B_1 C_2 D_2 E_1$
13	$A_1 B_1 C_2 D_2 E_2$	29	$A_1 B_1 C_2 D_1 E_2$
14	$A_2 B_1 C_2 D_2 E_2$	30	$A_2 B_1 C_2 D_1 E_2$
15	$A_1 B_2 C_1 D_2 E_2$	31	$A_1 B_1 C_1 D_2 E_2$
16	$A_2 B_2 C_1 D_2 E_2$	32	$A_2 B_1 C_1 D_2 E_2$

A = cover

B = tendon diameter

C = total tendon area

D = reinforcing rod diameter

E = total reinforcing rod area



can be handled in a similar fashion.

Interestingly enough, the thirty-two "distinct" combinations turned out, in fact, to be only six distinct cases. The reason for this drastic reduction is straightforward: the diameter of reinforcing rods and tendons is not an important parameter when compared with the total steel area. Tables 13 and 14 summarize the results. It has been stated previously that many small rods vice fewer large ones tend to improve impact resistance. However, as these Tables illustrate, the variation of rod and/or tendon size has no effect on section properties, providing the total steel area (and the steel's center of gravity) remains constant. This conclusion also supports the various Codes' (ACI, British, etc.) usage of total steel area in computational work.

Two glaring generalities are obvious from Table 14: (a) as cover thickness increases, concrete equivalent area, moment of inertia and section modulus all increase, but height of neutral axis above the baseline decreases; and (b) as steel area increases (whether rod, tendon, or both), concrete equivalent area, moment of inertia and section modulus similarly increase, but unlike (a), height of the neutral axis also increases. The different reaction of neutral axis location in (a) and (b), despite the same increasing trend in concrete equivalent area, moment



TABLE 14

COMPUTER RESULTS OF THE THIRTY-TWO COMBINATIONS  
OF FIVE KEY PARAMETERS (FOR  $n = 7$ )

Cases from Table 13	<u>1,3,5,9, 13,17, 23,29</u>	<u>2,4,6, 10,14, 18,24,30</u>	<u>7,19, 21,27</u>	<u>8,20, 22,28</u>	<u>11,15, 25,31</u>	<u>12,16, 26,32</u>
Cover, m	0.0317	0.0444	0.0317	0.0444	0.0317	0.0444
Steel Area, $m^2$	1.0	1.0	0.9	0.9	1.1	1.1
Moment of Inertia, $m^4$	3942.2	4069.3	3899.7	4026.8	3984.8	4111.9
Height of Neutral Axis above Baseline, m	12.09	12.07	12.05	12.04	12.12	12.1
Section Modulus at deck in $m^3$	345.37	356.15	340.73	351.52	350.01	360.8
Section Modulus at keel	326.20	337.02	323.49	334.32	328.91	339.7
Equivalent Concrete Area	38.37	39.68	37.99	39.30	38.75	40.06



of inertia and section modulus, can be explained by the fact that the steel area is also increasing in (b), whereas steel area is constant in (a).

A qualifying statement is necessary at this juncture. The variation in neutral axis location is ultimately due to the treatment of transverse reinforcement in the revised computer program. As it is written, the program neglects transverse steel in tension, considering the space it occupies as a void with no bonding strength. By deducting certain factors from both the sum of the areas and the sum of the moments, the neutral axis location will fluctuate as portrayed above. However, by conducting the program without these deductions, the neutral axis remains constant at mid-depth. In the latter instance, moment of inertia figures average about two percent greater.

Two of the original five key parameters (tendon diameter and reinforcing rod diameter) have already been eliminated. It is also apparent that two other parameters (total tendon area and total reinforcing bar area) can be combined under one all-inclusive parameter: total steel area. Thus, while maintaining overall midship section depth and breadth constant, there are actually only two (out of the original five) key parameters, namely, concrete cover thickness (i.e., concrete area) and total steel area.

However, consideration of "equivalent concrete area"





gives rise to another key parameter. Recalling the definition of equivalent concrete area from equation (73),

$$A_{eq} = A_g - A_s + nA_s \quad (73)$$

it follows that modular ratio ( $n = E_s/E_c$ ) is also an important variable. In essence, there are, therefore, three primary parameters (holding midship section depth and breadth constant) which effect moment of inertia and section modulus: concrete cover thickness, total steel area, and modular ratio.

4. Effect of the Three Primary Parameters. With a lesser number of parameters, it is possible to increase the number of variables without becoming too unwieldy. Consequently, the range of consideration will be widened by increasing to five the number of values for each parameter. The values to be analyzed for these three primary parameters are listed below:

(a) cover thickness: 0.0254 m (1.0 in), 0.0317 m (1.25 in), 0.0381 m (1.5 in), 0.0444 m (1.75 in), and 0.0508 m (2.0 in);

(b) total steel area (for half the midship section):  $0.8 \text{ m}^2$ ,  $0.9 \text{ m}^2$ ,  $1.0 \text{ m}^2$ ,  $1.1 \text{ m}^2$ , and  $1.2 \text{ m}^2$ ; and

(c) modular ratio:  $n = 5, 7, 9, 11$ , and  $13$ .

For each value of modular ratio there are twenty-five distinct combinations of cover thickness and steel area. There is, thus, a potential for 125 different results, six



of which have already been portrayed in Table 14.

After conducting this particular computer experiment, it was indeed verified that there are 125 distinct values for moment of inertia. These results can be illustrated in several ways, Appendix K being a tabular method. Perhaps the most instructive means, however, is graphically.

In order to avoid any misconception in the interpretation of the ensuing graphs, gross concrete area will be plotted in lieu of concrete cover thickness. This is appropriate since an increase in cover was achieved by physically augmenting both sides of each section slice by the amount of added cover thickness, which in turn enlarged the gross concrete area. The values to be used, with their corresponding cover thicknesses, are as follows:

<u>cover (m)</u>	<u>gross concrete area (m<sup>2</sup>)</u>
0.0254 (1.0")	33.90
0.0317	34.55
0.0381	35.20
0.0444	35.85
0.0508 (2.0")	36.50

Although the terminology differs from prior usage, gross concrete area will be designated " $A_c$ " and total steel area " $A_s$ ". (Recall that values of  $A_c$ ,  $A_s$ , and  $I$  are for one-half the midship section).



Figure 14 is a graph of moment of inertia ( $I$ ) versus modular ratio ( $n$ ) for a constant gross concrete area ( $A_c$ ). The two extreme cases of  $A_c$  are shown, the solid curves representing a gross concrete area of  $33.9 \text{ m}^2$  (which corresponds to a cover of 1 inch) and the dotted curves representing  $A_c = 36.5 \text{ m}^2$  (a corresponding cover of 2 inches). Three basic conclusions are obvious: (1) as modular ratio increases (for constant  $A_s$  and  $A_c$ ), moment of inertia increases; (2) as steel area increases (for constant  $n$  and  $A_c$ ), moment of inertia increases; and (3) as concrete area increases (for constant  $n$  and  $A_s$ ), moment of inertia also increases. In other words, by holding any two of the three primary parameters constant, the moment of inertia is directly proportional to the third parameter.

Two other observations are apparent from Figure 14. Firstly, the curves of steel area ( $A_s$ ) "flare" (for constant  $A_c$ ) as  $n$  increases; or in other words, the slope is steeper for larger  $A_s$ . Secondly, as concrete area increases (for constant  $A_s$ ), the slopes do not vary, but merely shift to a higher moment of inertia. Consequently, three additional conclusions can be made: (1) for a constant concrete area, moment of inertia increases more rapidly (as  $n$  increases) for larger values of steel area; (2) for a constant concrete area, moment of inertia increases more (as  $A_s$  increases) for larger values of



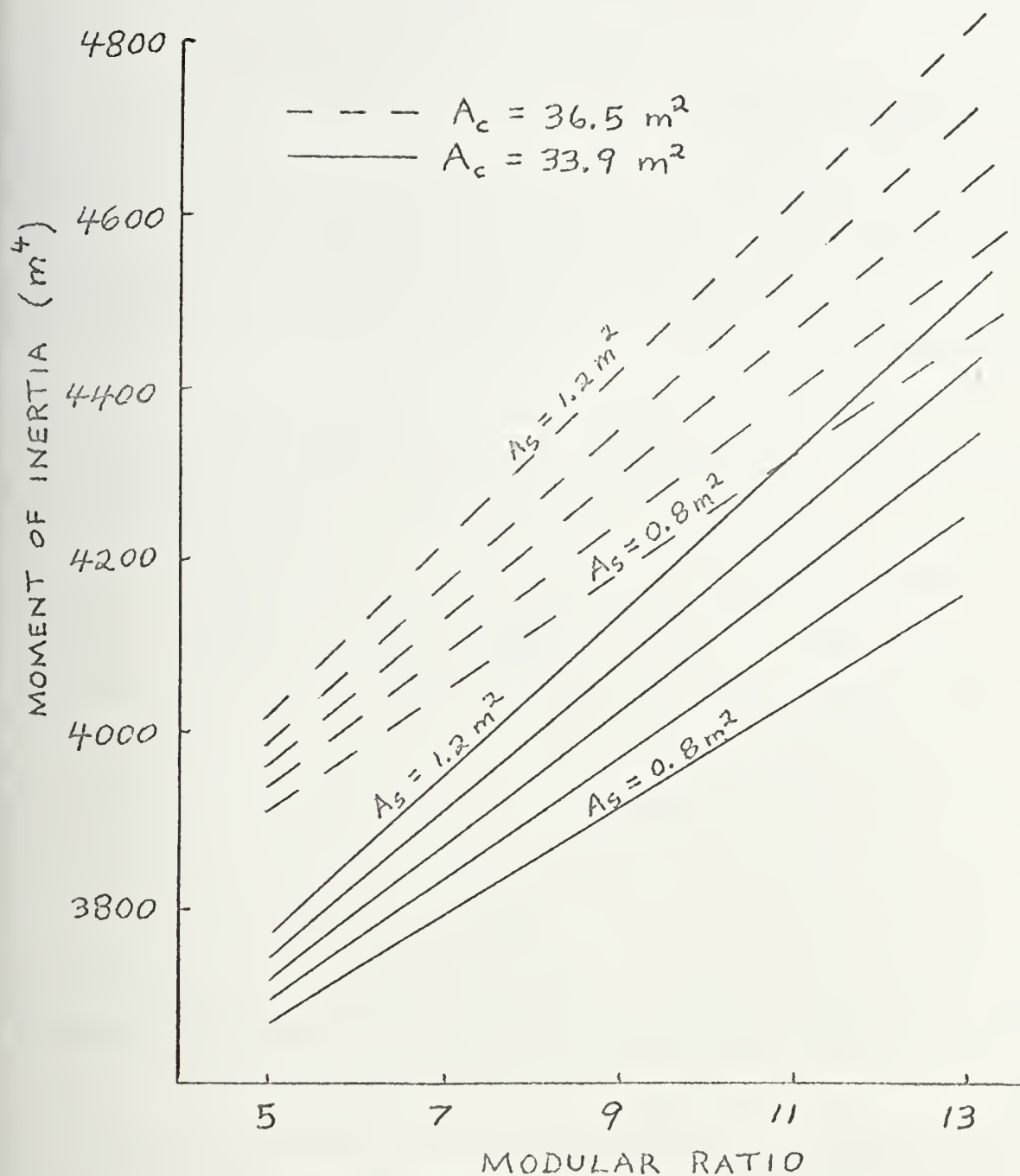


FIGURE 14

MOMENT OF INERTIA vs. MODULAR RATIO  
(for constant concrete area)





modular ratio; and (3) for constant steel area, moment of inertia increases uniformly (as  $n$  increases) for increasing amounts of concrete area.

Figures 15 through 19 are five additional ways of plotting some of the results tabulated in Appendix K. Despite their diversity of appearance, each graph confirms the above six conclusions based on Figure 14.

The foregoing conclusions were based on (a) holding two parameters constant while increasing the third, and (b) holding just one parameter constant while increasing the remaining two. Several more conclusions can be drawn by maintaining one parameter constant, while increasing the second but decreasing the third. Figures 20 through 22, modifications of Figures 17 through 19, are illustrative.

Figure 20 demonstrates the effect on moment of inertia of increasing modular ratio and decreasing concrete area (only one increment at a time), while holding steel area constant. It is seen that moment of inertia increases linearly (the opposite is obviously true for a decrease in  $n$  and an increase in  $A_c$ ).

Figure 21 shows that by maintaining a constant concrete area, moment of inertia similarly increases with increasing modular ratio and decreasing steel area. The difference, however, is that (unlike Figure 20) the relationship is non-linear.



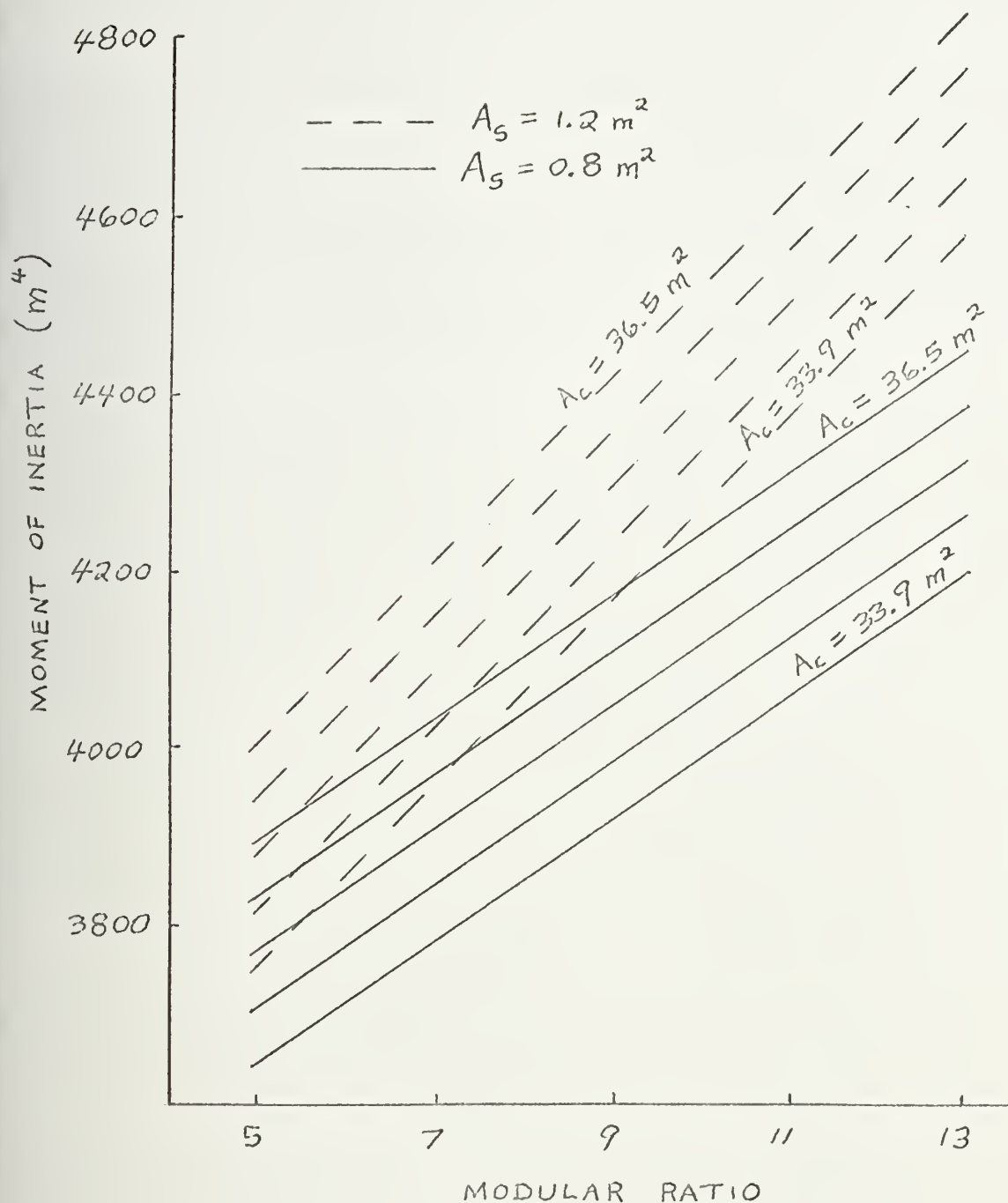


FIGURE 15

MOMENT OF INERTIA vs. MODULAR RATIO  
(for constant steel area)



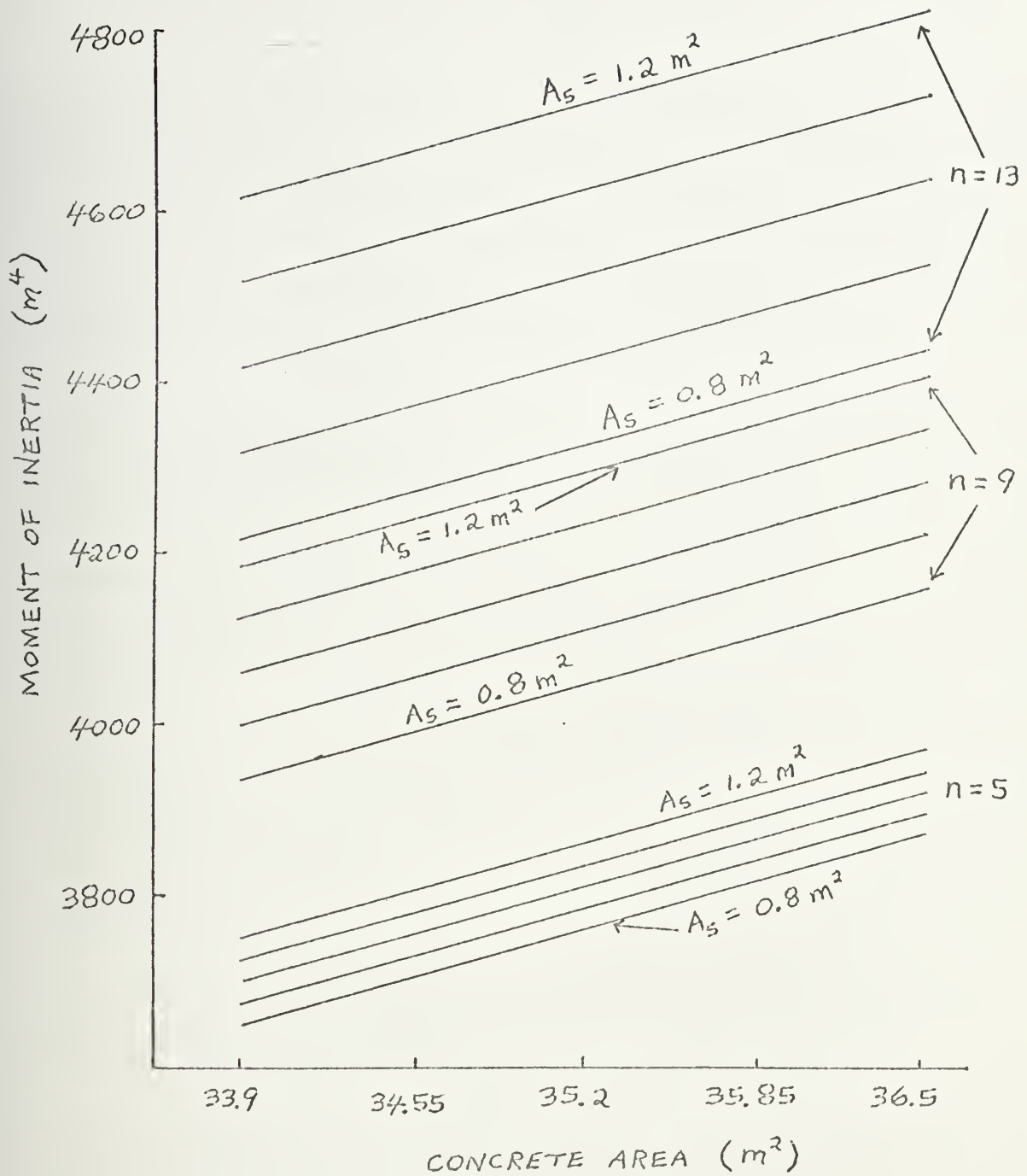


FIGURE 16

MOMENT OF INERTIA vs. CONCRETE AREA  
(for constant modular ratio)



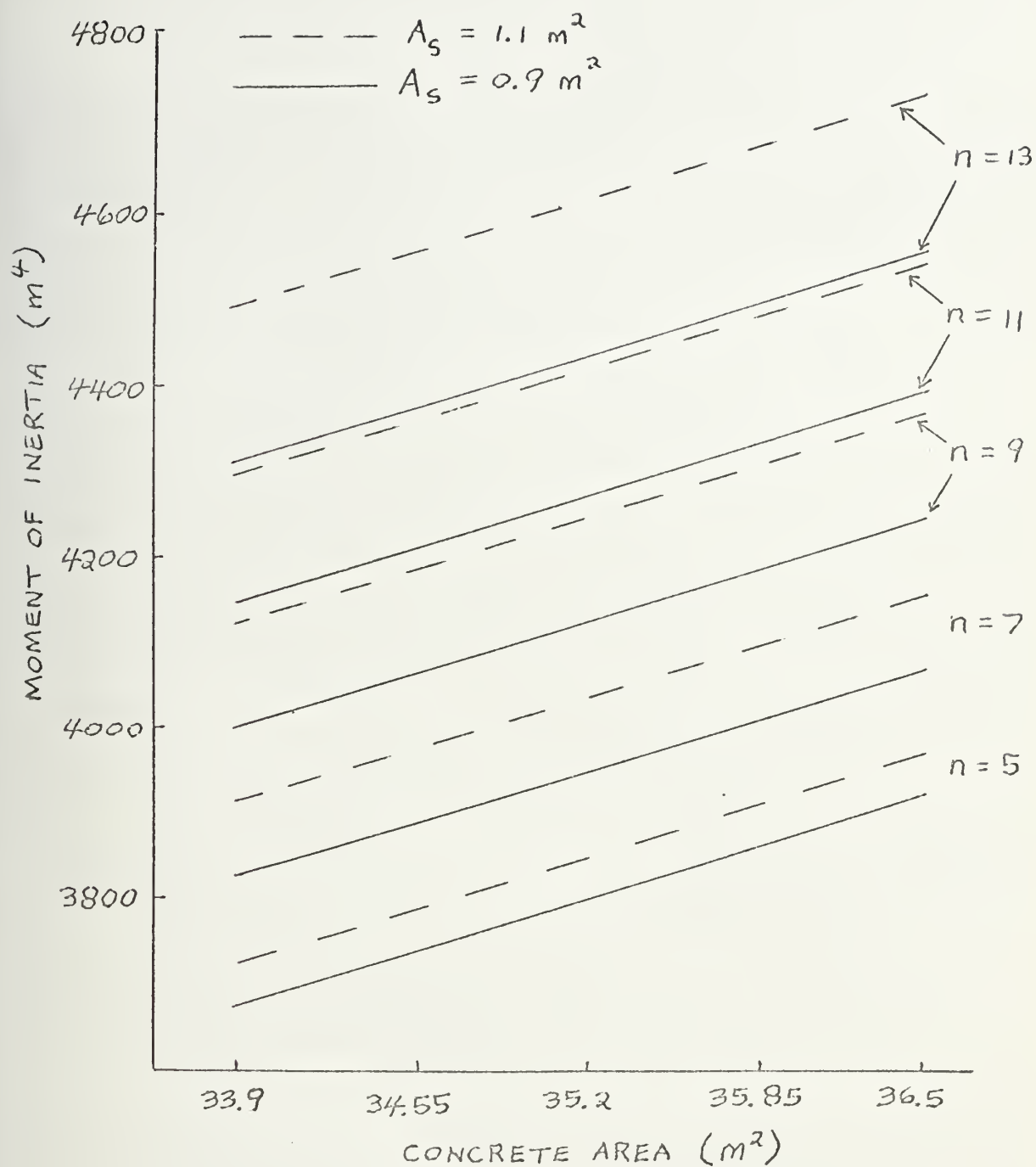


FIGURE 17

MOMENT OF INERTIA vs. CONCRETE AREA  
(for constant steel area)





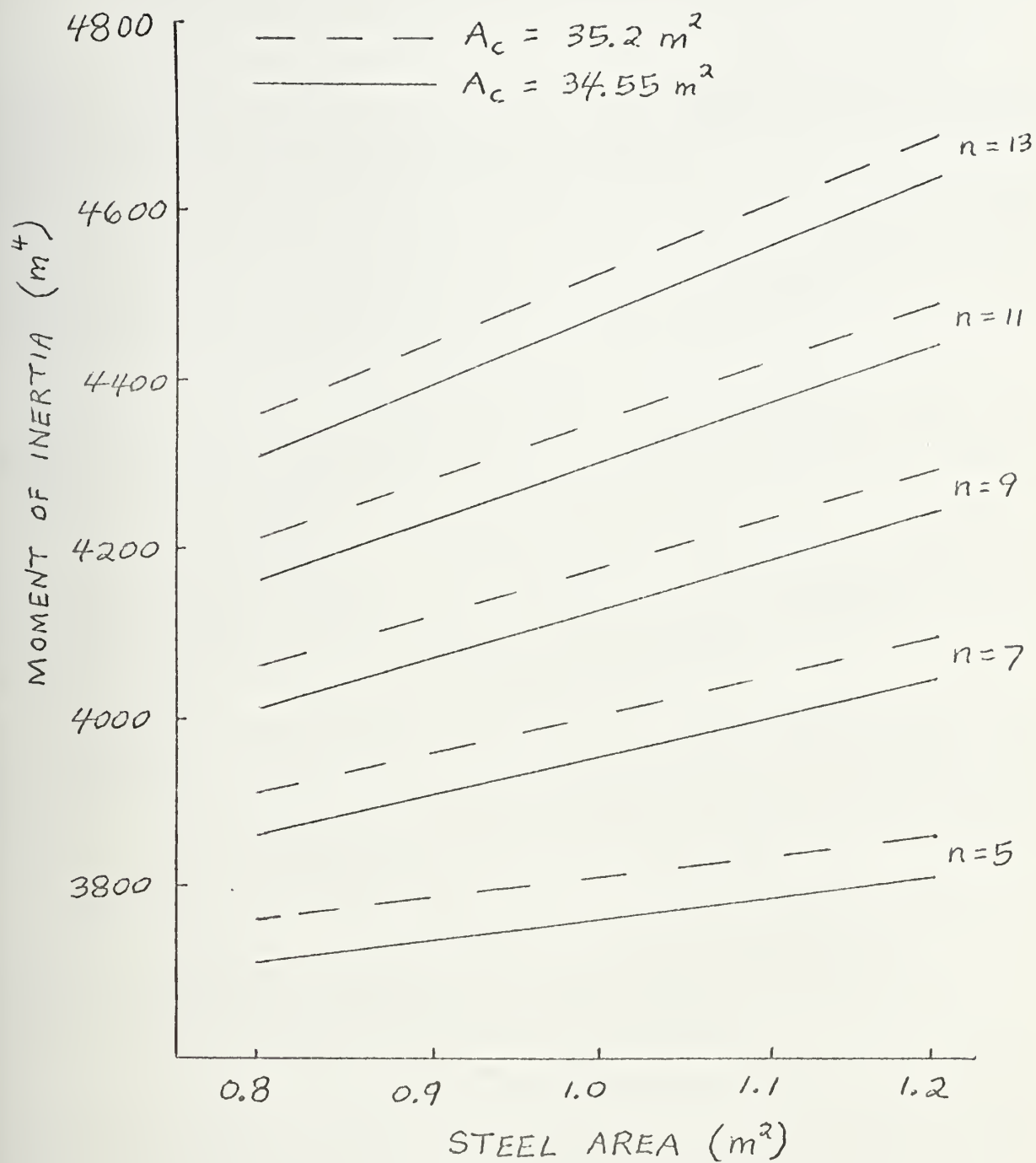


FIGURE 18

MOMENT OF INERTIA vs. STEEL AREA  
(for constant concrete area)



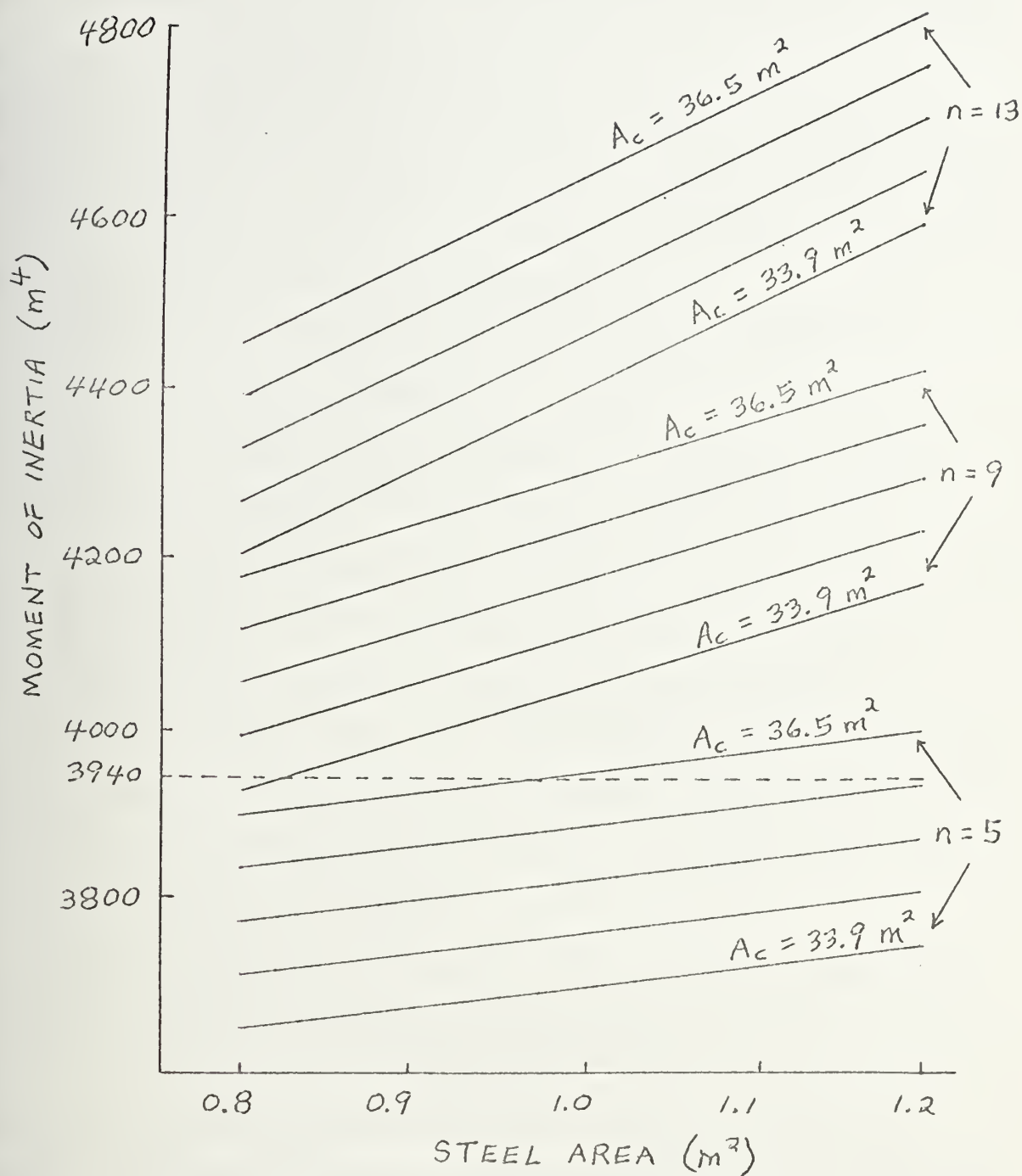


FIGURE 19

MOMENT OF INERTIA vs. STEEL AREA  
(for constant modular ratio)



Figure 22 indicates the influence that modular ratio has on moment of inertia. In fact, the effect on moment of inertia of decreasing steel area and increasing concrete area varies, depending upon the value of modular ratio. For  $n = 5, 7$  and  $9$ , moment of inertia increases with increasing  $A_c$  and decreasing  $A_s$ ; however, for  $n = 11$  and  $13$ , moment of inertia decreases.

It is apparent also from Figures 20 and 21 that modular ratio has a significant influence on moment of inertia. In both instances moment of inertia increased with increasing modular ratio, despite the fact that concrete area decreased in the former and steel area decreased in the latter. A quick perusal of Appendix K will demonstrate that moment of inertia increases with increasing modular ratio even when both concrete area and steel area decrease (one increment at a time). Hence, a broad generalization seems to be: "as modular ratio goes, so goes moment of inertia."

Of the remaining two parameters, Figure 21 tends to indicate that steel area has a greater influence on moment of inertia than does concrete area. This is due to the nonlinearity of the relationship: with decreasing  $A_s$ , moment of inertia increases (with increasing  $n$ ), although the increase is slightly reduced below the linear relationship of decreasing  $A_c$  in Figure 20. This, of course, confirms the last three conclusions derived from Figure 14.



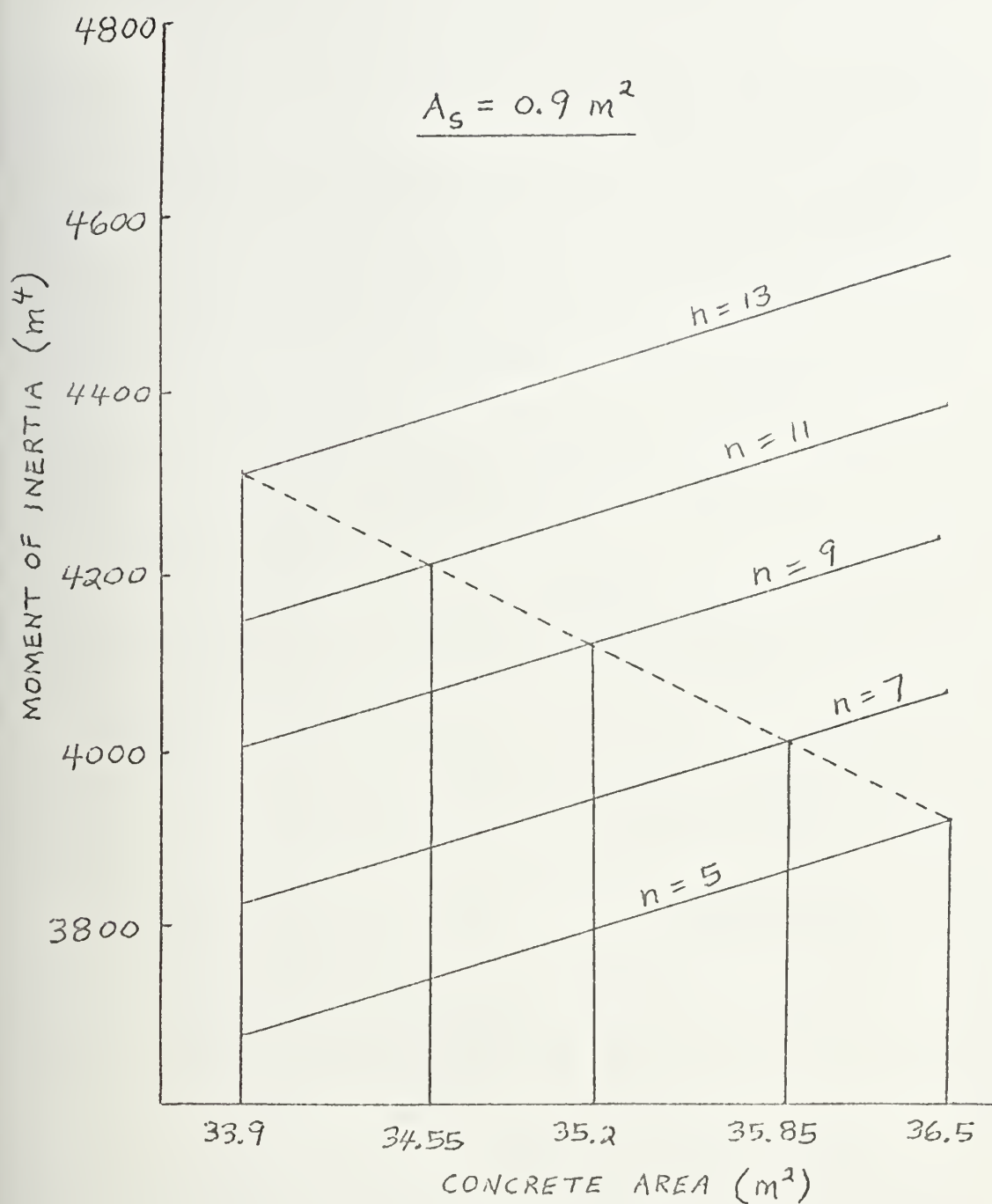


FIGURE 20

EFFECT ON MOMENT OF INERTIA OF INCREASING  
MODULAR RATIO AND DECREASING CONCRETE AREA





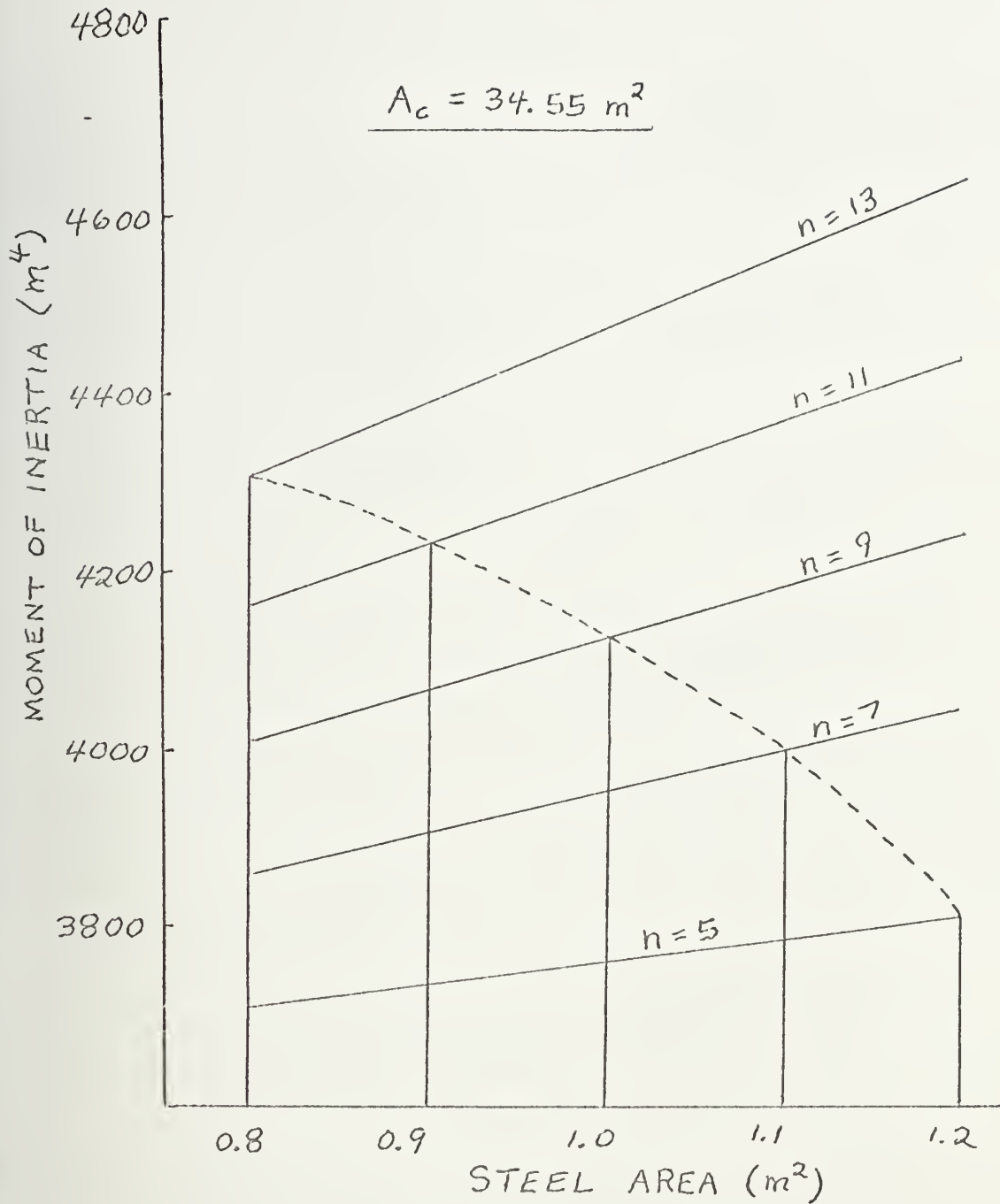


FIGURE 21

EFFECT ON MOMENT OF INERTIA OF INCREASING  
MODULAR RATIO AND DECREASING STEEL AREA



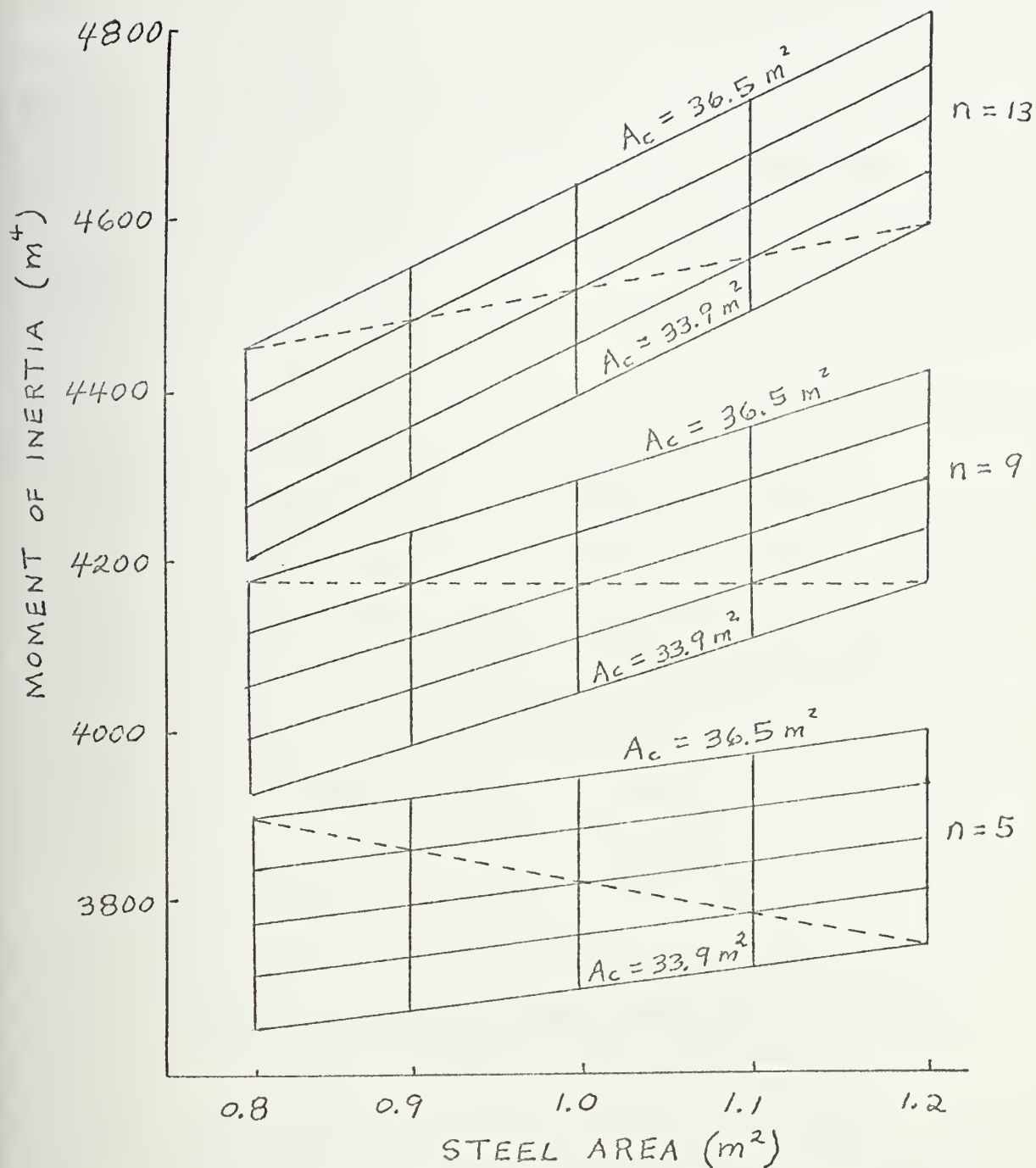


FIGURE 22

EFFECT ON MOMENT OF INERTIA OF INCREASING  
CONCRETE AREA AND DECREASING STEEL AREA



5. Minimum Weight Considerations. An advantage which accrues as a result of plotting concrete area vice cover thickness on Figures 14 through 19 is that the total weight of the midship section can be readily ascertained. For any given point on one of the graphs, the weight per unit length of one-half the midship section ( $W_{ms}$ ) is simply:

$$W_{ms} = \rho_s A_s + \rho_c (A_c - A_s) \quad (76)$$

where steel and concrete densities are given in Appendix D, and  $A_s$  and  $A_c$  are taken directly from the graph.

As discussed earlier, minimization of weight is a prime design consideration for a concrete ship. A trivial solution to this minimum weight problem is to merely select the point on a graph with the lowest steel area, lowest concrete area, and lowest modular ratio. Unfortunately, the correspondingly low moment of inertia may not be sufficient to attain the required section modulus.

A more meaningful approach to the problem is to start with a given moment of inertia ( $I$ ), locate the divers and sundry points on the graphs which satisfy this requirement, apply equation (76), and select the minimum result. The horizontal dotted line at  $I = 3940 \text{ m}^4$  on Figure 19 was drawn to facilitate location of such points. Appendix L summarizes the calculations and results for this case, as well as for an arbitrarily-chosen moment of inertia of  $4350 \text{ m}^4$ .



It can be seen from Figure 19 that in order to maintain moment of inertia at  $3940 \text{ m}^4$ , modular ratio must be less than or equal to  $n = 9$ ; if a larger modular ratio is desired, the steel area must be reduced below  $A_s = 0.8 \text{ m}^2$  and/or the concrete area must be reduced below  $A_c = 33.9 \text{ m}^2$ . Similarly, to maintain  $I = 4350 \text{ m}^4$ , modular ratio cannot be less than  $n = 9$ ; a smaller modular ratio will in turn require a steel area greater than  $A_s = 1.2 \text{ m}^2$  and/or a concrete area exceeding  $A_c = 36.5 \text{ m}^2$ .

An intuitively obvious conclusion is that, in order to hold moment of inertia constant, if concrete area is increased (for a given modular ratio), then steel area must be decreased. What is not so obvious, however, is that for the same increase in concrete area, it is not necessary to decrease the steel area as much for larger modular ratios as it is for smaller ratios. For example, an increase in concrete area of  $0.65 \text{ m}^2$  (corresponding to an increase in cover thickness of 0.25 inch) requires a decrease in steel area of  $0.25 \text{ m}^2$ ,  $0.15 \text{ m}^2$ ,  $0.1 \text{ m}^2$ ,  $0.084 \text{ m}^2$ , and  $0.065 \text{ m}^2$  for a modular ratio of  $n = 5, 7, 9, 11$ , and  $13$ , respectively.

Appendix L also points to the following significant conclusions: (1) As modular ratio increases (while maintaining moment of inertia constant), the weight per unit length of the midship section decreases. This is consistent with the preceding paragraph, in that for  $n = 7$ , as





concrete area decreases by  $0.65 \text{ m}^2$ , the steel area increases by  $0.15 \text{ m}^2$ ; whereas for  $n = 11$ , the steel area increases by only  $0.084 \text{ m}^2$ . (2) For all modular ratios except  $n = 5$ , the weight decreases as concrete area decreases and steel area increases, again while holding moment of inertia constant; (for  $n = 5$ , the weight increases as concrete area decreases and steel area increases).

The general overall conclusion to be reached is that for a midship section of minimum weight, a design should be strived for which results in both a high modular ratio and a low concrete area.

Since minimum weight is a desirable (if not optimum) attribute in a concrete ship, it is apparent that the preceding graphs can be a useful tool. A note of caution, however, is advisable. Even as a mechanical tool should be applied only for the purpose to which it is intended, so too with these computer results. It must be recollected that all the foregoing data is for a given ship configuration (depth = 23.5 m and breadth = 44.0 m) and total bending moment (700,000 tonnes-meter). It is not unreasonable to assume, however, that the basic conclusions can be extended to other situations.

#### D. Stress Diagram

The preceding section concluded with the statement



that both a high modular ratio and a low concrete area are desirable qualities to achieve minimum weight in a midship section. It was also averred that in order to attain a larger modular ratio (for a constant moment of inertia), the steel area and/or the concrete area must be reduced. The critical question logically arises as to what effect such a reduction in steel and concrete area has on the stress in the major components (concrete, ordinary reinforcing rods, and tendons) of a post-tensioned reinforced concrete midship section.

For the specific example referred to previously ( $n = 7$ ;  $A_s = 1.0 \text{ m}^2$ ;  $A_c = 34.55 \text{ m}^2$ , or, concrete cover = 1.25 inch; and  $I = 3940 \text{ m}^4$ ), the weight of one-half the midship section was found to be  $W_{ms} = 75,225 \text{ kg/m}$ . If it is wished to increase the modular ratio of this example to  $n = 11$ , then the steel area must be reduced below  $A_s = 0.8 \text{ m}^2$  and/or the concrete must be reduced below  $A_c = 33.9 \text{ m}^2$  (or, a concrete cover less than 1.0 inch). Since it is not recommended to have a concrete cover less than 1.0 inch, the concrete area will only be reduced from  $A_c = 34.55$  to  $33.9 \text{ m}^2$ ; the required amount of steel area to yield a moment of inertia equalling  $3940 \text{ m}^4$  is, extrapolating from Figure 14,  $A_s = 0.64 \text{ m}^2$ . Equation (76) then gives the corresponding midship section weight as  $W_{ms} = 71,805 \text{ kg/m}$ , a 4.55 percent saving in weight from the  $n = 7$  case.



A convenient technique by which the stresses in these two examples can be compared is the stress diagram. It is only necessary to make two assumptions, namely, that the post-tensioning steel area equals 45 percent of the total steel area and that the post-tensioning force equals 78,300 tonnes. (These two assumptions are, of course, flexible and can be varied for comparison purposes.) Recalling that the total midship section area is  $2A_c$  and the total steel area is  $2A_s$ , the following actual and equivalent areas can be readily calculated:

	<u>Actual Area</u>	<u>Equivalent Area</u>
Concrete	$2A_c - 2A_s$	$2A_c - 2A_s$
Tendons	$0.45(2A_s)$	$n(0.45)(2A_s)$
Rods	$0.55(2A_s)$	$n(0.55)(2A_s)$

Since the post-tensioning force induces compression into the concrete (and hence also in the ordinary reinforcing rods), the equivalent concrete area in initial compression is:

$$A_{eq} = (2A_c - 2A_s) + n(0.55)(2A_s) \quad (77)$$

where  $A_c$  and  $A_s$  are values taken from Figures 14 through 19.

The stresses are then calculated from the combined stress formula:

$$f = P/A \pm M/S \quad (51)$$

where  $P$  is the post-tensioning force,  $M$  is the total bending moment, and  $S$  is the section modulus (determined



from the computer program). The P/A-term represents the initial, pre-launching stresses, whereas the  $\pm M/S$ -term represents the additional stresses due to bending.

The pre-launching stresses (in  $\text{kg/cm}^2$ ) are calculated from equations (78) through (80). The initial concrete stress is:

$$f_c = 7830/A_{eq} \quad (78)$$

where  $A_{eq}$  is found from equation (77). The initial stress in the ordinary reinforcement is, thus, from equation (4):

$$f_s = n f_c \quad (79)$$

and the initial stress in the post-tensioning tendons is:

$$f_{ps} = 7830/(0.45)(2A_s) \quad (80)$$

Equations (78) and (79) are compressive stresses, whereas equation (80) is a tensile stress.

Assuming a total bending moment of 700,000 tonnes-meter, the additional stresses (in  $\text{kg/cm}^2$ ) due to bending are then calculated from equations (81) and (82). The bending stress in the concrete is:

$$f_{cb} = \pm 70,000/S \quad (81)$$

and the bending stress in both ordinary reinforcement and post-tensioning tendons is:

$$f_{sb} = \pm (n)(70,000)/S \quad (82)$$

For a sagging wave bending moment, the above bending stresses are positive (+) at the keel and negative (-) at the deck, where a plus sign (+) denotes tension.

The initial and bending stresses are summed





algebraically for each of the three components (concrete, rods, and tendons) to give the total stress. The results of these calculations, as well as other pertinent data, are summarized in Table 15. These results are then used to construct the stress diagram in Figure 23. (Since this figure is not drawn to scale it is urged that Table 15 be referred to in conjunction with Figure 23).

It can be concluded, therefore, that by increasing modular ratio (for a constant moment of inertia), the accompanying decrease in both steel and concrete area sizably increases the stress in both ordinary reinforcing rods and post-tensioning tendons. On the other hand, stress in the concrete remains virtually unchanged. The significant point to be made is that the critical stress in a post-tensioned reinforced concrete ship is the tensile stress in the concrete; and this stress is scarcely affected in the above example, in fact, it actually decreases slightly (from 12.3 to 10.6 kg/cm<sup>2</sup>).

Two formulae were presented in Chapter II for the maximum permissible tensile stress in concrete, namely, equations (9) and (10). The average of these two expressions yields a stress of 40 kg/cm<sup>2</sup> for the previous example; it is obvious, therefore, that the stress actually experienced is well below this maximum allowable value. Thus, the present work has, in essence, made a



TABLE 15

EFFECT ON TOTAL STRESS OF VARYING MODULAR RATIO

Modular ratio	7	11
$A_s$ ( $m^2$ )	1.0	0.64
$A_c$ ( $m^2$ )	34.55	33.9
$I$ ( $m^4$ )	3940.0	3940.0
$W_{ms}$ (kg/m)	75,225.0	71,805.0
Initial stress ( $kg/cm^2$ ):		
tendons	+8,700.0	+13,594.0
rods	-732.9	-1,159.4
concrete	-104.7	-105.4
Bending stress (sagging):		
steel (deck)	-784	-1,243
steel (keel)	+819	+1,276
concrete (deck)	-112	-113
concrete (keel)	+117	+116
Total stress ( $kg/cm^2$ ):		
tendons (deck)	+7,916	+12,351
tendons (keel)	+9,519	+14,870
rods (deck)	-1,517	-2,402
rods (keel)	+86	+117
concrete (deck)	-216.7	-218.4
concrete (keel)	+12.3	+10.6
Figure 23	solid line	dotted line

Note: tension = +, and compression = -



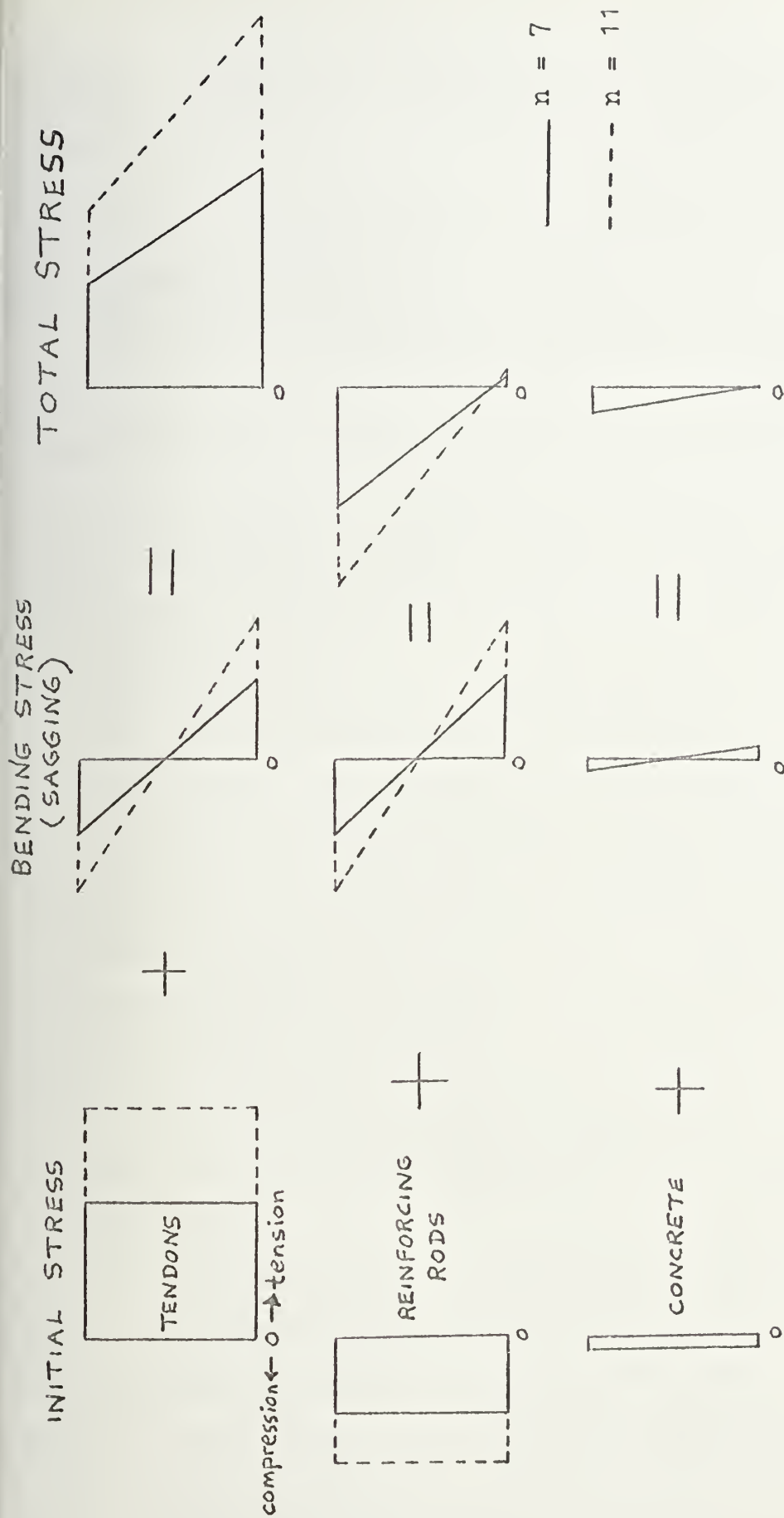


FIGURE 23  
STRESS DIAGRAM FOR A POST-TENSIONED REINFORCED  
CONCRETE TANKER MIDSHIP SECTION



complete circle: by commencing with a discussion of permissible stresses, and having now ultimately returned, it appropriately terminates at that same point.

#### E. Recommendations

The application of post-tensioned reinforced concrete to ship construction is a novel idea. As in all new design concepts, the possibilities for further investigation and evaluation present an exciting challenge to the naval architect and marine engineer. Some areas for future work, a direct outgrowth of the present thesis, are discussed below.

1. The preceding section calculated the stress in the three major components of a post-tensioned reinforced concrete tanker midship section. As was demonstrated, the critical stress (namely, the concrete tensile stress) was significantly below the maximum permissible stress. This indicates that perhaps the midship section selected is not the optimum configuration, since it was earlier assumed that such an "optimum" would occur when the steel and concrete attained their maximum allowable stresses simultaneously.

The next step would, thus, be to determine the optimum (i.e., minimum weight) midship section configuration, given the maximum stresses in the concrete, tendons and rods. The procedure would, in effect, be a reversal of the





present work in which a midship section configuration was selected and then the stresses were calculated.

2. Due to the innate heaviness of concrete structures, the primary optimization criterion for a post-tensioned reinforced concrete ship has been the minimization of weight. However, as mentioned in Chapters II and III, another important consideration is the economic factor; it is rather likely that a concrete ship will not be built if it does not offer a significant reduction in cost over its "tried and tested" steel counterpart. In fact, Evans (93) asserts that the final assessment of a new material depends upon "whether it is worth the price in competition with the steels." There are other considerations, of course, besides cost of construction and structural weight (e.g., structural reliability and service life), but cost and weight are deemed the principal ones. Cost and weight are actually interrelated: minimizing hull structural weight reduces total expenditures (initial cost is less due to lower material cost, and operating costs are less as a result of savings in fuel costs) and increases total earnings (revenues are greater due to increased payload capability). A least-weight midship section design, however, would undoubtedly lead to prohibitive costs, whereas a least-cost design would result in excessive weight. Indeed, the optimum design of a midship section should probably be



a compromise between minimum weight and minimum cost. Tables 5 and 6, as well as the other cost data in Chapter II, may serve as a convenient starting point, although it must be noted that concrete labor costs are not included.

3. Another interesting area for development is the determination of a relationship between ship payload (and/or ship principal dimensions) and the minimum required hull thickness. This relationship would most likely be based on maximum permissible stress considerations; shear stresses would also have to be taken into account, as they have a determining effect on the side shell thickness. If such a relationship were indeed possible, the task of selecting the optimum midship section configuration (concrete cover thickness, post-tensioning tendon area, and ordinary reinforcing rod area) would be greatly simplified.

4. Since post-tensioned reinforced concrete ships are such a new concept, the Regulatory Agencies have not as yet updated their requirements. Preliminary work could, thus, be commenced to determine the required values of section modulus for a given ship length and ship type. Resulting recommendations would undoubtedly be of assistance to the various Agencies.

5. The section on "cracking of concrete" suggests another important area of investigation, namely, the impact resistance of concrete ships. If the extent of



probable damage to such a ship hull (whether from collision, grounding, or torpedo attack) can be ascertained, a potential for post-tensioned reinforced concrete ships might conceivably be found even in naval applications.



## APPENDIX A

CONVERSION TABLE

Due to the impending metrication program in the United States, and since most shipbuilding Regulatory Agencies (e.g., Lloyds and Det Norske Veritas) and other countries already use the metric system, it behooves us to become familiar with its terminology. The following conversion table assists in this endeavor.

<u>METRIC</u>	<u>U.S.</u>	<u>RECIPROCAL</u>
Length:		
1 cm	0.394 in	2.54
1 m	3.28 ft	0.305
Mass, force:		
1 g	0.0353 oz	28.35
1 kg	2.205 lb	0.454
1 t	2205 lb	0.00045
Density:		
1 kg/m <sup>3</sup>	0.0624 lb/ft <sup>3</sup>	16.02
Pressure, stress:		
1 kg/cm <sup>2</sup>	14.22 lb/in <sup>2</sup>	0.0703
1 N/mm <sup>2</sup>	145 lb/in <sup>2</sup>	0.0069
Concrete mixes:		
100 kg/m <sup>3</sup>	168.6 lb/yd <sup>3</sup>	0.0059





## APPENDIX B

EFFECT ON BEAM DEPTH OF VARYING MODULAR RATIO

Merely for the sake of argument, let the following be given:

beam breadth (width)	$b = 20"$
steel stress	$f_s = 16,000 \text{ psi}$
concrete stress	$f_c = 600 \text{ psi}$
bending moment	$M = 2 \times 10^6 \text{ in-lb}$

Now, by varying  $n$  from 15 to 6 in decrements of 3, determine the effect on  $d$  and  $A_s$ . Equations (37), (38), (34), (36) will be employed to calculate  $k$ ,  $j$ ,  $d$ , and  $A_s$ , respectively.

1. For  $n = 15$

$$\begin{aligned}
 k &= 1/(1 + f_s/nf_c) \\
 &= 1/(1 + 16,000/(15)(600)) \\
 &= 1/2.777 \\
 &= 0.36
 \end{aligned}$$

$$\begin{aligned}
 j &= 1 - k/3 \\
 &= 1 - 0.36/3 \\
 &= 0.88
 \end{aligned}$$

$$\begin{aligned}
 d &= (2M/f_c b k j)^{0.5} \\
 &= (4,000,000/(600)(20)(0.36)(0.88))^{0.5} \\
 &= 32.44 \text{ in}
 \end{aligned}$$

$$\begin{aligned}
 A_s &= M/(f_s j d) \\
 &= 2,000,000/(16,000)(0.88)(32.44) = 4.38 \text{ in}^2
 \end{aligned}$$



2. Similarly, for  $n = 12$

$$k = 0.31$$

$$j = 0.8967$$

$$d = 34.63 \text{ in}$$

$$A_s = 4.025 \text{ in}^2$$

3. For  $n = 9$

$$k = 0.252$$

$$j = 0.916$$

$$d = 38.0 \text{ in}$$

$$A_s = 3.59 \text{ in}^2$$

4. For  $n = 6$

$$k = 0.184$$

$$j = 0.94$$

$$d = 43.9 \text{ in}$$

$$A_s = 3.03 \text{ in}^2$$

The key results in tabular form are:

<u>n</u>	<u>d (in)</u>	<u><math>A_s</math> (in<sup>2</sup>)</u>	<u>Moment Arm jd (in)</u>	<u>Distance of Neutral Axis from Top, kd (in)</u>
15	32.44	4.38	28.55	11.68
12	34.63	4.025	31.05	10.74
9	38.0	3.59	34.81	9.58
6	43.9	3.03	41.27	8.08



## APPENDIX C

EFFECT ON BEAM DEPTH OF VARYING STEEL STRESS

The same values for  $b$ ,  $f_c$ , and  $M$  are adopted as in Appendix B, and  $n = 15$ . Now, by varying steel stress ( $f_s$ ), equations (37), (38), (34), and (36) are again used to calculate  $k$ ,  $j$ ,  $d$ , and  $A_s$ , respectively. The procedure is then repeated for  $n = 6$ . The results are tabulated below:

<u>For <math>n = 15</math></u>						
<u><math>f_s</math> (psi)</u>	<u><math>k</math></u>	<u><math>j</math></u>	<u><math>d</math> (in)</u>	<u><math>A_s</math> (in<sup>2</sup>)</u>	<u><math>jd</math> (in)</u>	<u><math>kd</math> (in)</u>
16,000	0.36	0.88	32.44	4.38	28.55	11.68
20,000	0.31	0.90	34.63	3.22	31.05	10.74
30,000	0.23	0.92	39.63	1.82	36.58	9.11
40,000	0.184	0.94	43.9	1.21	41.27	8.08
50,000	0.153	0.95	48.0	0.88	45.55	7.32

<u>For <math>n = 6</math></u>						
<u><math>f_s</math> (psi)</u>	<u><math>k</math></u>	<u><math>j</math></u>	<u><math>d</math> (in)</u>	<u><math>A_s</math> (in<sup>2</sup>)</u>	<u><math>jd</math> (in)</u>	<u><math>kd</math> (in)</u>
16,000	0.184	0.94	43.9	3.03	41.27	8.08
20,000	0.153	0.95	48.0	2.19	45.55	7.32
30,000	0.107	0.964	56.85	1.22	54.8	6.08
40,000	0.08	0.973	65.44	0.785	63.67	5.24
50,000	0.07	0.977	69.8	0.59	68.2	4.89

As noted in Chapter IV, the apparent conclusion is that steel area decreases and depth increases with



increasing steel stress. An additional significant result can be discerned by comparing the two tables; it is observed that two sets of identical values for depth (43.9 and 48.0) appear under both  $n = 15$  and  $n = 6$ .

Thus, it can be stated that, for constant depth, as the modular ratio ( $n$ ) increases, the stress in the steel also increases. The significance of this conclusion lies in the fact that stress in the concrete ( $f_c$ ) is the critical factor in reinforced concrete structures, and by increasing the steel stress (e.g., by increasing  $n$ ) the concrete stress is likely to decrease.





## APPENDIX D

EFFECT ON BEAM WEIGHT OF VARYING DEPTH

A simple analysis can be conducted by first establishing an expression for the beam weight (W). Letting  $\rho$ , V, A, and L represent density, volume, area, and length, respectively, where the subscripts c and s stand for concrete and steel, respectively, the following formula results:

$$\begin{aligned} W &= W_c + W_s \\ &= \rho_c V_c + \rho_s V_s \\ &= \rho_c A_c L + \rho_s A_s L \end{aligned} \quad (D1)$$

Or, in other words, the beam weight per unit length is equal to:

$$W/L = \rho_c A_c + \rho_s A_s \quad (D2)$$

If the area is given in squared inches, then the density must be expressed in lb/in<sup>3</sup>. Hence, steel density (490 lb/ft<sup>3</sup>) is 0.284 lb/in<sup>3</sup>, and concrete density (125.5 lb/ft<sup>3</sup> from Chapter II) is 0.073 lb/in<sup>3</sup>.

For purposes of illustration only, the total beam area (see Figure 7a) can be approximated as:

$$A = bd \quad (D3)$$

Since  $A = A_c + A_s$ , it follows that:

$$A_c = bd - A_s \quad (D4)$$

Thus, a value for concrete area ( $A_c$ ) can be determined from equation (D4), after depth (d) and steel area ( $A_s$ )



have been found from equations (34) and (36). Equation (D2) can then be used to solve for the weight per unit length.

Referring to information in Appendices B and C, the following results can be tabulated:

For constant steel stress

<u>n</u>	<u>d (in)</u>	<u>A<sub>S</sub> (in<sup>2</sup>)</u>	<u>A (eq. D3)</u>	<u>A<sub>C</sub> (eq. D4)</u>	<u>W/L (eq. D2)</u>
15	32.44	4.38	648.8	644.42	48.28
12	34.63	4.025	692.6	688.58	51.41
9	38.0	3.59	760.0	756.41	56.24
6	43.9	3.03	878.0	874.97	64.73

For constant modular ratio

(Use  $n = 15$ , since least weight is "best")

<u>f<sub>s</sub> (psi)</u>	<u>d</u>	<u>A<sub>S</sub></u>	<u>A</u>	<u>A<sub>C</sub></u>	<u>W/L</u>
16,000	32.44	4.38	648.8	644.42	48.28
20,000	34.63	3.22	692.6	689.38	51.24
30,000	39.63	1.82	792.6	790.78	58.25
40,000	43.9	1.21	878.4	877.19	64.37
50,000	48.0	0.88	960.0	959.12	70.27



## APPENDIX E

ANALYTICAL EXPRESSION FOR MINIMUM WEIGHT OF BEAM

A precise expression for the total beam area would include both the concrete cover thickness (c) and the diameter (D) of the steel reinforcing rods. Referring to Figure 7(a), the total beam area is:

$$A = b(d + D/2 + c) \quad (E1)$$

From equation (D4), the concrete area is:

$$\begin{aligned} A_c &= A - A_s \\ &= b(d + D/2 + c) - x(\pi D^2/4) \end{aligned} \quad (E2)$$

where  $x$  = the number of rods. The weight expression to be minimized is, thus, equation (D2):

$$\begin{aligned} W/L &= \rho_c A_c + \rho_s A_s \\ &= \rho_c (b(d + D/2 + c) - x\pi D^2/4) \\ &\quad + \rho_s (x\pi D^2/4) \end{aligned} \quad (E3)$$

The object is to differentiate equation (E3) with respect to depth (d), and then equate to zero in order to find the expression for depth which results in minimum weight. Assuming that beam width (b) and rod diameter (D) are also unknown, these must first be expressed in terms of depth (d). Solving for b in equation (34) yields:

$$b = 2M/d^2 f_c k j \quad (E4)$$

Equating equation (36) with the steel area portion of



equation (E2) results in:

$$D = (4M/f_s j d x \pi)^{0.5} \quad (E5)$$

Substitution of equations (E4) and (E5) into equation (E3) yields:

$$\begin{aligned} W/L = & e_c (2M/d f_c k j + 2Mc/d^2 f_c k j \\ & + (M/d^2 f_c k j)(4M/f_s j d x \pi)^{0.5} \\ & - M/f_s j d) + e_s (M/f_s j d) \end{aligned} \quad (E6)$$

Differentiating equation (E6) with respect to  $d$ , after simplifying the first term on the second line to  $2M^{1.5}/k j d^{2.5} f_c (f_s j x \pi)^{0.5}$ , and setting equal to zero results in:

$$\begin{aligned} & e_c (-2M/d^2 f_c k j - 4Mc/d^3 f_c k j \\ & - 5M^{1.5}/k j d^{3.5} f_c (f_s j x \pi)^{0.5} \\ & + M/d^2 f_s j) - e_s (M/d^2 f_s j) = 0 \end{aligned} \quad (E7)$$

Multiplying equation (E7) by  $(-k j d^{3.5}/M)$ :

$$\begin{aligned} & e_c (2d^{1.5}/f_c + 4d^{0.5} c/f_c + 5(M/f_s j x \pi)^{0.5}/f_c \\ & - k d^{1.5}/f_s) + k d^{1.5} e_s/f_s = 0 \end{aligned} \quad (E8)$$

Grouping common terms of  $d$  yields the equation:

$$\begin{aligned} & d^{1.5} (k e_c/f_s - k e_s/f_s - 2e_c/f_c) - d^{0.5} (4c e_c/f_c) \\ & = 5 e_c (M/f_s j x \pi)^{0.5}/f_c \end{aligned} \quad (E9)$$

Since the two expressions in parentheses on the left-hand side as well as the entire right-hand side of the equation are all constants, equation (E9) can be written as:

$$A d^{1.5} - B d^{0.5} = C \quad (E10)$$





where

$$\begin{aligned} A &= (kf_c(e_c - e_s) - 2f_s e_c)/f_s f_c \\ B &= 4c e_c / f_c \end{aligned} \quad (E11)$$

$$\text{and } C = 5e_c (M/f_s j \times \pi)^{0.5} / f_c$$

In Appendix D it was shown that  $e_c$  is less than  $e_s$ . Thus, the constant A in equation (E11) is a negative number, regardless of the stresses in either the concrete or steel. Consequently, the minimum weight criterion as expressed in equation (E10) becomes a mathematical impossibility, since the addition of two "minuses" does not equal a "plus".



## APPENDIX F

EFFECT ON STRESS AND SECTION MODULUS  
OF VARYING BEAM DEPTH

The failure to achieve a meaningful solution in Appendix E is due to the absence of any imposed stress limitations. With this in mind, the following maximum permissible stresses will be adopted, based on Chapter II:

1. Steel reinforcement:  $f_s = 0.8f_y$
2. Concrete in compression:  $f_c = 0.45f'_c$
3. Concrete in tension:  $f_t = 6.75(f'_c)^{0.5}$

For the concrete selected in Chapter II ( $f'_c = 7,000$  psi) and mild steel reinforcement ( $f_y = 40,000$  psi), these stress limitations become:

1. Steel reinforcement:  $f_s = 32,000$  psi
2. Concrete (compression):  $f_c = 3,150$  psi
3. Concrete (tension):  $f_t = 565$  psi

For purposes of illustration, a beam with overall depth = 52 inches and breadth = 20 inches is arbitrarily chosen; mild steel reinforcing bars with a diameter of 5/8 inch will be embedded in the tensile side of the beam with a concrete cover of 1-11/16 inches (i.e., the distance from the centroid of the bars to the bottom of the beam is 2 inches, and, using the notation of Figure 7(a), the effective depth is thus  $d = 50$  inches). Assuming there are 5 bars (i.e., leaving room for 5 more



bars, and still having 1-inch spacing between them), the steel area is then

$$A_s = 5\pi(0.625)^2/4 = 1.534 \text{ in}^2$$

The order of events to be followed in this illustration is:

1. Determine the location of the neutral axis, the moment of inertia ( $I$ ), and the section modulus at both top ( $S_t$ ) and bottom ( $S_b$ ) of the beam. The methodology explained in detail in the first section of Chapter V, and summarized in Table 12, is used.

2. With the neutral axis location ( $kd$  in Figure 7 notation) and the depth known, the constants  $k$  and  $j$  can be calculated, the latter from equation (38).

3. The maximum moment which the beam can withstand is determined by selecting the minimum of the following:

- a.  $M = f_s A_s j d$

- b.  $M = f_c b k j d^2 / 2$

4. The maximum stress in the top ( $f_t$ ) and bottom ( $f_b$ ) fibers of the beam can then be found by dividing the moment by the section modulus at the top and bottom of the beam respectively.

Table F1 summarizes the results. The first case is for a solid concrete beam, with no steel reinforcement; it is apparent that the stress in the bottom fiber of the beam ( $f_b = 706 \text{ psi}$ ) is excessive, in that the concrete tensile limit is only 565 psi. The second case is for a



beam of the same dimensions, but with steel reinforcement added; as expected, the moment of inertia increases, while the stress decreases to within acceptable limits.

The third case sees a reduction in half of the effective depth (i.e., from  $d = 50$  to  $d = 25$  in.); the moment of inertia similarly decreases, whereas the stress increases -- although it is still within allowable limits.

The fourth case is a further 50 percent reduction in effective depth (from  $d = 25$  to  $d = 12.5$  in.). The moment of inertia continues to decline and the stresses increase, but this time the bottom fiber stress exceeds the maximum permissible tensile stress in the concrete. Thus, the "optimum" solution is not a beam with the smallest depth, as Appendices D and E suggested, since such a minimal depth would result in unacceptable stresses; rather, the "optimum" solution occurs when both steel and concrete attain their maximum permissible stresses simultaneously.





TABLE F1

EFFECT ON STRESS AND SECTION MODULUS  
OF VARYING BEAM DEPTH

beam size (in)	steel 2 area (in <sup>2</sup> )	distance of neutral axis below top, in	moment, M (10 <sup>6</sup> in-lb)	moment of inertia, I (in <sup>4</sup> )	section modulus (inches cubed) $S_{(top)}$	section modulus (inches cubed) $S_{(bot)}$	stress $f_{top}$	stress (psi) $f_{bot}$
52 x 20	0.0	26.0	6.36	234,347	9013	9013	706	706
52 x 20	1.534	26.2	2.025	239,610	9145	9287	221	218
27 x 20	1.534	13.7	1.0	33,964	2479	2554	403	392
14.5 x 20	1.534	7.4	0.493	5,329	720	751	685	656



## APPENDIX G

EFFECT ON STRESS AND SECTION MODULUS  
OF VARYING STEEL AREA AND DISTRIBUTION

The fourth example in Appendix F resulted in unacceptable stress levels in the concrete bottom fibers. This appendix will consider the effect of doubling the steel reinforcement area. In so doing, two situations will be analyzed: (1) adding five more  $5/8$  inch bars to the existing row; and (2) placing the five additional bars in a second row. In the first case, the steel center of gravity remains 12.5 inches from the top (and 2 inches from the bottom) of the beam; on the other hand, the centroid of the steel shifts closer to the top in the second case, thereby reducing the effective depth. Assuming a concrete thickness of  $1-11/16$  inches between rows of reinforcement, the data summarized in Table G1 can then be calculated by applying the methodology of the first section in Chapter V.

The first case is identical to the fourth example in Appendix F. The second case (doubling the steel area, but keeping it in the same row) results in an increase in moment of inertia and section modulus and a decrease in stress. The third case (doubling the steel area, and distributing it in two rows) likewise increases the moment of inertia, albeit not as much as the second case,



since the steel is closer to the neutral axis. The stress nevertheless decreases at the bottom even though it increases at the top.

The critical stress in a reinforced concrete beam is the concrete tensile stress at the bottom. The significant point is that this stress decreases in both instances of increasing steel area.



TABLE G1

EFFECT ON STRESS AND SECTION MODULUS OF  
VARYING STEEL AREA AND DISTRIBUTION

beam size (in)	steel area (in <sup>2</sup> )	distance of neutral axis below top (in)	moment, M 10 <sup>6</sup> in-lb	moment of inertia I (in <sup>4</sup> )	section modulus (in <sup>3</sup> )		stress (psi)	
					S (top)	S (bot)	f (top)	f (bot)
14.5x20	1.534	7.4	0.493	5,329	720	751	685	656
14.5x20	3.068 (one row)	7.56	0.493	5,563	736	802	670	615
14.5x20	3.068 (two rows)	7.49	0.493	5,367	717	766	688	644





## APPENDIX H

DETERMINATION OF POST-TENSIONING STEEL AREA

1. In order to derive an expression for the required amount of post-tensioning steel area in a beam, recourse can be made to equations (52) and (53). The former is an equation for the bottom fiber stress:

$$f_b = F/A + Fe/S - M_d/S \quad (52)$$

and the latter expresses the top fiber stress:

$$f_t = F/A - Fe/S + M_d/S \quad (53)$$

where  $F$  is the post-tensioning force. Adding these two equations results in the following:

$$f_b + f_t = 2F/A \quad (H1)$$

Adopting the stress limitations of Appendix F, the maximum top fiber stress is +3,150 psi (compression) and the maximum bottom fiber stress is -565 psi (tension).

Substituting these values into equation (H1) yields:

$$F = 2585A/2 \quad (H2)$$

Since force = (area)(stress), then  $F = A_{ps}f_{ps}$ . It, thus, follows that the area of post-tensioning steel is:

$$\begin{aligned} A_{ps} &= F/f_{ps} \\ &= 2585A/2f_{ps} \end{aligned} \quad (H3)$$

2. Another method for determining the area of post-tensioning steel is to use equation (55):

$$M_u = 0.9(A_{ps}f_{ps}d(1 - 0.59q')) \quad (55)$$



where  $q' = A_{ps} f_{ps} / b d f'_c$ , and  $f_{ps} = f_{pu} (1 - 0.5 A_{ps} f_{pu} / b d f'_c)$ , from equation (56). The ultimate moment,  $M_u$ , can be found by substituting the maximum value of  $q = 0.4$  into equation (54):

$$M_u = b d^2 f'_c q (1 - 0.59q) \quad (54)$$

A quartic equation in terms of  $A_{ps}$  results, which in turn can be solved for the area of post-tensioning steel, albeit the solution is rather complex.

3. An alternative method for calculating  $A_{ps}$ , given the area of nonprestressed reinforcement ( $A_s$ ), is described at the end of Chapter IV.

4. As an example, consider a simple concrete rectangular cross-section with the following dimensions and characteristics:

$$b = d = 20 \text{ in.}$$

$$f'_c = 7,000 \text{ psi}$$

stress limitations of Appendix F

The required amount of ordinary reinforcement ( $A_s$ ) and post-tensioning tendons ( $A_{ps}$ ) can then be found as outlined below:

(a) From equation (49),

$$M = 0.15 f'_c b d^2 = 8.4 \times 10^6 \text{ in-lb}$$

(b) From equations (37) and (38),  $j$  is found to be 0.863.

(c) The required reinforcing steel area is then calculated from equation (36):



$$\begin{aligned}
 A_s &= M/f_s jd \\
 &= (8.4 \times 10^6)/(32,000)(0.863)(20) \\
 &= 15.21 \text{ in}^2
 \end{aligned}$$

(d) The required post-tensioning steel area can be determined from equation (72):

$$q' = A_{ps}f_{ps}/bdf'_c + A_sf_y/bdf'_c \quad (72)$$

$$\begin{aligned}
 \text{where } f_{ps} &= 0.7f_{pu} - 25,000 \text{ (from Chapter IV)} \\
 &= 0.7(143,000) - 25,000 \text{ (from Table 5)} \\
 &= 75,100 \text{ psi}
 \end{aligned}$$

and  $f_y = f_s/0.8 = 40,000 \text{ psi}$ . Adopting the value of  $q' = 0.4$ , as suggested in Chapter IV, equation (72) becomes:

$$0.4 = 0.027A_{ps} + 0.0143A_s \quad (H4)$$

Substituting the result  $A_s = 15.21 \text{ in}^2$  found in the preceding paragraph into equation (H4) yields:  $A_{ps} = 6.76 \text{ in}^2$

(e) A solution for  $A_{ps}$  can be found independently of  $A_s$  by resorting to equation (H3). Hence, the required area of post-tensioning steel is:

$$\begin{aligned}
 A_{ps} &= F/f_{ps} \\
 &= 2585A/2f_{ps} \\
 &= (2585)(20)(20)/(2)(75,100) \\
 &= 6.88 \text{ in}^2
 \end{aligned}$$

This requirement can be satisfied by using five 33 mm. tendons or eight 27 mm. tendons.

The two solutions for  $A_{ps}$ , arrived at independently in paragraphs (d) and (e), are reasonably similar (within



1.7 percent of each other), and thus tend to support the validity of the formulae derived in this appendix.

As a further check on the accuracy of the preceding equations, a beam with a depth of 30 inches will be considered. With the new values of  $M$ ,  $j$ , and  $d$ , the required area of ordinary reinforcing steel is:

$$\begin{aligned} A_s &= M/f_s j d \\ &= (18.9 \times 10^6)/(32,000)(0.864)(30) \\ &= 22.79 \text{ in}^2 \end{aligned}$$

Equation (72) now becomes:

$$0.4 = 0.0179A_{ps} + 0.0095A_s$$

and solving for the area of post-tensioning steel yields:

$$A_{ps} = 10.25 \text{ in}^2$$

An independent solution for  $A_{ps}$ , using equation (H3), yields:

$$\begin{aligned} A_{ps} &= (2585)(20)(30)/(2)(75,100) \\ &= 10.33 \text{ in}^2 \end{aligned}$$

The discrepancy in this instance is only 0.77 percent, thus lending further credence to the formulae developed herein.

The total steel percentage in both the preceding examples is 5.52 percent:

$$\begin{aligned} (A_s + A_{ps})/bd &= (15.21 + 6.88)/400 \\ &= (22.79 + 10.33)/600 \\ &= 0.0552 \end{aligned}$$

Therefore, for a constant gross cross-sectional area, if





the area of ordinary reinforcement ( $A_s$ ) is decreased, it is necessary to increase the post-tensioning steel area ( $A_{ps}$ ), and vice versa.



## APPENDIX I

DETERMINATION OF NONPRESTRESSED  
AND PRESTRESSED STEEL AREA

Referring to Figure 11, while ignoring the tendon duct area (treat it as part of the concrete), expanded versions of equations (65) and (66) can be written:

$$e_n = (eA_g - e_{ps}A_{ps} - e_sA_s)/A_n \quad (I1)$$

and

$$I_n = I_g + A_g(e_n - e)^2 - A_{ps}(e_n - e_{ps})^2 - A_s(e_n - e_s)^2 \quad (I2)$$

where terminology is as defined in Chapter IV. Equations (69) and (70) can be rewritten as follows, with comparison to equations (52) and (53):

$$f_t = N_p/A_n + M/S_{tn} \quad (I3)$$

and

$$f_b = N_p/A_n - M/S_{bn} \quad (I4)$$

Subtracting equation (I4) from (I3) results in:

$$\begin{aligned} f_t - f_b &= +M(1/S_{tn} + 1/S_{bn}) \\ &= 3150 - (-565) \\ &= 3715 \text{ psi} \end{aligned} \quad (I5)$$

by adopting the stress limitations of Appendix F.

Substitution of equations (67) and (68) into equation (I5) yields:

$$3715/M = (d - e_n)/I_n + e_n/I_n \quad (I6)$$

Given the depth (d) and moment (M), and assuming a



value for  $e_n$  (the distance to the centroid of  $A_n$ , where  $A_n = A_g - A_{ps} - A_s$ ), then equation (I6) can be solved for the net moment of inertia ( $I_n$ ). The resulting value is substituted into equation (I2). It is next necessary to assume the location of both the  $A_s$  and  $A_{ps}$  centroids ( $e_s$  and  $e_{ps}$ , respectively). Realizing that  $A_g = bd$ ,  $I_g = bd^3/12$ , and  $e = d/2$ , it is then possible to solve the simultaneous equations (I1) and (I2) for the two unknowns,  $A_s$  and  $A_{ps}$ .

As an illustration, the first example of Appendix H will be re-worked using the present method. Assuming that  $M = 2.35 \times 10^6$  in-lb and that  $e_n = 10.3$  in., equation (I6) is solved for the net moment of inertia;

$$\begin{aligned} I_n &= 20M/3715 \\ &= 12,651 \text{ in}^4 \end{aligned}$$

Now  $e = d/2 = 10$  in.,  $A_g = bd = (20)(20) = 400 \text{ in}^2$ , and  $I_g = bd^3/12 = 13,333 \text{ in}^4$ . Assuming further that  $e_s = 2$  in. (i.e., a cover thickness of about 1-3/4 in.) and  $e_{ps} = 5$  in., equations (I1) and (I2) reduce to:

$$\text{and} \quad 5.3A_{ps} + 8.3A_s = 120 \quad (I7)$$

$$28.1A_{ps} + 68.9A_s = 718 \quad (I8)$$

Solution of equations (I7) and (I8) results in:

$$\begin{aligned} \text{and} \quad A_s &= 3.28 \text{ in}^2 \\ A_{ps} &= 17.5 \text{ in}^2 \end{aligned}$$

These values differ from those obtained in Appendix H, but the discrepancy is attributable to all the assumptions



required of the present technique. Significantly, however, the total steel percentage is 5.2 percent, which is reasonably close to the 5.52 percent of Appendix H. It is nevertheless recommended that the method in Appendix H be employed in the preliminary design of the midship section for a post-tensioned reinforced concrete ship.





## APPENDIX J

MODIFIED COMPUTER PROGRAM TO CALCULATE  
THE SECTION MODULUS OF A POST-TENSIONED  
REINFORCED CONCRETE SHIP

To facilitate comprehension of the ensuing computer program, the terminology employed is defined chronologically below:

YR = modular ratio =  $E_s/E_c$

TAUPI = T.P. = transverse-reinforcement percentage factor

RDDIA = reinforcing rod diameter

TDNDIA = post-tensioning tendon diameter

RDARE = area of one reinforcing rod

TDNARE = area of one tendon

RDARSM = sum total of reinforcing rod areas

TDARSM = sum total of tendon areas

COVER = concrete cover thickness

IMR = number of reinforcing rods

JTENDN = number of tendons

RODIST = distance of rods to baseline

TNDIST = distance of tendons to baseline

TOP = top width of slice

BTM = bottom width of slice

TH = slice thickness

DBL = distance from bottom of slice to baseline



AREAST = area of steel

STLSM = sum total of steel area

AREA = net concrete area

AREASM = sum total of equivalent concrete area

XMOM = moment of a slice

TMOM = total sum of moments

XINRT = moment of inertia of a slice

SMINRT = sum total of moments of inertia

GAMMA =  $\text{TAUPI} * \text{STLSM}$  = amount of transverse  
reinforcement to deduct from AREASM

HTNA = height of neutral axis above baseline

DECKSM = section modulus at the deck

BTMSM = section modulus at the bottom (keel)

The computer program itself, including a typical input/  
output, appears on the following three pages.



```

0004R C THIS IS A PROGRAM TO CALCULATE THE SECTION MODULUS OF A
0004R C POST-TENSIONED REINFORCED CONCRETE TANKER MIDSHIP SECTION.
0004R C NOTE: RESULTS (E.G., SECTION MODULUS, MOMENT OF INERTIA,
0004R C AREA OF STEEL, ETC.) ARE FOR ONLY HALF THE MIDSHIP SECTION,
0004R C AND HENCE MUST CORRESPONDINGLY BE MULTIPLIED BY TWO.
0004R C DIMENSIONS ARE GIVEN IN METERS.
0004R INTEGER IR,IP
0004R DATA IR/8,IP/5/
0004R YR = 7.
0004R 705 READ(IR,710) DEPTH, BREDTH, ROARSM, TOARSM, RODIA, TONDIA, COVER
0004R 710 FORMAT(7F10.4)
0004R RDARE = (3.14159/4.)*RODIA**2.
0004R TONARE = (3.14159/4.)*TONDIA**2.
0004R HO = DEPTH/2.
0004R AREASH = 0.
0004R TMOM = 0.
0004R SMINRT = 0.
0004R STLSM = 0.
0004R I = 0
0004R WRITE(IP,715) DEPTH, BREDTH, ROARSM, TOARSM, RODIA, TONDIA, COVER
0004R 715 FORMAT('1',DEPTH,'F4.1,2X',BREDTH,'F4.1,2X',ROD AREA = ',
0004R XF4.2,2X',TENDON AREA = ',F4.2,2X',ROD DIAM=,F6.4,2X,
0004R X,TENDON DIAM=,F6.4,2X,COVER = ',F6.4)
0004R WRITE(IP,720)
0004R 720 FORMAT('0',I,ITEM,3X,TOP,6X,BOTTOM,4X,SLICE,4X,DISTANCE',
0004R X2X,NO,1,2X,DISTANCE,2X,NO,1,2X,DISTANCE,4X,AREA,5X,
0004R X,MOMENT,4X,MOMENT')
0004R WRITE(IP,725)
0004R 725 FORMAT('1,7X,WIDTH,5X,WIDTH,3X,THICKNESS',2X,TO BASE,1X,
0004R X,RODS,2X,TO BASE,1X,TENDON,1X,TO BASE,2X,(CONCRETE)',
0004R X4X,OF,7X,DF,1,37X,LINE,11X,LINE,11X,LINE,15X,SLICE',
0004R X5X,INERTIA,/)
0004R 730 READ(IR,735) TOP, BTM, TH, OBL, IMR, RDOIST, JTENON, TNDIST
0004R 735 FORMAT(4F8.2,14,F8.2,14,F8.2)
0004R I = I + 1
0004R AREAST = FLDAT(IMR)*ROARE + FLOAT(JTENON)*TONARE
0004R STLSM = STLSM + AREAST
0004R AREA = TOP*TH + AREAST
0004R AREAST = YR*AREAST
0004R CG = 0.5
0004R AREASH = AREASH + AREA + AREAST
0004R XMOM = YR*(FLDAT(IMR)*RDARE*RDOIST) + YR*(FLOAT(JTENON)*TONARE*
0004R XTNOIST) + AREA*(OBL + TH*CG)
0004R TMOM = TMOM + XMOM
0004R XINRT = YH*(FLOAT(IMR)*ROARE*(RDOIST**2.)) + YR*(FLDAT(JTENON)*
0004R XTNDARE*(TNDIST**2.)) + (AREA*(OBL+TH*CG)**2.) + (TH**2.)*AREA/12.
0004R SMINRT = SMINRT + XINRT
0004R WRITE(IP,740)I,TOP,BTM,TH,OBL,IMR,RDOIST,JTENON,TNOIST,AREA,XMOM,
0004R XINRT
0004R 740 FORMAT('1,15,F8.2,3F10.2,15,F11.2,16,F8.2,3F10.2)
0004R IF(I.LT.3) GO TO 730
0004R C THIS RUN IS FOR THE SAGGING CONDITION
0004R TAUPI = 2.19

```



```

05E2R      GAMMA = TAUPI*STLSM
05EER      AREASM = AREASM - GAMMA
05FAR      TMOM = TMOM - GAMMA*HD/2.
0612R      SMINRT = SMINRT - GAMMA*(HO/2.)*2.
0632R      HTNA = TMOM/AREASM
065AR      SMINRT = SMINRT - (AREASM*(HTNA*2.))
067ER      WRITE(IP,745) HTNA, SMINRT
067ER      745 FORMAT(//,'0',HEIGHT OF NEUTRAL AXIS ABOVE BASE LINE = ',F6.2/
067ER      X'0',MOMENT OF INERTIA ABOUT NEUTRAL AXIS = ',F10.1)
06F0R      DECKSM = SMINRT/(DEPTH - HTNA)
0704R      ATMSM = SMINRT/HTNA
0710R      WRITE(IP,750) DECKSM, BTMSM
0734R      750 FORMAT('0','SECTION MODULUS (DECK) = ',F10.2,'0','SECTION MODULUS (
0734R      X)BOTTOM) = ',F12.2)
0786R      WRITE(IP,755) AREASM, STLSM
07AAR      755 FORMAT('0','TOTAL AREA IN EQUIVALENT CONCRETE = ',F10.2,'0',
07AAR      X)AREA OF STEEL (UNCONVERTED TO EQUIVALENT CONCRETE) = ',F10.2)
0822R      GO TO 705
0826R      STOP
082CR      ENO
0800(S)  *II 0008(V) IR 000C(V) IP 0830(V) YR 0018(L) 705
084(L) 710 000(S) 01 083R(V) DEPTH 083C(V) BREATH 0840(V) RDARSM
084(V) TDARSM 084C(V) TONOA 0870(V) HO 0874(V) AREASM 087C(V) TMOM
0800(S) *A 086C(V) TONARE 088R(V) I 0130(L) 715 01E0(L) 722
0800(S) SMINRT 0884(V) STLSM 03A4(L) 735 0890(V) TOP 0894(V) BTM
028(L) 725 0350(L) 730 089C(V) DBL 08A0(V) IMR 08A4(V) JTENON
08AC(V) TH 0864(V) AREAST 000(S) FLOAT 08B8(V) AREA 088C(V) CG
08C(V) TMOM 0800(V) XINRT 059R(L) 742 08F4(V) TAUPI 08FC(V) GAMMA
0900(V) HTNA 067E(L) 745 0904(V) DECKSM 0908(V) BTMSM 0734(L) 750
07A(L) 755 000(S) *S 000(S) *V
      LENGTH OF PROGRAM IS X'090C'
      NO ERRORS IN *MAIN*
// XEG
EOF

```

```

PROGRAM LABELS:
2000 *MAIN* 3FB8 *V 3962 *A 300A $6 3056 *W 3EB4 *ERCNT
290C *I 3E7C *ZERO 3F0C *MES 3014 FLOAT 381C EXP 3C42 AINT
3A14 ALOG 3E78 *S 3B1C AEXP 3E82 *S 3E4E $8
30B* *COMP 3F8A *U 3EB4 *O 3FC6
ENTRY=POINTS:
290C *I 3962 *A 3A14 ALOG 3B1C AEXP 3B1C EXP 3C42 AINT
3014 FLOAT 3056 *W 3084 *COMP 300A $6 3E1C *RARG 3E4E $8
3E78 *S 3E7C *ZERO 3E80 *S 3EB4 *ERCNT 3EB6 *O 3FC2 *MES
3F96 *U 3FBC *V
COMMON=BLOCKS:
NONE

```





DEPTH = 23.5 BREADTH = 44.0 ROD AREA = 0.55 TENDON AREA = 0.45 ROD DIAM=0.0095 TENDON DIAM=0.0330 COVER = 0.0317

ITEM	TOP WIDTH	BOTTOM WIDTH	SLICE THICKNESS	DISTANCE TO BASE RODS LINE	NO. RODS	DISTANCE TO BASE TENDON LINE	NO. DISTANCE TO BASE LINE	AREA (CONCRETE)	MOMENT OF SLICE	MOMENT OF INERTIA
1	22.00	22.00	0.52	22.98	2569	23.24	174	11.11	312.01	7251.31
2	0.52	0.52	22.46	0.52	2622	11.75	178	11.34	161.07	2369.28
3	22.00	22.00	0.52	0.00	2569	0.26	174	11.11	3.49	1.16

HEIGHT OF NEUTRAL AXIS ABOVE BASE LINE = 12.09

MOMENT OF INERTIA ABOUT NEUTRAL AXIS = 3942.2

SECTION MODULUS (DECK) = 345.36

SECTION MODULUS (BOTTOM) = 326.20

TOTAL AREA IN EQUIVALENT CONCRETE = 38.37

AREA OF STEEL (UNCONVERTED TO EQUIVALENT CONCRETE) = 1.00



## APPENDIX K

EFFECT ON MOMENT OF INERTIA  
OF VARYING PRIMARY PARAMETERS

It was demonstrated in Chapter V that there are three primary parameters which affect the moment of inertia of a post-tensioned reinforced concrete ship, namely: concrete area ( $A_c$ ), steel area ( $A_s$ ), and modular ratio ( $n$ ). By considering five different values for each of these primary parameters, the computer program in Appendix J was applied and yielded 125 distinct values for the moment of inertia.

The five tables which follow (for  $n = 5, 7, 9, 11$ , and  $13$ , respectively) present the resulting moment of inertia figures (in  $m^4$ ); steel area (in  $m^2$ ) is on the left-hand column and concrete area (in  $m^2$ ) is on the bottom -- by selecting any two values for  $A_s$  and  $A_c$ , the corresponding value for moment of inertia can be simply read off the table.

		<u><math>n = 5</math></u>				
steel area	1.2	3754	3818	3881	3944	4007
	1.1	3721	3792	3856	3919	3981
	1.0	3704	3767	3831	3894	3956
	0.9	3679	3742	3805	3867	3931
	0.8	3653	3717	3780	3843	3906
		33.90	34.55	35.20	35.85	36.50
		concrete area				



n = 7

steel area	1.2	3965	4028	4091	4154	4216
	1.1	3922	3985	4048	4111	4173
	1.0	3879	3942	4005	4067	4131
	0.9	3836	3899	3962	4026	4088
	0.8	3793	3856	3920	3983	4045

33.90	34.55	35.20	35.85	36.50
concrete area				

n = 9

steel area	1.2	4176	4238	4301	4364	4425
	1.1	4115	4177	4240	4303	4365
	1.0	4055	4117	4180	4243	4305
	0.9	3994	4057	4120	4183	4245
	0.8	3933	3996	4059	4122	4184

33.90	34.55	35.20	35.85	36.50
concrete area				



n = 11

steel area	1.2	4386	4448	4511	4573	4635
	1.1	4308	4370	4432	4496	4557
	1.0	4230	4292	4355	4418	4480
	0.9	4151	4214	4277	4340	4401
	0.8	4073	4136	4199	4262	4324
		33.90	34.55	35.20	35.85	36.50
		concrete area				

n = 13

steel area	1.2	4597	4658	4721	4783	4844
	1.1	4500	4562	4625	4688	4748
	1.0	4405	4467	4530	4593	4654
	0.9	4309	4371	4434	4497	4558
	0.8	4213	4275	4338	4401	4463
		33.90	34.55	35.20	35.85	36.50
		concrete area				





## APPENDIX L

MINIMUM WEIGHT CONSIDERATIONS

With the aid of Figures 14 through 19, various combinations of concrete area, steel area, and modular ratio were selected with only one thing in common: they each had the same moment of inertia. Equation (76) was then employed to ascertain the effect on weight per unit length of the midship section ( $W_{ms}$ ). With  $A_s$  representing total steel area, and  $A_c$  signifying gross concrete area (before deducting  $A_s$ ), the results are summarized below for two different values of moment of inertia ( $I$ ).

$$\text{For } I = 3940 \text{ m}^4$$

<u>case</u>	<u>n</u>	<u><math>A_s \text{ (m}^2\text{)}</math></u>	<u><math>A_c \text{ (m}^2\text{)}</math></u>	<u><math>W_{ms} \text{ (kg/m)}</math></u>
1	5	1.2	35.85	79,002
2	5	0.95	36.5	78,849
3	7	0.8	35.42	75,805
4	7	1.0	34.55	75,225
5	7	1.15	33.9	74,794
6	9	0.717	34.55	73,574
7	9	0.817	33.9	72,852



For  $I = 4350 \text{ m}^4$

<u>case</u>	<u>n</u>	<u><math>A_s \text{ (m}^2\text{)}</math></u>	<u><math>A_c \text{ (m}^2\text{)}</math></u>	<u><math>W_{ms} \text{ (kg/m)}</math></u>
1	9	1.075	36.5	79,563
2	9	1.18	35.85	78,871
3	11	0.913	35.85	77,314
4	11	0.994	35.2	76,481
5	11	1.08	34.55	75,677
6	13	0.813	35.2	75,425
7	13	0.877	34.55	74,492
8	13	0.942	33.9	73,567



REFERENCES

1. Morgan, R.G., "Lambot's Boats," Concrete, Vol. 2, No. 3, March 1968, p. 128.
2. Nervi, P.L., "Ferro-cemento," chapter 4 in Structures, F.W. Dodge, New York, 1956.
3. Klieger, P. and A.H. Gustaferro, "Concrete for Underwater Structures," NRL Report 6167, November 1964, p. 120-9.
4. Bezukladov, V.F. et al., "Ship Hulls Made of Reinforced Concrete," translated by the Naval Ships Systems Command, Publication AD680042, Defense Documentation Center, November 1968.
5. Baitis, A.E., "The Vipers: Ferro-cement Planing Boat," Naval Engineers Journal, Vol. 83, No. 2, April 1971, p. 53-63.
6. Brauer, F.E., "Ferro-cement for Boats and Craft," Naval Engineers Journal, Vol. 85, No. 5, October 1973, p. 93-105.
7. Dinsenhacher, A.L. and F.E. Brauer, "Material development, Design, Construction, and Evaluation of a Ferro-cement Planing Boat," Marine Technology, Vol. 11, No. 3, July 1974, p. 277-96.
8. Collins, J.F. and J.S. Claman, "Ferro-cement for Marine Applications - An Engineering Evaluation," S.N.A.M.E. New England Section paper, March 1969.
9. Coveyou, T.T., "The 1973 University of Michigan Ferro-cement Canoe Project," Marine Technology, Vol. 11, No. 2, April 1974, p. 215-23.
10. "References on Ferro-cement in the Marine Environment," Technical and Research Report R-14, Task Group HS-6-4 (Ferro-cement) of Panel HS-6 (Materials) of the Hull Structure Committee, S.N.A.M.E., New York, October 1972.
11. Boyd, R.W., et. at., "Report of Special Committee on Concrete ships and Barges," American Concrete Institute Proceedings, Vol. 17, 1921, p. 285-91.
12. Vasta, J., "The Concrete Ship Program of World War II," S.N.A.M.E. Chesapeake Section paper, May 1952.



13. "Building Code Requirements for Reinforced Concrete" (ACI 318-71), American Concrete Institute, 1971.
14. Faber, J. and F. Mead, Reinforced Concrete, E. and F.N. Spon Ltd., London, 1965, 534 pp.
15. Ferguson, P.M., Reinforced Concrete Fundamentals, John Wiley and Sons, Inc., New York, 1973, 750 pp.
16. Timoshenko, S. and G.H. MacCullough, Elements of Strength of Materials, D. Van Nostrand Co., Inc., New York, 1940, p. 227-33.
17. Den Hartog, J.P., Strength of Materials, Dover Publications, Inc., New York, 1949, p. 127-31.
18. Magnel, G., Prestressed Concrete, McGraw-Hill Book Co., Inc., New York, 1954, 345 pp.
19. Chi, M. and F. Biberstein, Theory of Prestressed Concrete, Prentice-Hall, Inc., Englewood Cliffs, N.J., 1963, 252 pp.
20. Faber, J. and F. Mead, Ibid., chapter 15, p. 451-66.
21. Ferguson, P.M., Ibid., chapter 16, p. 613-39.
22. Moe, J., F. Stensrud and E. Vitiello, "A Feasibility Study of Prestressed Concrete Tanker Ships," Trondheim, October 1972.
23. Gerwick, Ben C., Jr., "Design and Construction of Prestressed Concrete Vessels," OTC 1886, May 1973.
24. Yee, A.A., K. Lum and V. Golveo, "Design and Construction of Oceangoing Pretensioned Concrete Barges," American Concrete Institute Proceedings, Vol. 72, No. 4, April 1975, p. 125-134.
25. Fundamentals of Prestressed Concrete Design, Prestressed Concrete Institute, Inc., Chicago, 1968, 133 pp.
26. The Structural Use of Concrete (CP 110), British Standards Institution, November 1972.
27. Troxell, G.E., H. Davis and J. Kelly, Composition and Properties of Concrete, McGraw-Hill Book Co., New York, 1968.





28. Evans, J.H. and J.C. Adamchak, Ocean Engineering Structures, The M.I.T. Press, 1969, p. 57-61.
29. Masubuchi, K., Materials for Ocean Engineering, The M.I.T. Press, 1970, p. 14.
30. Branson, D.E. and M.A. Sozen, "Deflections of Prestressed Concrete Members," American Concrete Institute Proceedings, Vol. 60, No. 12, December 1963, pp. 1697-1728.
31. Neville, A.M., Properties of Concrete, John Wiley and Sons, Inc., New York, 1963, 532 pp.
32. Lydon, F.D., Concrete Mix Design, Applied Science Publishers Ltd., London, 1972, 148 pp.
33. Design and Control of Concrete Mixtures, Portland Cement Association, Chicago, 1952, 68 pp.
34. Pulver, H.E., Construction Estimates and Costs, McGraw-Hill Book Co., New York, 1969, p. 127.
35. "Construction Scoreboard," Engineering News-Record, Vol. 193, No. 11, September 5, 1974, p. 27.
36. "Third Quarterly Cost Roundup," Engineering News-Record, Vol. 193, No. 13, September 19, 1974, p. 97.
37. "Materials Prices," Engineering News-Record, Vol. 193 No. 8, August 15, 1974, p. 40-1.
38. Armco Steel Corporation, Product Data: "Armco Crescent Reinforcing Bars," p. 2.
39. Rice, P.F. and E.S. Hoffman, Structural Design Guide to the ACI Building Code, Van Nostrand Reinhold Co., New York, 1972, 437 pp.
40. Kurt Orban Company, Inc., Technical Bulletin: "Stress Relieved Strand and Wire for Prestressed Concrete," p. 16.
41. Building Construction Cost Data, R.S. Means Company, Inc., Duxbury, Mass., 1974, p. 243.
42. "Materials Prices," Engineering News-Record, Vol. 193 No. 11, September 5, 1974, p. 30-1.



43. Gerwick, Ben C., Jr., Construction of Prestressed Concrete Structures, John Wiley and Sons, Inc., New York, 1971, 411 pp.
44. Inglis, C.E., Transactions of the Institute of Naval Architects, London, Vol. 55, 1913, p. 219.
45. Griffith, A.A., "The Phenomena of Rupture and Flaw in Solids," Philosophical Transactions of the Royal Society of London, Vol. 221, 1921, p. 163-98.
46. Irwin, G.R., "Analysis of Stresses and Strains Near the End of a Crack Traversing a Plate," Journal of Applied Mechanics, Vol. 24, 1957, p. 361-4.
47. Crowan, E., "Energy Criterion of Fracture," Technical Report No. 3, M.I.T., July 1954.
48. Kaplan, M.F., "Crack Propagation and the Fracture of Concrete," ACI Journal, Proceedings, Vol. 58, No. 28, November 1961, p. 591-610.
49. Moavenzadeh, F., R. Kuguel and L. Keat, "Fracture of Concrete," Research Report No. R68-5, M.I.T., March 1968.
50. Romualdi, J.P., and G.B. Batson, "Mechanics of Crack Arrest in Concrete," A.S.C.E. Proceedings, Vol. 89, No. EM3, June 1963, p. 147-67.
51. Lott, J.L., and C.E. Kessler, "Crack Propagation in Plain Concrete," University of Illinois T.A.M. Report No. 648, 1964.
52. Glucklich, J., "Fracture of Plain Concrete," A.S.C.E. Proceedings, Vol. 89, No. EM6, September 1963, p. 127-38.
53. Bianchini, A.C., C.E. Kesler and J.L. Lott, "Cracking of Reinforced Concrete Under External Load," in Causes, Mechanism and Control of Cracking in Concrete, ACI Publication SP-20, 1968, p. 73-85.
54. Broms, B.B., "Crack Width and Crack Spacing in Reinforced Concrete Members," ACI Journal, Proceedings, Vol. 62, No. 10, October 1965, p. 1237-56.
55. Mather, B., "Cracking Induced by Environmental Effects," in Causes, Mechanism and Control of Cracking in Concrete, p. 67-72, 1968.



56. Kaar, P.H., "An approach to the Control of Cracking in Reinforced Concrete," in Causes, Mechanism and Control of Cracking in Concrete, p. 141-57, 1968.
57. PCI Design Handbook, Prestressed Concrete Institute, Chicago, 1971.
58. Romualdi, J.P. and J.A. Mandel, "Tensile Strength of Concrete Affected by Uniformly Distributed and Closely Spaced Short Lengths of Wire Reinforcement," ACI Journal, Proceedings, Vol. 61, No. 6, June 1964, p. 657-72.
59. Romualdi, J.P., Ramay, M.R. and S.C. Sanday, "Prevention and Control of Cracking by Use of Short Random Fibers," ACI Publication SP-10, 1968, Paper No. 10.
60. Leopold, Reuven, "Naval Surface Ship Design," M.I.T. Professional Summer Course, July 8-19, 1974.
61. Olszah, W., "Influence of Bond and Cracking on Corrosion of Reinforcement, on Watertightness, and on Stiffness," Proceedings, Symposium on Bond and Crack Formation in Reinforced Concrete (Stockholm, 1957).
62. Recommendations for an International Code of Practice for Reinforced Concrete, Comite Europeen du Beton, Paris, 1964 (English translation by the American Concrete Institute, 1965), 156 pp.
63. Guyon, Y., Limit-State Design of Prestressed Concrete, John Wiley and Sons, New York, 1972, 485 pp.
64. Leonhardt, Fritz, "To New Frontiers for Prestressed Concrete Design and Construction," Journal of the Prestressed Concrete Institute, Vol. 19, No. 5, September-October 1974, p. 54-69.
65. Regan, P.E. and C.W. Yu, Limit State Design of Structural Concrete, John Wiley and Sons, New York, 1973, 325 pp.
66. Gergely, P. and L.A. Lutz, "Maximum Crack Width in Reinforced Concrete Flexural Members," in ACI Publication SP-20, 1968, p. 87-117.





67. Hognestad, E., "High Strength Bars as Concrete Reinforcement, Part 2 - Control of Flexural Cracking," Journal, PCA Research and Development Laboratories, Vol. 4, No. 1, January 1962, p. 46-63.
68. Abeles, P.W., An Introduction to Prestressed Concrete, Concrete Publications, Ltd., London, 1966.
69. Uhlig, H.H., Corrosion and Corrosion Control, John Wiley and Sons Inc., New York, 1971, p. 13-16.
70. Lorman, W.R., J.J. Hromadik, D.A. Davis, D.F. Griffin, M.J. Wolfe and H.S. Zwibel, "Mobile Ocean Basing System - A Concrete Concept," Naval Civil Engineering Laboratory, 1971.
71. Gerwick, Ben C., Jr., "Prestressed Concrete in Marine Structures," Civil Engineering, Vol. 29, No. 11, November 1959, p. 46-9.
72. Black, Peter, Strength of Materials, Pergamon Press, London, 1966, p. 153.
73. Granet, Irving, Strength of Materials for Engineering Technology, Reston Publishing Co., Inc., Reston, Virginia, 1973, pp. 220-224.
74. Commentary of the "Building Code Requirements for Reinforced Concrete" (ACI 318-71), American Concrete Institute, 1974.
75. "TUFWIRE Products for Prestressed Concrete," Armco Steel Corp., 1968, p. 4.
76. Shaikh, A.F. and D.E. Branson, "Non-Tensioned Steel in Prestressed Concrete Beams," Journal of the Prestressed Concrete Institute, Vol. 15, No. 1, February 1970, pp. 14-36.
77. Abeles, P.W., "Partial Prestressing and Possibilities for Its Practical Application," PCI Journal, Vol. 4, No. 1, June 1959, pp. 35-51.
78. Abeles, P.W., "Partial Prestressing in England," PCI Journal, Vol. 8, No. 1, February 1963, pp. 51-72.
79. Abeles, P.W., "Studies of Crack Widths and Deformation Under Sustained and Fatigue Loading," PCI Journal, Vol. 10, No. 6, December 1965.





80. Hutton, S.G. and R.E. Loov, "Flexural Behavior of Prestressed, Partially Prestressed, and Reinforced Concrete Beams," ACI Journal, Proceedings, Vol. 63, No. 12, December 1966, pp. 1401-1408.
81. Naaman, A.E., "Ultimate Moment Design in Prestressed Concrete," submitted for possible publication in the PCI Journal, September 1974.
82. "American Association of State Highway Officials, Section 5 - Reinforced Concrete - Standard Specifications for Highway Bridges," Washington, D.C., 1973.
83. Leonhardt, Fritz, Prestressed Concrete Design and Construction, Wilhelm Ernst and Sohn, Munich, 1964, 677 pp.
84. Milto, A.A., "Construction of Prestressed Concrete Vessels," Proceedings of the FIP Symposium on Concrete Sea Structures, Tbilisi, September 1972, pp. 202-205.
85. Power, C.A., "The Development of Prestressed Concrete Barges in Fiji," Proceedings of the FIP Symposium on Concrete Sea Structures, Tbilisi, September 1972, pp. 12-17.
86. "Recommendations for the Design of Concrete Sea Structures," FIP Commission, London, October 1973, 40 pp.
87. Turner, F.H., and E.C.B. Corlett, "Prestressed Concrete Carriers for the Transportation and Storage of Cryogenic Liquids," Proceedings of the FIP Symposium on Concrete Sea Structures, Tbilisi, September 1972, pp. 18-25.
88. Closner, J.J., DeBeck, L.F., Legatos, N.A., Marchaj, T.J., and B.C. Gerwick, Jr., "Prestressed Concrete Proposed for LNG Carriers," Ocean Industry, February 1974, pp. 105-112.
89. Turner, F.H., "The Contranstor Concept for Cryogenic Carriers," Ocean Industry, November 1974, pp. 54-56.
90. St. Denis, M., "On the Structural Design of the Midship Section," David W. Taylor Model Basin Report C-555, October 1954, 100 pp.



91. Comstock, J.P., ed., Principles of Naval Architecture, Society of Naval Architects and Marine Engineers, 1967, p. 183.
92. Keays, K., Computer program entitled "Dyckerhoff and Widmann Concrete LNG Tanker Midship Section Modulus," September 1974.
93. Evans, J.H., editor, Ship Structural Design Concepts, Ship Structure Committee, 1974, Chapters 1 and 24.



Thesis  
E656 Ertner

163419

Post-tensioned rein-  
forced concrete as ap-  
plied to the construc-  
tion of ships.

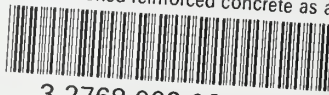
Thesis  
E656 Ertner

163419

Post-tensioned rein-  
forced concrete as ap-  
plied to the construc-  
tion of ships.

thesE656

Post-tensioned reinforced concrete as ap



3 2768 002 06224 2

DUDLEY KNOX LIBRARY